Modeling Drivers' Acceleration and Lane Changing Behavior

by

Kazi Iftekhar Ahmed
B. Sc. Eng. (Civil)
Bangladesh Univ. of Eng. and Technology (BUET), Dhaka, Bangladesh (1991)

M.S. in Transportation
Massachusetts Institute of Technology, Cambridge, MA (1996)

Submitted to the Department of Civil and Environmental Engineering
in partial fulfillment of the requirements for the degree of

Doctor of Science in
Transportation Systems and Decision Sciences
at the
MASSACHUSETTS INSTITUTE OF TECHNOLOGY

February 1999

Author

. . . . . .
Department of Civil and Environmental Engineering
January 8, 1999

Certified by

. . . . . .
Moshe E. Ben-Akiva
Professor of Civil and Environmental Engineering
Thesis Supervisor

Certified by

. . . . . .
Dr. Haris N. Koutsopoulos
Operations Research Analyst
Thesis Supervisor

Accepted by

. . . . . .
Andrew J. Whittle
Chairman, Departmental Committee on Graduate Studies

Modeling Drivers' Acceleration and Lane Changing Behavior

by

Kazi Iftekhar Ahmed

Submitted to the Department of Civil and Environmental Engineering
on January 8, 1999, in partial fulfillment of the
requirements for the degree of
Doctor of Science in
Transportation Systems and Decision Sciences

Abstract

This thesis contributes to the development of microscopic traffic performance models which includes the acceleration and lane changing models. It enhances the existing models and develops new ones. Another major contribution of this thesis is the empirical work, i.e., estimating the models using statistically rigorous methods and microscopic data collected from real traffic.

The acceleration model defines two regimes of traffic flow: the car–following regime and the free–flow regime. In the car–following regime, a driver is assumed to follow his/her leader, while in the free–flow regime, a driver is assumed to try to attain his/her desired speed. A probabilistic model, that is based on a time headway threshold, is used to determine the regime the driver belongs to. Heterogeneity across drivers is captured through the headway threshold and reaction time distributions. The parameters of the car–following and free–flow acceleration models along with the headway threshold and reaction time distributions are jointly estimated using the maximum likelihood estimation method.

The lane changing decision process is modeled as a sequence of three steps: decision to consider a lane change, choice of a target lane, and gap acceptance. Since acceptable gaps are hard to find in a heavily congested traffic, a forced merging model that captures forced lane changing behavior and courtesy yielding is developed. A discrete choice model framework is used to model the impact of the surrounding traffic environment and lane configuration on drivers' lane changing decision process.

The models are estimated using actual traffic data collected from Interstate 93 at the Central Artery, located in downtown Boston, MA, USA. In addition to assessing the model parameters from statistical and behavioral standpoints, the models are

validated using a microscopic traffic simulator. Overall, the empirical results are encouraging, and demonstrate the effectiveness of the modeling framework.

Thesis Supervisor: **Moshe E. Ben-Akiva**
Title: Professor of Civil and Environmental Engineering
Massachusetts Institute of Technology

Thesis Supervisor: **Dr. Haris N. Koutsopoulos**
Title: Operations Research Analyst
Volpe National Transportation Systems Center
Cambridge, MA, USA.

To

Abbu, Ammu,

my son, Sabih,

and
my wife, Lubna

Thesis Committee

Moshe E. Ben-Akiva (Chairman)
Professor
Department of Civil and Environmental Engineering
Massachusetts Institute of Technology

Haris N. Koutsopoulos
Operations Research Analyst
Volpe National Transportation Systems Center

Ismail Chabini
Assistant Professor
Department of Civil and Environmental Engineering
Massachusetts Institute of Technology

Mithilesh Jha
Research Associate
Center for Transportation Studies
Massachusetts Institute of Technology

Acknowledgments

I acknowledge with deep sense of gratitude the guidance, invaluable advice, and constant inspiration provided by my supervisors Prof. Moshe Ben–Akiva and Dr. Haris Koutsopoulos during the course of my studies. I feel privileged to get the opportunity to work with them for the last five years. I have learned a lot from them during the course of this research.

I am grateful to the other members of my dissertation committee—Prof. Ismail Chabini and Dr. Mithilesh Jha, for their advice, feed back, and inspiration during the course of this research.

My special thanks goes to the following individuals without whose contribution this thesis could not be completed: Dr. Qi Yang, Dr. Kalidas Ashok, Prof. Rabi Mishalani, Prof. Michel Bierlaire, Alan Chachich, Dave Cuneo, Masroor Hasan, Dr. Owen Chen, Russel Spieler, Tania Amin, Khwaja Ehsan, Shahnaz Islam, and Prof. Shafiqul Islam.

I am also thankful to the CA/T project at the ITS Research Program for financially supporting my five years of studies at MIT.

I would like to thank my friends, fellow students, and administrative staff at the CEE Department, CTS, and ITS Office, that made my life at MIT an enjoyable experience, especially, Adriana, Amalia, Andras, Atul, Bruno, Cheryl, Chris, Cynthia, Denise, Didier, Dinesh, Dale, Deiki, Dong, Hari, Hong, Jeff, Jessei, John, Jon, Joan, Juli, Krishna, Lisa, Mark, Masih, Nagi, Niranjan, Pat, Paula, Peter, Prodyut Da, Shenoi, Scott, Sreeram, Sridevi, Sudhir, Susan, Tomer, Winston, and Yan.

Thanks are due to fellow Bangladeshis Adnan, Fahria and Zeeshan, Minu and Monjur, Oni and Arif, Rima, Rita and Mukul, Rumi and Saquib, Sabah and Mahmood, and Shampa and Sabet, for their friendship and support.

Finally, I wish I knew a better way to express my indebtedness to my wife, Lubna, my three year old son, Sabih, for their unconditional support, endless love, to my parents for their encouragement and inspiration throughout my life that helped me outgrow again and again.

Contents

List of Figures

List of Tables

Chapter 1

Introduction

1.1 The Problem

Traffic congestion in and around the urban areas of the world is a major problem. Congestion during peak hours extends for longer periods each day. Congestion adversely affects mobility, safety, and air quality. These cause direct economic losses due to delays and accidents, and indirect economic losses due to environmental impact. In most cases, the capacity of the existing roadway systems cannot be increased by adding additional lanes due to space, resource, or environmental constraints. Potential ways to address the congestion problem are to improve the utilization of the existing systems through better traffic management and operations strategies, and improve the geometric design of roads and highways.

Traffic operations in the congested sections of roadways is very complex, since different drivers employ different techniques to travel through such sections while interacting with other drivers. To understand the occurrence of bottlenecks and to devise solutions for it, a comprehensive analysis of vehicle to vehicle interactions is essential. This requires the development of traffic theories to explain driver behavior at the microscopic level, the main elements of which are the acceleration and lane changing dimensions.

Drivers' acceleration behavior, when they are in the car–following regime, has been studied extensively since the 1950s. In this regime, drivers are assumed to

follow their leaders. However, estimation of these models using microscopic data, for example, speed of a subject and its leader, gap length, acceleration applied by the subject, collected from real traffic has not received much attention. On the other hand, researchers started paying attention to the acceleration behavior in the free–flow regime beginning early 1980s. In the free–flow regime, drivers are not close to their leaders and therefore, have the freedom to attain their desired speed. The parameters of the general acceleration model, that captures drivers' acceleration decision in both the car–following and free–flow regimes, have not been estimated.

The principal focus of research in modeling drivers' lane changing behavior has been on modeling the gap acceptance behavior at stop controlled T–intersections. The gap acceptance phase is a part of the lane changing process. Researchers started paying attention to the lane changing model as microscopic traffic simulation emerged as an important tool for studying traffic behavior and developing and evaluating different traffic control and management strategies. However, the existing lane changing models are rule–based and do not explicitly capture variability within driver and between drivers. Furthermore, the model parameters have not been estimated formally.

In this thesis, we present a comprehensive framework for modeling drivers' acceleration and lane changing behavior. This includes enhancing existing models, developing new ones, providing framework for model estimation, and finally, estimating the models using statistically rigorous method and microscopic data collected from real traffic.

1.2 Motivation

Research in Intelligent Transportation Systems (ITS) is being performed to develop traffic management and operations strategies to deal with problems associated with congestion. The number of strategies needed to be tested for a transportation system may be large and field testing would be prohibitively expensive. For this purpose, 'microscopic traffic simulation' is a suitable tool. An important element of a traffic simulator is the set of driver behavior models that is used to move vehicles in the

network. This includes the acceleration[1] and lane changing models. Reliability of simulation results depends heavily on these underlying driver behavior models.

Near on– and off–ramps or weaving sections, drivers often change to the lanes that are connected to their destinations. These areas are potential locations for bottleneck formation when the fraction of drivers trying to change lanes is high. Lane changing operations are critical in selecting geometric configuration of such areas (AASHTO 1990). Drivers' lane changing behavior has direct influence on the capacity and safety of such areas (HCM 1985). Therefore, a detailed understanding of drivers lane changing behavior is necessary.

Traffic engineers use the mean of the minimum acceptable gap length at intersections to estimate the capacities of and delays at intersections and pedestrian crossings. Therefore, the mean has to be estimated as accurately as possible; this requires a thorough understanding of the gap acceptance process. Gap acceptance behavior also affects the design of the length of an acceleration lane which is an important design element from capacity and safety perspectives.

Microscopic driver behavior models play a very important role in the analysis of traffic flow characteristics in the presence of ITS technologies, such as lane use sign, variable message signs, traffic control, and route guidance. Macroscopic speed–flow–density relationship assumes homogeneous speed and density for a given freeway segment and treats capacity as an exogenous parameter. In the presence of ITS technologies, these assumptions may not be realistic (Yang 1993). Capacity can be influenced not only by drivers' acceleration pattern, but also by the number of lane changes taking place. A better understanding of driver acceleration and lane changing behavior is, therefore, essential to model the impact of the ITS Technologies on the traffic flow relationships.

Rear–end collision accounted for 2.2 million automobile crashes in 1990, which was 19% of the total number of crashes in the US in that year (NSC 1992). NSC (1992) also reported that nearly half of these crashes were due to drivers following their leaders too closely. In such cases, drivers are not able to decelerate fast enough

[1]Acceleration refers to both acceleration and deceleration unless deceleration is mentioned.

when their leaders decelerate at unexpectedly high rates. Studying safety in the car–following situations is, therefore, very important to the design of an Automated Highway Systems and Intelligent Cruise Control (Chen 1996). To evaluate safety in car–following situations, a detailed understanding of drivers car–following behavior and braking reaction time is required.

In conclusion, there is a need for improving the current understanding of drivers' acceleration and lane changing behavior at a microscopic level.

1.3 Thesis Objectives

The main objective of this thesis is to advance the state of the art in modeling drivers' acceleration and lane changing behavior. The models need to be estimated using real driver data and have to be assessed from statistical and behavioral standpoints.

The acceleration model should capture drivers acceleration behavior in both the car–following and free–flow regimes. In the car–following regime, drivers follow their leaders and try to match their leaders' speed, whereas, in the free–flow regime, they try to attain their desired speed. The headway threshold, that is used to determine the regime a driver belongs to, should be modeled as a random variable to capture variability between drivers. In addition, the reaction time (or the time lag of response to stimulus) should be modeled to be sensitive to the traffic conditions. Furthermore, the sensitivity of different factors on the car–following acceleration and deceleration decisions may not be same, different set of parameters should be allowed while estimating the models.

Modeling a lane changing decision process is very complex due to its latent nature and the number of factors a driver considers before reaching a decision. The only observable part is a successful lane change operation. The exact time at which a driver decides to change lanes cannot be observed except in a few specialized situations, for example, turning left/right at an intersection. In addition, the influence of past lane changes, such as time elapsed since the most recent lane change, on the current lane changing behavior further complicates the modeling of such a process. Therefore, the

modeling effort should find a balance between simplicity in modeling and representing reality.

1.4 Thesis Contributions

This thesis advances the state of the art in modeling drivers' acceleration and lane changing behavior. It enhances the existing models and develops new ones. Another major contribution of this thesis is the empirical work, i.e., estimating the models using statistically rigorous methods and microscopic data collected from real traffic. More specifically,

- Contribution to the modeling framework:
  - The car–following model, which captures drivers' acceleration behavior when they are following their leader, is extended by assuming that the stimulus is a nonlinear function of the lead relative speed and capturing the impact of traffic conditions ahead of the driver. These are significant improvements over the existing models that restrict the impact of the lead relative speed (the stimulant) on the acceleration response to be linear and do not model the impact of traffic conditions ahead of the driver except for the position and speed of the leader.
  - The existing models restricts the lead relative speed (the stimulant) and other factors (such as subject speed, gap in front of the subject) that affect the acceleration decision to be observed at the same time. This corresponds to an assumption that drivers base their decisions on the traffic environment at the time they were stimulated into action. We relax this assumption by allowing drivers to update their perception of the traffic environment during the decision making process.
  - A headway threshold distribution is introduced that allows any driver behavior to be captured (aggressive or conservative). The headway threshold

defines whether a driver is following its leader or trying to attain its desired speed.

  - An individual driver specific reaction time is introduced which is allowed to be sensitive to the traffic situations under consideration.
  - A probabilistic lane changing model is developed that captures drivers' lane changing behavior under both the mandatory and discretionary lane changing situations. This is a significant improvement over the existing deterministic rule–based lane changing models.
  - The proposed lane changing model allows for different gap acceptance model parameters for mandatory and discretionary lane changing situations. It also captures the variability within driver and between drivers in the lane changing decision process.
  - A forced merging model is proposed that captures merging in heavily congested traffic by gap creation either through force or through courtesy yielding.

- Contribution to model estimation:

  - A methodology to estimate instantaneous speed and acceleration (that is required for model estimation) from discrete trajectory data (that can be obtained from real traffic) is developed.
  - All the components of the acceleration model are estimated jointly using real microscopic traffic data. The component models are the car–following acceleration and deceleration models, the free–flow acceleration model, and the headway threshold and reaction time distributions. Estimation results demonstrate the robustness of the modeling framework.
  - Separate car–following model parameters under acceleration and deceleration situations are allowed in the estimation. This captures the fact that, the sensitivity of different factors on drivers' acceleration behavior may not be same under these two situations.

- Separate gap acceptance models for the mandatory and discretionary lane changing situations are estimated.
- The proposed lane changing model and the forced merging model are estimated using the maximum likelihood estimation method.

1.5 Thesis Outline

In Chapter 2, a literature review of the existing acceleration and lane changing models is presented. The acceleration and the lane changing models are presented in chapters 3 and 4 respectively. In Chapter 5, data needs of this research is presented. First, a methodology to estimate instantaneous speed and acceleration from discrete trajectory data is presented. Then, the data source and the data extracted from this source to estimate different driver behavior models are presented. Estimation results of all the models described in chapters 3 and 4 are presented in Chapter 6. In Chapter 7, validation of the acceleration model and a part of the lane changing model, using a microscopic traffic simulator, is presented. Conclusions and directions for future research are presented in Chapter 8.

Chapter 2

Literature Review

In this chapter, a literature review of the acceleration and lane changing models is presented. Findings from this review are summarized at the end of the chapter.

2.1 Acceleration Models

The models capturing drivers' acceleration behavior can be classified as:

- Car–following models,
- General acceleration models.

The car–following models capture acceleration behavior in the car–following regime. In this regime, the drivers are close to their leaders and follow their leaders (see Figure 2-1). The general acceleration models capture acceleration behavior in both

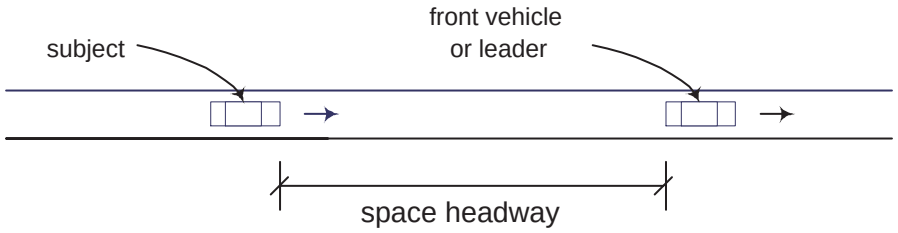

Figure 2-1: The subject and the front vehicle.

the car–following and free–flow regimes. In the free–flow regime, drivers are not close to their leaders and therefore, have the freedom to attain their desired speed.

Drivers' acceleration behavior, when they are in the car–following regime, has been studied extensively since the 1950s. Estimation of these models using microscopic data, for example, speed of a subject and its leader, gap length, acceleration applied by the subject, has not received much attention. Simple correlation analysis was used to estimate the models in most cases.

Researchers started paying attention to the acceleration behavior in the free–flow regime in the early 1980s as microscopic simulation emerged as an important tool for studying traffic behavior and developing and evaluating different traffic control and management strategies. However, the parameters of a general acceleration model, that captures drivers' acceleration behavior in both the car–following and free–flow regimes, have not been estimated.

Previous research on each of these categories and the estimation of the brake reaction time is presented next.

2.1.1 Car–Following Models

The general form of the car–following models developed in the late 1950s is as follows:

$$response_n(t) = sensitivity_n(t - \tau_n) \ \times \ stimulus_n(t - \tau_n) \tag{2.1}$$

where,

$$\begin{aligned} t &= \text{time of observation,} \\ \tau_n &= \text{reaction time for driver } n, \\ response_n(t) &= \text{acceleration applied at time } t. \end{aligned}$$

The reaction time, τ_n, includes the perception time (time from the presentation of the stimulus until the foot starts to move) and the foot movement time. The front

relative speed[1] (see Figure 2-1) is generally considered as the stimulus and sensitivity is a proportionality factor that may be a function of factors such as subject speed, space headway.

Chandler et al. (1958) developed the first car–following model that is a simple linear model. Mathematically, the model can be expressed as

$$a_n(t) = \alpha \; \Delta V_n^{front}(t - \tau_n) \tag{2.2}$$

where,

$$\begin{aligned}
a_n(t) &= \text{acceleration applied by driver } n \text{ at time } t, \\
\alpha &= \text{constant}, \\
\Delta V_n^{front}(t - \tau_n) &= [V_n^{front}(t - \tau_n) - V_n(t - \tau_n)] : \text{stimulus}, \\
V_n(t - \tau_n) &= \text{subject speed at time } (t - \tau_n), \\
V_n^{front}(t - \tau_n) &= \text{leader or front vehicle speed at time } (t - \tau_n).
\end{aligned}$$

A driver responds to the stimulus at time $(t - \tau_n)$ by applying acceleration at time t. The same sensitivity terms are used for both the acceleration and deceleration situations. They estimated the model using the correlation analysis method and microscopic car–following data. The data was collected from a sample of 8 drivers driving test vehicles in a two lane two way road in real traffic for 20 to 30 minutes. For each driver, the data included discrete measurements of the acceleration, speed, space headway, and relative speed over the time of observation. For different values of τ and α, correlations between the observed and the estimated accelerations were computed. The values of τ and α that yielded the highest correlation were used as the estimates of τ and α for each driver. The estimated τ and α averaged over all samples were 1.5 seconds and 0.37 second^{-1} respectively.

A major limitation of the above model is the assumption of a constant sensitivity

[1] In this thesis, relative speed with respect to another vehicle is defined as the speed of that vehicle less the speed of the subject.

for all situations. Gazis et al. (1959) address it by incorporating the space headway (see Figure 2-1) between the two vehicles in the sensitivity term. Their model is as follows:

$$a_n(t) = \frac{\alpha}{\Delta X_n(t-\tau_n)} \Delta V_n^{front}(t-\tau_n) \tag{2.3}$$

where, $\Delta X_n(t-\tau_n)$ denotes the space headway at time $(t-\tau_n)$. The model was estimated using microscopic data collected from the car–following experiments in the Holland Tunnel and the Lincoln Tunnel in New York and at the General Motors test track. The parameters α and τ were estimated for each driver of each data set using correlation analysis. For each data set, the values of the parameters averaged over all samples were reported as the estimates. Table 2.1 summarizes the estimation results.

Table 2.1: Estimation results of the model developed by Gazis et al. (1959).

Data collection site	Number of drivers	α (mph)	τ (second)
GM Test Track	8	27.4	1.5
Holland Tunnel	10	18.3	1.4
Lincoln Tunnel	16	20.3	1.2

The mean reaction time measured at the test track varied from 1.0 to 2.2 seconds.

Edie (1961) pointed out that, the model given by Equation 2.3 suffers from two limitations. First, from a behavioral standpoint, the follow–the–leader theory is not applicable at low densities. Second, the macroscopic speed–density relationship derived from Equation 2.3 yields infinite speed as the density approaches zero. Define,

u = speed of a stream of traffic at density k,

c = integration constant,

k_j = jam density.

Assuming that traffic is in a steady–state and ignoring the reaction time, integrating

both sides of Equation 2.3 yields:

$$\begin{aligned} \int a\ dt &= \int \frac{\alpha}{\Delta X}\Delta V\ dt \\ \Rightarrow u &= c + \alpha\ \ln\left(\Delta X\right) \\ \Rightarrow u &= c + \alpha\ \ln\left(\frac{1}{k}\right) \\ \text{at } k = k_j, u = 0 &\Rightarrow c = \alpha\ \ln(k_j) \\ \Rightarrow u &= \alpha\ \ln\left(\frac{k_j}{k}\right) \end{aligned} \tag{2.4}$$

In this equation, α corresponds the stream speed at maximum flow. This equation is the macroscopic speed–density relationship developed by Greenberg (1959). It does not yield free–flow speed at zero density.

Edie addressed the above mentioned limitations by changing the sensitivity term and the model is as follows:

$$a_n(t) = \alpha \frac{V_n(t-\tau_n)}{\Delta X_n(t-\tau_n)^2}\ \ \Delta V_n^{front}(t-\tau_n) \tag{2.5}$$

Sensitivity is now proportional to the speed and inversely proportional to the square of the headway. Equation 2.5 can be integrated (as was done to obtain the model given by Equation 2.4) to obtain a model that yields free-flow speed as the density approaches zero. This model performed better than the model proposed by Gazis et al. (1959) at low densities. However, the stimulus term is still a function of the front relative speed, which is not realistic at low densities, in particular, when the headways are high.

Instead of using the sensitivity–stimulus formulation to explain the car–following acceleration decision, Newell (1961) suggested the following relationship between the speed and the headway:

$$V_n(t) = G_n\ \Delta X_n(t-\tau_n) \tag{2.6}$$

where, G_n is a function whose form determines the specification of the car–following models that are presented above. Different forms of G_n were assumed for the acceleration and deceleration decisions. Although, the model had the advantage of integrability to obtain different macroscopic speed–flow–density relationships, no attempt was reported to obtain a quantitative result to validate the model.

The car–following model developed by Gazis et al. (1961), known as the *General Motors Nonlinear Model*, is the most general one. The model is given by:

$$a_n(t) = \alpha \ \frac{V_n(t)^{\beta}}{\Delta X_n(t-\tau_n)^{\gamma}} \ \ \Delta V_n^{front}(t-\tau_n) \tag{2.7}$$

where, α, β, and γ are model parameters. The sensitivity is proportional to the speed raised to the power β and inversely proportional to the headway raised to the power γ. The parameter α is a constant and the front relative speed is the stimulus. The models developed earlier by Chandler et al. (1958)and Gazis et al. (1959) can be derived from this model as special cases. It should be mentioned that the macroscopic flow–speed relationship developed by Greenshields (1934) can be derived from the GM Model by setting $\beta = 0$ and $\gamma = 2$. No rigorous framework for estimating the model was provided.

Bexelius (1968) suggested that instead of following only the immediate leader, drivers in a car–following situation also follow the vehicles ahead of the leader. Mathematically, the model is given by:

$$a_n(t) = \sum_{i=1}^{N} \lambda_i \ \ (V_n^i(t-\tau_n) - V_n(t-\tau_n)) \tag{2.8}$$

where, λ_i and $V_n^i(t-\tau_n)$ are the sensitivity and speed associated with the i-th front vehicle and N is the number of drivers. However, the model was not estimated and validated.

May and Keller (1967) estimated the GM Model (Equation 2.7) using a macroscopic relationship between speed and density that was derived by Gazis et al. (1961). In addition to using integer values of β and γ, May and Keller (1967) also used non–

integer values and found higher correlation coefficients for the non–integer cases. The estimated parameters are presented in Table 2.2. Since they used a macroscopic relationship between speed and density, reaction time could not be identified.

Table 2.2: Estimation results of the GM Model by May and Keller (1967).

Parameter	Estimates with integer β and γ	Estimates with non–integer β and γ
α	1.35×10^{-4}	1.33×10^{-4}
β	1.0	0.8
γ	3.0	2.8
free speed (u_f), mph	48.7	50.1
jam density (k_j), vpm	∞	220
optimum speed, mph	29.5	29.6
optimum density (k_o), vpm	60.8	61.1
maximum flow, vph	1795	1810
macroscopic model	$u = u_f\ e^{-0.5(k/k_o)^2}$	$u = u_f\ \left(1 - \left(\frac{k}{k_j}\right)^{1.8}\right)^5$

Leutzbach (1968) proposed a *psycho–physical spacing model* that addresses two limitations of the car–following models from a behavioral standpoint. First, drivers do not follow their leaders at large spacings, and second, drivers cannot perceive small differences in front relative speeds and therefore, do not react to such differences. Leutzbach introduced the term "perceptual threshold" to define a relative speed threshold which is a function of the space headway. The threshold is smaller at low space headways and gradually increases with space headway. A driver reacts to the stimulus, the front relative speed, only when the stimulus exceeds the perceptual threshold. At a certain large space headway, the threshold becomes infinity, i.e., a driver no longer follows its leader beyond that space headway. An important finding of his research is that the perceptual threshold for negative relative speed is smaller than that for positive relative speed. This implies that the sensitivity of spacing and front relative speed on drivers' acceleration and deceleration decisions are different. Leutzbach, however, did not provide any mathematical formulation of the proposed model, nor provided any direction as to how the perceptual threshold can be estimated.

Recently, Ozaki (1993) estimated the GM Model (Equation 2.7) parameters. He used regression analysis to estimate a model for drivers' reaction time and correlation analysis to estimate parameters α, β and γ.

Ozaki listed four actions to identify reaction time. Figure 2-2 shows the definition of reaction time corresponding to these actions. The actions are:

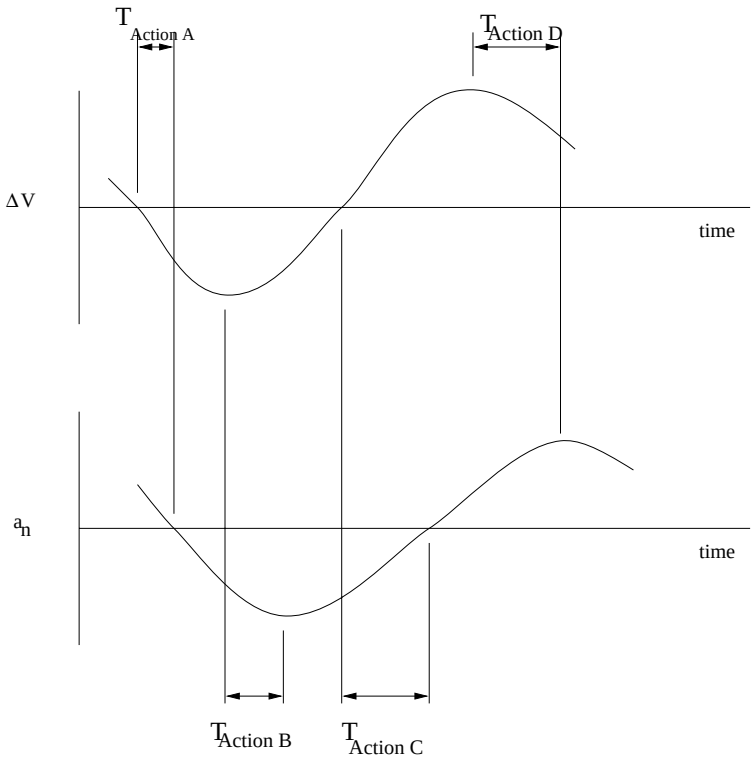

Figure 2-2: Definition of reaction time corresponding to the four actions (source: Ozaki, 1993).

Action A start of deceleration: time elapsed since the relative speed became zero and the subject, who was accelerating at that instant of time, started decelerating;

Action B maximum deceleration: time elapsed since the relative speed reached its minimum value (negative) and the subject applied the maximum deceleration;

Action C start of acceleration: time elapsed since the relative speed became zero and the subject, who was decelerating at that instant of time, started accelerating;

Action D maximum acceleration: time elapsed since the relative speed reached its maximum value (positive) and the subject applied the maximum acceleration.

These definitions of reaction time are not consistent with those suggested by earlier car–following model researchers and the Traffic Engineering Literature (Gerlough and Huber 1975). These researchers defined the reaction time as the summation of perception and foot movement times. Depending on the deceleration capability of a vehicle, its driver may start reacting at different times. For example, a driver driving a vehicle with powerful brakes may not decelerate, even after realizing that its leader is slower, until the driver gets very close. This does not imply that the driver's reaction time is larger as suggested by Ozaki. He, however, made an important observation: traffic conditions, such as the headway and the acceleration of the leader, influence the reaction time.

To estimate the car–following model parameters, he first identified the reaction time using the definition of reaction time for different actions listed above. Then, the correlation between the observed acceleration and estimated acceleration (obtained by using the explanatory variables lagged by the reaction time and setting the car–following model parameters to present numbers) was calculated for different values of the parameters. The combination that yielded the maximum correlation was reported as the estimates.

Ozaki assumed a different set of parameters for the acceleration and the deceleration decisions; this captures the fact that different factors, such as subject speed, front relative speed, and headway, may not have the same impact on driver's acceleration and deceleration decisions. The parameters α, β and γ were estimated to be 1.1, -0.2, and 0.2 respectively for the acceleration model, and 1.1, 0.9, and 1.0 respectively for the deceleration model.

Aycin and Benekohal (1998) developed a car–following model which estimates the acceleration rate at any instant of time. Acceleration for the next time instant is then computed by adding the product of the acceleration rate estimate and the time difference to the current acceleration. This guarantees continuity in the acceleration profile for a given driver. Equations of laws of motion are used to compute the

acceleration rate required for a driver to attain its leader's speed while maintaining a *preferred time headway*. The *preferred time headway* is defined as a headway the driver wants to maintain under steady–state car–following conditions. For each driver in the car–following data set that traveled at speeds within ±5 ft/sec of its leader's speed, the discrete time headways measurements over time were averaged. Then, the average was taken as the driver's *preferred time headway*. The *preferred time headway* values ranged from 1.1 to 1.9 seconds with a mean of 1.47 seconds. The effect of reaction time is explicitly modeled. According to this model, drivers are assumed to be in the car–following regime if the clear gap (see Figure 2-1) is less than 250 feet. This rule ignores variability between drivers. The reaction time was not estimated using a rigorous method. It was assumed to be 80% of the estimated *preferred time headway*.

2.1.2 General Acceleration Models

The models presented above apply to the car–following regime only. When the headways are large, drivers do not follow their leader, instead they try to attain their desired speeds. Developing an appropriate acceleration model for the free–flow regime is important for microscopic simulation models.

Gipps (1981) developed the first general car–following model that is applicable to both the car–following and free–flow regimes. This model calculates a maximum acceleration for a driver such that the speed would not exceed a desired speed, and the clear gap would be at least a minimum safe distance. Mechanical limitations of vehicles were captured by using the parameters maximum acceleration and most severe deceleration. Equations of laws of motion were used in the above computations. The parameters of the models were not estimated rigorously and the reaction time was set arbitrarily for all drivers.

Benekohal and Treiterer (1988) developed a car–following simulation model, called CARSIM, to simulate traffic in both normal and stop–and–go conditions. The acceleration for a vehicle is calculated for five different situations and the most binding acceleration is used to update the vehicle's speed and position. These situations are

- the subject (i.e., the following vehicle) is moving but has not reached its desired speed;
- the subject has reached its desired speed;
- the subject was stopped and starts from a standstill position;
- the subject's movement is governed by the car–following algorithm in which a space headway constraint is satisfied; and,
- the subject is advancing according to the car–following algorithm with a non–collision constraint.

Equations of laws of motion are used in the above computations. In addition, a comfortable and a maximum allowable deceleration are assumed to limit the output from the acceleration models within a reasonable boundary. The reaction times of drivers are randomly generated, and shorter reaction times are assigned at higher densities. No rigorous framework for parameter estimation was presented and the reaction time distribution parameters were adopted from Johansson and Rumer (1971) which is presented in Section 2.1.3.

Yang and Koutsopoulos (1996) developed a general acceleration model that is used in MITSIM, a microscopic traffic simulator. Based on headway, a driver is assigned to one of the three following regimes:

- the emergency regime, if the current headway is less than a lower threshold;
- the car–following regime, if the current headway is greater than the lower threshold but less than an upper threshold; and finally,
- the free–flow regime, if the current headway is greater than the upper threshold.

In the emergency regime, a driver applies the necessary deceleration to avoid colliding with its leader and increase headway. The *GM Model* (Equation 2.7) is used to determine the acceleration rate in the car–following regime. Different set of parameters are used for positive and negative relative speed cases. In the free–flow regime, a driver

tries to attain its desired speed by applying a maximum acceleration if the current speed is less than the desired speed or a normal deceleration otherwise. The model parameters were not estimated using field data.

Subramanian (1996) developed a general acceleration model that captures drivers' acceleration behavior in both the car–following and free–flow regimes. A space headway threshold distribution was assumed that determines which regime a driver is in at any instant of time. In the car–following regime, drivers are assumed to follow their leader, and in the free–flow regime, they are assumed to try to attain their desired speed. He, however, estimated only the car–following model parameters using data that was collected in 1983 from a section of Interstate 10 Westbound near Los Angeles (Smith 1985).

His specification of the car–following model is an extension of the *GM Model* (Equation 2.7) and is given by:

$$a_n(t) = \alpha \frac{V_n(t-\tau_n)^{\beta}}{\Delta X_n(t-\tau_n)^{\gamma}} \Delta V_n^{front}(t-\tau_n) + \epsilon_n^{cf}(t) \tag{2.9}$$

where, $\epsilon_n^{cf}(t)$ is the random term associated with driver n at time t. He modeled the reaction time as a random variable to capture the variability within driver and between drivers. Variables $\epsilon_n^{cf}(t)$ and τ_n are assumed to be distributed normal and truncated lognormal respectively.

He estimated separate models for acceleration and deceleration observations. The estimation results are presented in Table 2.3. The estimated mean reaction time was larger than those reported by Johansson and Rumer (1971) and Lerner et al. (1995), and the mean reaction time estimate for the deceleration decision was higher than that for the acceleration decision—a counter intuitive result. He also estimated the *GM Model* using different headway thresholds and concluded that the headway threshold has significant impact on the parameter estimates.

Table 2.3: Estimation results of the GM Model by Subramanian (1996).

parameter	Model for acceleration estimate	Model for deceleration estimate
α	9.21	15.24
β	-1.67	1.09
γ	-0.88	1.66
std. dev(ϵ^{cf})	0.780	0.632
mean(τ), sec.	1.97	2.29
std. dev(τ)	1.38	1.42

Note: acceleration in ft/sec^2, speed in ft/sec, space in feet.

2.1.3 Estimation of the Brake Reaction Time

In this section, we present the studies that were conducted to obtain the brake reaction time of drivers driving in real traffic.

Johansson and Rumer (1971) estimated the distribution of the brake reaction time from a sample of 321 drivers traveling in a real traffic. The subjects were instructed to apply the brake pedal as soon as they hear a sound. The time elapsed from the moment the sounds were made to the moment the drivers' brake light turned on were recorded as the brake reaction time. The brake reaction time varied from 0.4 to 2.7 seconds with a median, mean, and standard deviation of 0.89, 1.01, and 0.37 seconds respectively and a 90 percentile value of 1.5 seconds. These numbers may be biased downwards, since the sound, to which the drivers reacted, might have reduced the perception time, and hence the reaction time.

Recently, Lerner et al. (1995) estimated the reaction time distribution from a sample of 56 drivers driving in real traffic. To estimate the brake reaction time for unexpected situations (to mimic real driving conditions), subjects were not informed that they were participating in a brake reaction time study. When a subject reached the test site at 40 mph speed, a large yellow highway crash barrel was released approximately 200 ft in front of the vehicle. The barrel was chained so that it was held within the median. The time elapsed since a barrel is released to the instant a driver

applies brake was recorded as the driver's reaction time. The brake reaction time varied from 0.7 to 2.5 seconds with a median, mean, and standard deviation of 1.44, 1.51, and 0.39 seconds respectively.

2.2 Lane Changing Models

In this section, a literature review of the lane changing models is presented followed by a literature review of the gap acceptance models.

The principal focus of research in modeling drivers' lane changing behavior has been on modeling the gap acceptance behavior at stop controlled T–intersections. The gap acceptance phase is a part of the lane changing process.

Gipps (1986) presented a lane changing decision model to be used in a microscopic traffic simulator. The model was designed to cover various urban driving situations where traffic signals, obstructions, and the presence of heavy vehicles (for example, bus, truck, semi–trailer) affect a driver's lane selection decision. Three major factors were considered in the lane changing decision process: necessity, desirability, and safety. Different driving conditions were examined including the ones where a driver may face conflicting goals. However, different goals were prioritized deterministically, and inconsistency and non–homogeneity in driver behavior were not modeled. The terms inconsistency implies that a driver may behave differently under identical conditions at different times, while the term non–homogeneity implies that different drivers behave differently under identical conditions. The model parameters were not estimated formally.

CORSIM (FHWA 1998) is a microscopic traffic simulator that uses FREESIM to simulate freeways and NETSIM to simulate urban streets. In CORSIM, a lane change is classified as either mandatory (MLC) or discretionary (DLC). A driver performs an MLC when the driver must leave the current lane and performs a DLC when the driver perceives the driving conditions in the target lane to be better, but, a lane change is not required. The necessity or desirability of changing lanes is determined by computing a risk factor that is acceptable to a driver which is a function of a

driver's position relative to the object that gives rise to the need for a lane change. A default set of model parameters are provided with the flexibility of using user provided parameters. The gap acceptance behavior is not modeled in a systematic manner. Minimum gap lengths for different situations are listed and all drivers are assumed to have identical gap acceptance behavior.

Yang and Koutsopoulos (1996) developed a rule–based lane changing model that is applicable only for freeways. Their model is implemented in MITSIM. A lane change is classified as either mandatory (MLC) or discretionary (DLC). Unlike Gipps (1986), they used a probabilistic framework to model drivers' lane change behavior when they face conflicting goals. A driver considers a discretionary lane change only when the speed of the leader is below a desired speed, and checks neighboring lanes for opportunities to increase speed. Two parameters, impatience factor and speed indifference factor, were used to determine whether the current speed is low enough and the speeds of the other lanes are high enough to consider a DLC. They also developed a gap acceptance model that captures the fact that the critical gap length (defined as the minimum acceptable gap length) under an MLC situation is lower than that under a DLC situation. They pointed out that, for a case of merging into a traffic parallel to the current lane, a gap is acceptable only when both the lead and lag gaps are acceptable. However, no formal parameter estimation was done and a framework to do so was not developed.

Recently, Ahmed et al. (1996) developed a framework for a general lane changing model that captures lane changing behavior under both the MLC and DLC situations. Lane change is modeled as a sequence of four steps: decision to consider a lane change, choice of a target lane, acceptance of gaps in the target lane, and performing the lane change maneuver. A discrete choice framework is used to model these decision elements that allows for modeling impact of different traffic and roadway environment on driver behavior. From a model estimation view point, the utilities capturing the first and the fourth steps cannot be uniquely identified in the absence of any indicator available to the analyst differentiating these two steps. They estimated parameters of the model only for a special case: merging from a freeway on–ramp. They used

the data collected in 1983 from a site at Interstate 95 northbound near the Baltimore Washington Parkway (Smith 1985).

In this case, it was assumed that drivers have already decided to change to the adjacent freeway and therefore, the decision process involved acceptance of a gap and the actual lane change maneuver. Following Yang and Koutsopoulos (1996), a gap is considered acceptable only when both the lead and lag gaps are acceptable. Figure 2-3 shows the definition of the lead and lag gaps. The lead and lag critical

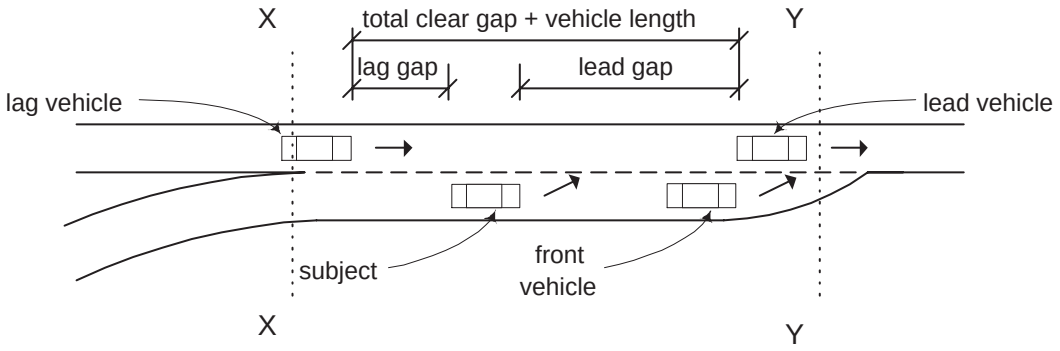

Figure 2-3: The subject, lead, lag, and front vehicles, and the lead and lag gaps.

gap lengths were assumed to be lognormally distributed and whether a lane change will take place immediately, given the gap is acceptable, was modeled using a binary logit model.

The estimated lead critical gap for driver n at time t is

$$G_n^{cr,lead}(t) = \exp[2.72 - 0.055\ \nu_n + \epsilon_n^{lead}(t)] \tag{2.10}$$

where,

$G_n^{cr,lead}(t)$ = lead critical gap (feet),

ν_n = driver specific random term that is constant for a given driver, assumed distributed standard normal,

$\epsilon_n^{lead}(t)$ = random term that varies across different components of a gap for a given driver, across different gaps for a given individual,

as well as across drivers, $\epsilon_n^{lead}(t) \sim \mathcal{N}(0, 1.61^2)$.

The estimated lag critical gap for driver n at time t is

$$G_n^{cr,lag}(t) = \exp[-9.32 + 0.1170 \min(\Delta V_n^{lag}(t), 10) + 0.1174 \max(\Delta V_n^{lag}(t) - 10, 0) + 1.57 \delta_n^{1stGap}(t) + 1.88 \ln(L_n^{rem}(t)) + 1.90 \nu_n + \epsilon_n^{lag}(t)] \quad (2.11)$$

where,

$$\begin{aligned}
G_n^{cr,lag}(t) &= \text{lag critical gap (feet)}, \\
\Delta V_n^{lag}(t) &= \text{lag vehicle speed – subject speed (mph)}, \\
\delta_n^{1stGap}(t) &= \begin{cases} 1 & \text{if } delay_n(t) = 0 \\ 0 & \text{otherwise.} \end{cases} \\
delay_n(t) &= \text{time elapsed since } MLC \text{ conditions apply (seconds)}, \\
L_n^{rem}(t) &= \text{remaining distance to the point at which lane change must be completed (feet)}, \\
\epsilon_n^{lag}(t) &\sim \mathcal{N}(0, 1.31^2).
\end{aligned}$$

The estimated model of changing lanes, given that both the lead and lag gaps are acceptable, is:

$$\mathrm{P}_n(change\ lanes\ at\ time t \mid gap\ acc.) = \frac{1}{1 + \exp(1.90 - 0.52\ delay_n(t))} \quad (2.12)$$

The gap acceptance model, however, cannot be applied to a case of forced merging or merging through courtesy yielding. In this case, gaps of acceptable lengths may not exist due to high congestion level, and in order to merge gaps have to be created.

2.2.1 Gap Acceptance Models

Different gap acceptance models were developed in the 1960s and 1970s based on the assumption on the distribution of the critical gap length. Herman and Weiss (1961) assumed the critical gap to be exponentially distributed, Drew et al. (1967) assumed a lognormal distribution, and Miller (1972) assumed a normal distribution. They, however, did not capture the effect of previously rejected gaps on the critical gap.

In general, data collected for estimating gap acceptance models is panel in nature, i.e., it contains one or more observations from each individual. Different observations from a given sample are likely to be correlated which may introduce bias in the parameter estimates. Daganzo (1981) used a probit model formulation appropriate for panel data to estimate the gap acceptance model parameters for drivers merging from the minor leg of a stop controlled T–intersection to the major leg. The critical gap for driver n at time t is assumed to have the following functional form:

$$G_n^{cr}(t) = G_n + \epsilon_n^{cr}(t) \tag{2.13}$$

where,

G_n = component of critical gap attributable to driver n,

$\epsilon_n^{cr}(t)$ = random term that varies across different gaps for a given driver as well as across different drivers.

G_n, and $\epsilon_n^{cr}(t)$ are assumed to be mutually independent. Further, he assumed $G_n \sim \mathcal{N}(G, \sigma_G^2)$ and $\epsilon_n^{cr}(t) \sim \mathcal{N}(0, \sigma_\epsilon^2)$. The individual specific random term, G_n, captures the correlation between different observations from driver n. The model has the flexibility to incorporate the impact of other factors on a driver's gap acceptance behavior by varying the mean of the distribution of G_n. However, he had estimability problems and the estimated critical gap lengths were not guaranteed to be non–negative.

Mahmassani and Sheffi (1981) used the data that Daganzo (1981) used and ad-

dressed the estimability problem by ignoring panel data formulation, i.e., they treated the data as cross–sectional data. They assumed the critical gap to be normally distributed. The mean of the critical gap was allowed to be a function of explanatory variables, a framework that allows for incorporating the impact of different factors on a driver's gap acceptance behavior. The variable *number of gaps rejected*, capturing the impatience factor, was found to have a significant impact on drivers gap acceptance behavior.

The Highway Capacity Manual (HCM 1985), or HCM, uses the mean critical gap length of drivers at an intersection to estimate the delay at and the capacity of that intersection. The HCM defined the critical gap for a two–way stop controlled intersection as the median of all acceptable gap lengths. A major limitation of this definition is that an observation of a large gap accepted by a driver provides no information about the minimum acceptable gap length. In the revised HCM procedure, the critical gap is defined as the largest observed rejected gap length. This definition is again flawed, since one very conservative driver can greatly increase the estimate. In addition, Cassidy et al. (1995) listed other deficiencies of this approach. First, only a subset of the data is used and all accepted gaps shorter than the largest one is not included in the estimation. Second, inconsistency in driver behavior (accepting a gap smaller than a previously rejected gap) is addressed either by discarding or by modifying the data. However, the benefit of using the HCM definition of a critical gap is ease in estimation.

Kita (1993) used a logit model to estimate the gap acceptance model for the case of merging from a freeway on–ramp. The impact of different factors on drivers' gap acceptance behavior was modeled by using a random utility model. Although he used panel data, he did not use an appropriate panel data formulation. In addition to the gap length, relative speed of the subject with respect to the mainline vehicles and the remaining distance of the acceleration lane were found to have impact on drivers' gap acceptance behavior.

Cassidy et al. (1995) used Kita's approach to model the gap acceptance behavior at a stop controlled T–intersection. They, too, ignored the panel data formulation

and found that a gap acceptance function with disaggregate factors have significantly more predictive power than a function that includes only the mean gap length.

2.3 Summary

A summary of the findings from the literature review is presented below.

- Modeling acceleration behavior:
  - Primary attention of the research has been on modeling drivers' acceleration behavior in the car–following regime.
  - The impact of stimulus (the front relative speed) on the car–following acceleration was assumed to be linear.
  - The reaction time was modeled but not estimated rigorously in most cases.
  - Variability within driver and between drivers were not captured in most cases.
  - The headway threshold, that determines whether a driver is in the car–following regime or in the free–flow regime, is modeled deterministically in most cases.
  - A general acceleration model was proposed by Subramanian (1996). The model captures acceleration behavior in both the car–following and free–flow regimes. It also captures the inconsistency in driver behavior. A probabilistic framework was used to model variability in headway threshold and reaction time. However, only the car–following part of the model was estimated.
- Modeling lane changing behavior:
  - Modeling drivers' gap acceptance behavior has been the primary focus of the research in modeling drivers' lane changing behavior.

- A majority of the research in modeling drivers' gap acceptance behavior used panel data. However, model formulation appropriate for panel data was not used while estimating the parameters.
- A model capturing drivers' lane change decision process was developed by Ahmed et al. (1996). However, the model is not applicable to mandatory lane changing situations in a heavily congested traffic where gaps of acceptable lengths are hard to find. The parameters of the discretionary lane changing model have not been estimated.
- The impact of an acceleration decision, which determines drivers speed, on the lane changing decision is modeled by using speed as an explanatory variable in the lane changing model.

The acceleration model proposed in this thesis builds on the earlier work by Subramanian (1996) and extends his model. The impact of the stimulus on the car–following acceleration is allowed to be a nonlinear function of the lead relative speed and the sensitivity term is extended to capture the impact of traffic conditions ahead of the subject and its leader. In addition, all the components of the acceleration model are estimated jointly using microscopic data collected from real traffic. On the other hand, the lane changing model proposed in this thesis extends the model proposed by Ahmed et al. (1996) to capture merging behavior in heavily congested traffic and the model is estimated using statistically rigorous methods and real driver data.

Chapter 3

The Acceleration Model

In this chapter, a rigorous framework for estimating the parameters of the acceleration model is presented that builds on the previous work by Subramanian (1996) and extends it. The proposed model consists of two components: the car–following model and the free–flow acceleration model. The car–following model is applied when a driver follows its leader (i.e., the vehicle in front). The free–flow acceleration model is applied when a driver tries to attain its desired speed and is not following its leader.

This chapter starts with a presentation of the conceptual framework and specification of the model. Next, the likelihood function that is necessary for estimating the model is formulated.

3.1 Introduction

Based on a headway threshold, a driver is assumed to be in one of the two following regimes: the car–following regime and the free–flow regime. If the current headway is less than the threshold, the driver is assumed to be in the car–following regime and follow its leader (see Figure 3-1). Speed selection (and hence the acceleration decision) is governed by the speed of the leader. Otherwise, the driver is assumed to be in the free–flow regime in which case speed selection is governed by its desired speed.

The existing car–following models (for example, Gazis et al. (1961), Subramanian

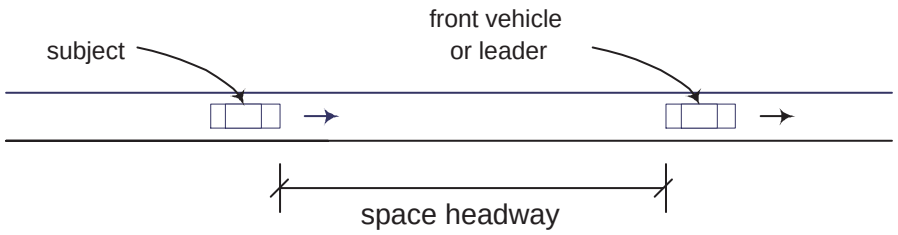

Figure 3-1: The subject and the front vehicle.

(1996)) restrict the stimulus of the acceleration to be a linear function of the front relative speed and do not capture the impact of traffic conditions ahead of the driver except the speed and position of its leader. The front relative speed is defined as the speed of the leader less the subject speed. In this chapter, we use the terms front relative speed and relative speed interchangeably.

In the car–following regime, the sensitivity of different factors, such as speed, headway, and front relative speed, on drivers' acceleration decision under acceleration and deceleration situations may be different. For example, consider two cases: one with a positive relative speed with a certain magnitude and the other with a negative relative speed with the same magnitude, and all other factors are identical. The acceleration in case one is likely to be less than the deceleration (in absolute terms) in case two due to safety concerns involved.

The model proposed in this thesis relaxes the restriction that the car–following stimulus is a linear function of the front relative speed and captures the impact of traffic conditions ahead of the subject on the car–following sensitivity by using as explanatory variable the density ahead of the subject. Separate car–following model parameters under acceleration and deceleration situations are allowed in the estimation.

The model proposed in this thesis, however, does not explicitly capture the impact of lane changing decisions on the acceleration decision. For example, a driver may accelerate or decelerate to fit into a gap in an adjacent lane. Instead, random terms are used in all component models that capture the effect of unobserved factors. This is left as a subject for further research and is discussed in Chapter 8.

3.2 The Acceleration Model

A driver is assumed to be in the car–following regime if the headway is less than a threshold, and in the free–flow regime otherwise. Mathematically, the acceleration model can be expressed as:

$$a_n(t) = \begin{cases} a_n^{cf}(t) & \text{if } h_n(t-\tau_n) \leq h_n^* \\ a_n^{ff}(t) & \text{otherwise} \end{cases} \tag{3.1}$$

where,

$$\begin{aligned} t &= \text{time of observation,} \\ \tau_n &= \text{reaction time of driver } n, \\ a_n(t) &= \text{acceleration at time } t, \\ a_n^{cf}(t) &= \text{car–following acceleration at time } t, \\ a_n^{ff}(t) &= \text{free–flow acceleration at time } t, \\ h_n(t-\tau_n) &= \text{time headway[1] at time } (t-\tau_n), \\ h_n^* &= \text{unobserved headway threshold for driver } n. \end{aligned}$$

Reaction time refers to the delay in a driver's response to a stimulus, or the response lag. It includes both the perception (time from the presentation of the stimulus until the foot starts to move) and foot movement times. Since these two cannot be identified uniquely from the observed data, the term reaction time is used to designate the summation of the two.

We define the headway threshold, h_n^*, in terms of time headway as opposed to space headway for two reasons. First, previous research (for example, Winsum and

[1] Time headway is defined as:

$$h_n(t) = \frac{\Delta X_n(t)}{V_n(t)}, \quad V_n(t) > 0$$

where, $V_n(t)$ and $\Delta X_n(t)$ denote the subject speed and the space headway (see Figure 3-1) at time t respectively. In this research, headway is used to designate time headway unless otherwise mentioned.

Heino (1996), Aycin and Benekohal (1998)) indicates that drivers maintain certain time headways independent of speed in a steady–state car–following situations. And second, equal space headways have identical acceleration regimes (car–following versus free–flow) although speeds may be very different, while the time headway does not suffer from this limitation.

Specification of the car–following and free–flow acceleration models and the distributions of the headway threshold and reaction time are presented next.

3.2.1 The Car–Following Model

Since, it is hypothesized that the expected value of the acceleration distribution is greater than zero when the relative speed is positive, the model corresponding to a positive relative speed is called the car–following acceleration model. Similarly, the model corresponding to a negative relative speed is called the car–following deceleration model. The model can be expressed as follows:

$$a_n^{cf,g}(t) \;=\; s[X_n^{cf,g}(t-\xi\tau_n)] \;\; f[\Delta V_n(t-\tau_n)] + \epsilon_n^{cf,g}(t) \tag{3.2}$$

where,

$$\begin{aligned}
g &\in \{acc, dec\} \\
s[X_n^{cf,g}(t-\xi\tau_n)] &= \text{sensitivity, a function of } X_n^{cf}(t-\xi\tau_n), \\
X_n^{cf,g}(t-\xi\tau_n) &= \text{vector of explanatory variables affecting the car–following} \\
&\quad \text{acceleration sensitivity observed at time } (t-\xi\tau_n), \\
\xi &\in [0,1], \text{ a parameter for sensitivity lag,} \\
f[\Delta V_n(t-\tau_n)] &= \text{stimulus, a function of relative speed, } \Delta V_n(t-\tau_n), \\
\Delta V_n(t-\tau_n) &= \left(V_n^{front}(t-\tau_n) - V_n(t-\tau_n)\right), \\
V_n(t-\tau_n) &= \text{subject speed at time } (t-\tau_n), \\
V_n^{front}(t-\tau_n) &= \text{front vehicle speed at time } (t-\tau_n),
\end{aligned}$$

$\epsilon_n^{cf,g}(t)$ = random term associated with the car–following acceleration of driver n at time t.

The acceleration (or deceleration) applied by driver n at time t is proportional to the stimulus, a function of the front relative speed at time $(t - \tau_n)$. The reaction time, τ_n, varies from driver to driver, and therefore, is modeled as a random variable. The sensitivity term is the proportionality factor, a function of explanatory variables (discussed below) observed $\xi\tau_n$ seconds earlier. The parameter for the sensitivity lag, ξ, varies between 0 and 1.

The stimulus term is a function of the relative speed. Figure 3-2 (a) shows the expected effect of the relative speed on drivers' acceleration decision. At low relative

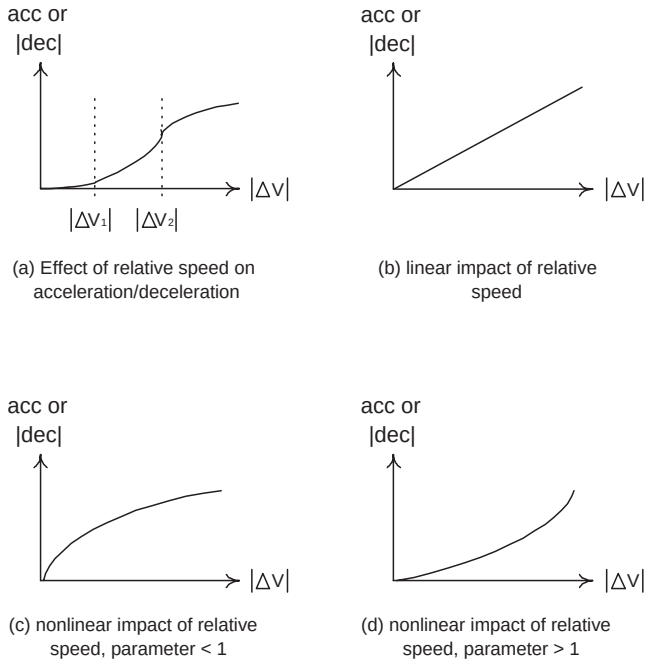

Figure 3-2: Impact of the relative speed on drivers' acceleration decision.

speeds, drivers' acceleration response may not be significant as they may not be able to perceive a small magnitude of the relative speed. For relative speeds beyond a certain threshold, $|\Delta V_1|$, drivers get a better sense of the stimulus and therefore, acceleration increases at an increasing rate. Beyond another threshold, $|\Delta V_2|$, the acceleration applied by a driver is limited by the acceleration capacity of the vehicle

and hence, acceleration increases at a decreasing rate until it reaches the maximum acceleration.

The effect of the relative speed on the car–following acceleration discussed above can be captured by assuming a piecewise nonlinear function of the relative speed of the following form:

$$f[\Delta V_n(t-\tau_n)] = \Delta V1_n(t-\tau_n)^{\lambda_1^g} + \Delta V2_n(t-\tau_n)^{\lambda_2^g} + \Delta V3_n(t-\tau_n)^{\lambda_3^g} \qquad (3.3)$$

where,

$$\begin{aligned}
\Delta V1_n(t-\tau_n) &= \min(|\Delta V_n(t-\tau_n)|, |\Delta V_1|) \\
|\bullet| &= \text{absolute value,} \\
\Delta V2_n(t-\tau_n) &= \max(0, \min(|\Delta V_n(t-\tau_n)| - |\Delta V_1|, |\Delta V_2| - |\Delta V_1|) \\
\Delta V3_n(t-\tau_n) &= \max(0, |\Delta V_n(t-\tau_n)| - |\Delta V_2|)
\end{aligned}$$

The breakpoints, $|\Delta V_1|$ and $|\Delta V_2|$, should be chosen such that they are reasonable from a behavioral standpoint. In order to replicate the impact of the relative speed on the acceleration as shown by the curve in Figure 3-2 (a), both λ_1^g and λ_2^g should be greater than one while λ_3^g should be less than one. In addition, λ_1^g should be less than λ_2^g.

Figure 3-2 (b) shows the linear approximation of the impact of the relative speed on acceleration which has been used by existing models. This implies the following:

$$f[\Delta V_n(t-\tau_n)] = |\Delta V_n(t-\tau_n)| \qquad (3.4)$$

The functional form given by Equation 3.3 can be simplified by allowing only one parameter:

$$f[\Delta V_n(t-\tau_n)] = |\Delta V_n(t-\tau_n)|^{\lambda^g} \qquad (3.5)$$

Figures 3-2 (c) and (d) show the effect of the relative speed on the acceleration using

this specification for $\lambda^g < 1$ and $\lambda^g > 1$ respectively. We apriori expect λ^g to be less than one for both the acceleration and deceleration due to the existence of a maximum value for acceleration and deceleration that a driver can apply in reality. The parameter λ^g can be tested statistically to determine whether it is significantly different from one. Note that, $\lambda^g = 1$ corresponds to the specification given by Equation 3.4.

The *GM Model* (Equation 2.7) assumed the sensitivity term to be a nonlinear function of the subject speed at time t and the space headway at time $(t - \tau_n)$. It allowed a single set of parameters for both the acceleration and deceleration decisions. Mathematically, this is given by:

$$s[X_n^{cf}(t - \xi\tau_n)] = \alpha \frac{V_n(t)^\beta}{\Delta X_n(t - \tau_n)^\gamma} \tag{3.6}$$

where, α, β, and γ are constant parameters, and ξ is set to 0 and 1 for speed and space headway respectively. We extend the *GM Model* by allowing different sets of parameters for the car–following acceleration and deceleration sensitivities, by incorporating the density of traffic as explanatory variable into the sensitivity term, and by allowing the time at which the explanatory variables are observed to be a parameter to be estimated:

$$s[X_n^{cf,g}(t - \xi\tau_n)] = \alpha^g \frac{V_n(t - \xi\tau_n)^{\beta^g}}{\Delta X_n(t - \xi\tau_n)^{\gamma^g}} \; k_n(t - \xi\tau_n)^{\rho^g} \tag{3.7}$$

where,

$$\begin{aligned} \alpha^g, \beta^g, \gamma^g, \rho^g &= \text{constant parameters,} \\ k_n(t - \xi\tau_n) &= \text{density of traffic ahead of the subject within} \\ &\quad \text{its view at time } (t - \xi\tau_n). \end{aligned}$$

The parameter ξ captures the fact that drivers may update their perception of the traffic environment during the acceleration decision making process. Restricting ξ to be equal to one implies that drivers do not update their perception of the traffic

environment and react (accelerate/decelerate) based on the traffic conditions at the time they observe the stimulus. In other words, $\xi = 1$ implies that the lag for sensitivity and stimulus are equal, while, $\xi < 1$ implies that lag for sensitivity is smaller than that for stimulus.

There are apriori expectations regarding the signs of the various parameters. The constant α^g in the sensitivity term should be positive and negative for the acceleration and deceleration models respectively. In the car–following regime under acceleration situations, drivers are likely to apply a lower acceleration at high speeds compared to low speeds and therefore, the corresponding parameter β^{acc} should be negative. On the other hand, under deceleration situations, drivers are likely to apply a higher deceleration at high speeds compared to low speeds which implies that β^{dec} should be positive. The sign of the parameter γ^{acc} can either be negative or positive. Under acceleration situations, drivers may apply a higher acceleration when space headways are larger, implying a negative headway parameter, γ^{acc} (i.e., the space headway should be in the numerator of the sensitivity). However, as the space headway increases, drivers may tend to follow the speed of the lead vehicle less and if this is the case, γ^{acc} would be positive. Under deceleration situations, drivers are likely to apply smaller decelerations at larger headways, implying a positive headway parameter, γ^{dec}.

Traffic conditions ahead of the subject and its leader are likely to change more rapidly at high densities than at low densities. Due to this, higher uncertainty is involved in predicting the position and speed of the leader in the near future. In addition, high traffic density represents lack of maneuverability compared to low traffic density for both the subject and its leader. As a result, drivers are expected to be more conservative at high densities than at low densities. Hence, at high densities the subject is likely to accelerate at a lower rate, while decelerate at a higher rate. These imply that, ρ^{acc} and ρ^{dec} are expected to be negative and positive respectively.

The random term captures the effect of omitted variables. It is assumed to be independent for different decisions of a given driver as well as for different drivers. The correlation between different acceleration decisions of a given driver is assumed

to be captured through the reaction time and headway threshold distributions. This implies:

$$\begin{aligned} \epsilon_n^{cf,g}(t) &\sim \mathcal{N}(0, \sigma^2_{\epsilon^{cf,g}}) \\ \text{cov}\left(\epsilon_n^{cf,g}(t), \epsilon_{n'}^{cf,g'}(t')\right) &= \begin{cases} \sigma^2_{\epsilon^{cf,g}} & \text{if } g = g', t = t', n = n' \\ 0 & \text{otherwise} \end{cases} \end{aligned} \tag{3.8}$$

3.2.2 The Free–Flow Acceleration Model

When the headway is greater than the threshold, the driver has the freedom to attain its desired speed. Hence, the acceleration applied by a driver in this regime is assumed to have the following functional form:

$$a_n^{ff}(t) = \lambda^{ff}\left[V_n^*(t-\tau_n) - V_n(t-\tau_n)\right] + \epsilon_n^{ff}(t) \tag{3.9}$$

where,

$$\begin{aligned} \lambda^{ff} &= \text{constant sensitivity,} \\ V_n^*(t-\tau_n) &= \text{desired speed of the driver,} \\ \left[V_n^*(t-\tau_n) - V_n(t-\tau_n)\right] &= \text{stimulus,} \\ \epsilon_n^{ff}(t) &= \text{random term associated with the free–flow} \\ &\quad \text{acceleration of driver } n \text{ at time } t. \end{aligned}$$

The desired speed of a driver is defined as the speed the driver wants to maintain after considering the speed limit of the section it is traveling, vehicle's mechanical capability, the effect of surrounding traffic, the roadway and weather conditions, and the geometry of the roadway section. The desired speed is assumed to have the following functional form:

$$V_n^*(t-\tau_n) = X_n^{DS}(t-\tau_n)\beta^{DS} \tag{3.10}$$

where,

$$\begin{aligned} X_n^{DS}(t-\tau_n) &= \text{vector of explanatory variables affecting the desired speed } (DS), \\ \beta^{DS} &= \text{constant parameters.} \end{aligned}$$

Replacing the specification of $V_n^*(t-\tau_n)$ in Equation 3.9, the free–flow acceleration model becomes

$$a_n^{ff}(t) = \lambda^{ff}\left[X_n^{DS}(t-\tau_n)\beta^{DS} - V_n(t-\tau_n)\right] + \epsilon_n^{ff}(t) \tag{3.11}$$

In this model, the acceleration at time t is assumed to be proportional to the stimulus—the difference between the driver's desired speed and current speed at time $(t-\tau_n)$. The sensitivity term is assumed to be a constant.

If the desired speed is higher than the current speed, drivers are expected to accelerate and vice versa. The magnitude of the applied acceleration (deceleration) depends on the difference between the current and the desired speeds.

Important explanatory variables affecting the desired speed of a driver include geometry of the roadway (curvature, grade, lane width), pavement surface quality (roughness, presence of pot holes), weather conditions, the speed limit of the roadway section, density of traffic ahead of the subject, speed of the vehicles ahead of the subject (which is also a proxy for density and maneuverability), type of the vehicle, and characteristics of the driver. For example, in a curved road or roadway with grades (particularly upgrade) or in a roadway with rough pavement, vehicles tend to slow down (thus the desired speed of drivers reduce) even when there is no lead vehicle. Similarly, drivers often set their desired speed relative to the speed limit of the roadway section. To estimate models with these site specific factors, data from different sites is necessary.

High density of traffic ahead of a driver within the driver's view, or a lower speed of the lead vehicle reduces desired speed, as might be expected. And finally, heavy vehicles (for example, bus, truck, semi–trailer etc. that have length greater than 9.14 meters or 30 ft (AASHTO 1990)) have lower acceleration and deceleration capability and hence respond slowly to free–flow conditions.

We further assume that, $\epsilon_n^{ff}(t)$ is normally distributed with zero mean and a variance $(\sigma^2_{\epsilon^{ff}})$, i.e., $\epsilon_n^{ff}(t) \sim \mathcal{N}(0, \sigma^2_{\epsilon^{ff}})$, and $\epsilon_n^{ff}(t)$ is independent of the random terms $\epsilon_n^{cf,acc}(t)$ and $\epsilon_n^{cf,dec}(t)$ for a given driver[2].

Note that, since the desired speed of a driver cannot be observed, extending the free–flow acceleration model to have different sensitivity under acceleration and deceleration situations cannot be done without increasing the complexity of the current framework.

3.2.3 The Headway Threshold Distribution

The headway threshold, h_n^*, is assumed to be truncated normally distributed with truncation on both sides. This distribution is given by:

$$f(h_n^*) = \begin{cases} \frac{\frac{1}{\sigma_h}\phi\left(\frac{h_n^* - \mu_h}{\sigma_h}\right)}{\Phi\left(\frac{h^*_{max} - \mu_h}{\sigma_h}\right) - \Phi\left(\frac{h^*_{min} - \mu_h}{\sigma_h}\right)} & \text{if } h^*_{min} \le h_n^* \le h^*_{max} \\ 0 & \text{otherwise} \end{cases} \tag{3.12}$$

where,

$$\begin{aligned} \mu_h, \sigma_h &= \text{constant mean and standard deviation of the untruncated distribution,} \\ h^*_{min}, h^*_{max} &= \text{minimum and maximum value of } h_n^* \text{ (parameters to be estimated),} \\ \phi() &= \text{probability density function of a standard normal random variable,} \end{aligned}$$

[2]As mentioned above, the correlation between the car–following and the free–flow acceleration decisions is assumed to be captured through the reaction time and headway threshold distributions.

$\Phi()$ = cumulative distribution function of a standard normal random variable.

The advantage of using a truncated normal distribution with mean, variance, and the truncation ends (h^*_{min} and h^*_{max}) as parameters is that the distribution is not restricted to be skewed to a particular direction. For instance, a distribution skewed to the left implies that, the probability of a driver being aggressive is higher than that of being conservative, since, an aggressive driver is expected to have a shorter headway threshold compared to a conservative driver. The above treatment of the headway distribution is a generalization over Subramanian (1996) who used a shifted truncated lognormal distribution that restricts the distribution to be skewed to the left.

Using Equation 3.12, the probability that driver n, who is $h_n(t)$ behind its leader, is in the car–following regime is given by:

$$
\begin{aligned}
&\mathrm{P}_n(\text{car–following at time } t) \\
&= \mathrm{P}\left(h_n(t) \leq h^*_n\right) \\
&= \begin{cases} 1 & \text{if } h_n(t) \leq h^*_{min} \\ 1 - \frac{\Phi\left(\frac{h_n(t)-\mu_h}{\sigma_h}\right) - \Phi\left(\frac{h^*_{min}-\mu_h}{\sigma_h}\right)}{\Phi\left(\frac{h^*_{max}-\mu_h}{\sigma_h}\right) - \Phi\left(\frac{h^*_{min}-\mu_h}{\sigma_h}\right)} & \text{if } h^*_{min} < h_n(t) \leq h^*_{max} \\ 0 & \text{otherwise} \end{cases}
\end{aligned}
\tag{3.13}
$$

At very large headways, it is unlikely that a driver would be in a car–following regime. Hence, the corresponding probability is zero for headways greater than h^*_{max}. Similarly, at very low headways it is unlikely that a driver would be in a free–flow regime and the corresponding probability of car–following is one for headways less than h^*_{min}.

3.2.4 The Reaction Time Distribution

The reaction time is assumed to be truncated log-normally distributed (i.e., skewed to the left) as suggested by Subramanian (1996). This implies that the probability of

a driver having a smaller reaction time is higher than that of having a larger reaction time. This was also supported by Johansson and Rumer (1971) and Lerner et al. (1995). Truncation is assumed since reaction time is finite. The distribution is as follows:

$$f(\tau_n) = \begin{cases} \dfrac{1}{\Phi\left(\dfrac{\ln(\tau_{max}) - \mu_\tau}{\sigma_\tau}\right)\tau_n \sigma_\tau \sqrt{2\pi}} \, \mathrm{e}^{-\frac{1}{2}\left(\frac{\ln(\tau_n) - \mu_\tau}{\sigma_\tau}\right)^2} & \text{if } 0 < \tau_n \leq \tau_{max} \\ 0 & \text{otherwise} \end{cases} \tag{3.14}$$

where,

$$\begin{aligned} \tau_n &= \text{reaction time of driver } n, \\ \mu_\tau &= \text{mean of the distribution of } \ln(\tau_n), \\ \sigma_\tau &= \text{standard deviation of the distribution of } \ln(\tau_n), \\ \tau_{max} &= \text{upper bound of the distribution of } \tau_n \text{ (parameter to be estimated).} \end{aligned}$$

The mean, median, and variance of the above distribution are as follows:

$$\text{mean} = \exp(\mu_\tau + 0.5\sigma_\tau^2) \frac{\Phi\left(\dfrac{\ln(\tau_{max}) - \mu_\tau}{\sigma_\tau} - \sigma_\tau\right)}{\Phi\left(\dfrac{\ln(\tau_{max}) - \mu_\tau}{\sigma_\tau}\right)} \tag{3.15}$$

$$\text{median} = \exp\left(\mu_\tau + \sigma_\tau \Phi^{-1}\left(0.5\Phi\left(\frac{\ln(\tau_{max}) - \mu_\tau}{\sigma_\tau}\right)\right)\right) \tag{3.16}$$

$$\text{variance} = e^{2\mu_\tau + \sigma_\tau}\left(e^{\sigma_\tau^2} - 1\right) \frac{\Phi\left(\dfrac{\ln(\tau_{max}) - \mu_\tau}{\sigma_\tau} - 2\,\sigma_\tau\right)}{\Phi\left(\dfrac{\ln(\tau_{max}) - \mu_\tau}{\sigma_\tau}\right)} \tag{3.17}$$

The mean of the distribution of $\ln(\tau_n)$, μ_τ, is assumed to be a function of explanatory variables:

$$\mu_\tau = X_n^\tau \, \beta^\tau \tag{3.18}$$

where,

$$\begin{aligned} X_n^\tau &= \text{vector of explanatory variables,} \\ \beta^\tau &= \text{model parameters.} \end{aligned}$$

Important factors affecting the reaction time include age, mental condition, visibility, weather conditions, roadway geometry, vehicle characteristics, vehicle speed, and traffic conditions. Older drivers are expected to have longer reaction times. Poor visibility increases driving difficulty and drivers are expected to be more alert. This implies a reduction in reaction time. During rain or snow drivers are expected to be more alert compared to good weather conditions. Roadway sections with high curvature and/or high grade make driving more difficult and hence would make drivers more alert. At high speeds drivers are expected to be more alert compared to low speeds due to safety reason. Traffic conditions (such as the density of traffic and the gap in front of the subject) may also affect reaction time. Drivers may be more alert in congested traffic compared to free flow traffic due to higher uncertainty involved in predicting future traffic conditions.

3.3 Likelihood Function Formulation

Using Equation 3.2 and the hypothesis that a driver in the car–following regime will accelerate if the leader is faster and vice versa, the distribution of the car–following acceleration, conditional on τ_n, is given by:

$$f\left(a_n^{cf}(t) \mid \tau_n\right) = f\left(a_n^{cf,acc}(t) \mid \tau_n\right)^{\delta[\Delta V_n(t-\tau_n)]} f\left(a_n^{cf,dec}(t) \mid \tau_n\right)^{(1-\delta[\Delta V_n(t-\tau_n)])} \tag{3.19}$$

where,

$$\delta[\Delta V_n(t-\tau_n)] = \begin{cases} 1 & \text{if } \Delta V_n(t-\tau_n) \geq 0 \\ 0 & \text{otherwise} \end{cases}$$

Using Equations 3.2 and 3.8, the distribution of the car–following acceleration, conditional on τ_n, are as follows:

$$f\left(a_n^{cf,g}(t) \mid \tau_n\right) = \frac{1}{\sigma_{\epsilon^{cf,g}}}\phi\left(\frac{a_n^{cf,g}(t) - s[X_n^{cf,g}(t-\xi\tau_n)] \quad f[\Delta V_n(t-\tau_n)]}{\sigma_{\epsilon^{cf,g}}}\right) \tag{3.20}$$

where, $g \in \{acc, dec\}$. The free–flow acceleration distribution, conditional on τ_n, is given by:

$$f\left(a_n^{ff}(t) \mid \tau_n\right) = \frac{1}{\sigma_{\epsilon^{ff}}}\phi\left(\frac{a_n^{ff}(t) - \lambda^{ff}[X_n^{DS}(t-\tau_n)\beta^{DS} - V_n(t-\tau_n)]}{\sigma_{\epsilon^{ff}}}\right) \tag{3.21}$$

Combining Equations 3.19 and 3.21, and using Equation 3.1, the distribution of acceleration for driver n at time t, conditional on h_n^* and τ_n, is as follows:

$$f\left(a_n(t) \mid h_n^*, \tau_n\right) = f\left(a_n^{cf}(t) \mid \tau_n\right)^{\delta[h_n(t-\tau_n)]} \quad f\left(a_n^{ff}(t) \mid \tau_n\right)^{(1-\delta[h_n(t-\tau_n)])} \tag{3.22}$$

where,

$$\delta[h_n(t-\tau_n)] = \begin{cases} 1 & \text{if } h_n(t-\tau_n) \leq h_n^* \\ 0 & \text{otherwise} \end{cases}$$

As mentioned above, the reaction time and the headway threshold capture the correlation between different acceleration decisions at different times for a given driver. This implies that, conditional on τ_n and h_n^*, the T_n different observations of driver n are independent. Therefore, the conditional joint density of observing an acceleration pattern associated with driver n, $(a_n(1), a_n(2), \ldots, a_n(T_n))$, can be expressed as the product of the conditional densities of each element of the pattern. Mathematically, this can be expressed as follows:

$$f(a_n(1), a_n(2), \ldots, a_n(T_n) \mid h_n^*, \tau_n) = \prod_{t=1}^{T_n} f(a_n(t) \mid h_n^*, \tau_n) \tag{3.23}$$

The unconditional distribution that constitutes the likelihood function for driver

n is:

$$f(a_n(1), a_n(2), \ldots, a_n(T_n)) = \int_0^{\tau_{max}} \int_{h^*_{min}}^{h^*_{max}} f(a_n(1), a_n(2), \ldots, a_n(T_n) \mid h^*, \tau) f(h^*)\ f(\tau)\ dh^*\ d\tau \quad (3.24)$$

Finally, assuming that the acceleration observations from different drivers in the sample are independent, the log–likelihood function is given by:

$$\mathcal{L} = \sum_{n=1}^{N} \ln[f(a_n(1), a_n(2), \ldots, a_n(T_n))] \quad (3.25)$$

Maximizing the likelihood function would provide the MLE estimate of the model parameters.

3.4 Conclusions

In this chapter, a rigorous framework for specifying and estimating the general acceleration model is presented that allows for joint estimation of all component models. The component models are the car–following acceleration and deceleration models, the free–flow acceleration model, and the headway threshold and reaction time distributions.

The proposed model builds on the earlier work by Subramanian (1996) and extends it. First, separate model parameters under acceleration and deceleration situations in the car–following regime are allowed in the likelihood function formulation. Second, the sensitivity of the car–following acceleration is extended to capture the effect of traffic conditions ahead of the driver, in addition to the relative position and speed of its leader. Third, it allows the time at which the explanatory variables of the car–following acceleration sensitivity are observed to be a parameter to be estimated (as opposed to restricting it to be the time at which the stimulus is observed). Fourth, the stimulus of the car–following acceleration is extended by making it a nonlinear function of the lead relative speed. And finally, a more general headway threshold

distribution is used that allows any driver behavior to be captured (aggressive or conservative).

Chapter 4

The Lane Changing Model

In this chapter, the lane changing model is presented. Lane changes are classified as either mandatory or discretionary. When a lane change is required due to, for example, a lane drop, the operation is called a mandatory lane change (MLC). On the other hand, when lanes are changed by a driver to improve perceived driving conditions, the operation is called a discretionary lane change (DLC).

The proposed mandatory lane changing model extends the work by Ahmed et al. (1996) by developing a new model for heavily congested traffic. Under heavily congested traffic, gaps of acceptable lengths are hard to find. Hence, a forced merging model is proposed which captures merging by gap creation either through courtesy yielding of the lag vehicle in the target lane or through the subject forcing the lag vehicle to slow down.

This chapter begins by presenting the conceptual framework of the proposed lane changing model. The model along with the likelihood function formulation is presented next. Then, the complexities associated with modeling the impact of past lane changing decisions on the current lane changing decision are discussed. This chapter concludes by presenting the conceptual framework, the model, and the likelihood function formulation of the forced merging model.

4.1 Introduction

A lane change decision process is assumed to have the following three steps:

- decision to consider a lane change (either a DLC or an MLC),
- choice of a target lane, and
- acceptance of a gap in the target lane.

Modeling such a process is extremely complicated. First, the entire lane change decision process is latent in nature. All that is observed is the execution of the lane change decision—the final acceptance of a gap. Second, the time at which a lane change decision is made cannot be observed in general[1]. Furthermore, once a decision to change lanes is made, a driver may continue to search for gaps or may change its mind—all of which are unobserved. Finally, the lane changing decision is continuous in nature.

To simplify the modeling, time is discretized. Furthermore, drivers are assumed to make decisions about lane changes at every discrete point in time irrespective of the decisions made during earlier time periods. In other words, we do not explicitly model the impact of past lane changing decisions on the current lane changing decision. The complexities associated with capturing such behavior are discussed in Section 4.2.4. The impact of past decisions on the current decision, however, is captured in the proposed forced merging model. Due to their different structures, the lane changing and forced merging models are presented separately.

[1]Merging from an on–ramp to a freeway is a notable exception, since as soon as a driver arrives at the merging point, the driver would recognize the necessity of performing a mandatory lane change.

4.2 The Lane Changing Model

4.2.1 Conceptual Framework

The lane changing model structure is shown in Figure 4-1. As mentioned above, except for the completion of the execution of the lane change, the whole decision process is latent in nature. The latent and observable parts of the process are represented by ovals and rectangles respectively.

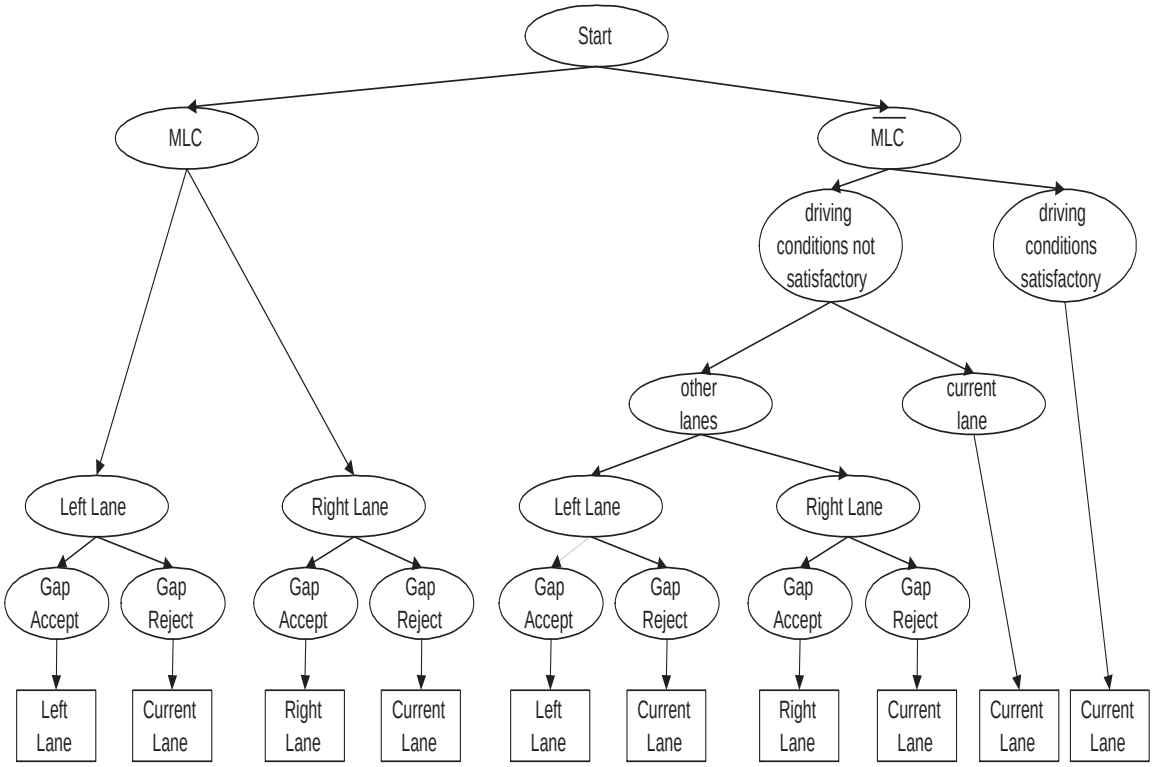

Figure 4-1: The lane changing model structure.

The MLC branch in the top level corresponds to the case when a driver decides to respond to the MLC condition[2]. Explanatory variables that affect such decision include remaining distance to the point at which lane change must be completed, the number of lanes to cross to reach a lane connected to the next link, delay (time elapsed since the MLC conditions apply), and whether the subject vehicle is a heavy

[2]When a mandatory lane changing situation does not apply, the probability of responding to MLC is set to zero.

vehicle (bus, truck, semi–trailer etc.). Drivers are likely to respond to the MLC situations earlier if it involves crossing several lanes. A longer delay makes a driver more anxious and increases the likelihood of responding to the MLC situations. And finally, due to lower maneuverability and larger gap length requirement of heavy vehicles as compared to their non–heavy counterparts, they have a higher likelihood of responding to the MLC conditions.

The $\overline{MLC}$ branch corresponds to the case where either a driver does not respond to an MLC condition, or that MLC conditions do not apply. A driver then decides whether to perform a discretionary lane change (DLC). This comprises of two decisions: whether the driving conditions are satisfactory, and if not satisfactory, whether any other lane is better than the current lane. The term driving conditions satisfactory implies that the driver is satisfied with the driving conditions of the current lane. Important factors affecting the decision whether the driving conditions are satisfactory include the speed of the driver compared to its desired speed, presence of heavy vehicles in front and behind the subject, if an adjacent on–ramp merges with the current lane, whether the subject is tailgated etc. If the driving conditions are not satisfactory, the driver compares the driving conditions of the current lane with those of the adjacent lanes. Important factors affecting this decision include the difference between the speed of traffic in different lanes and the driver's desired speed, the density of traffic in different lanes, the relative speed with respect to the lag vehicle in the target lane, the presence of heavy vehicles in different lanes ahead of the subject etc. In addition, when a driver considers DLC although a mandatory lane change is required but the driver is not responding to the MLC conditions, changing lanes opposite to the direction as required by the MLC conditions may be less desirable. If a driver decides not to perform a discretionary lane change (i.e., either the driving conditions are satisfactory, or, although the driving conditions are not satisfactory, the current is the lane with the best driving conditions) the driver continues in the current lane. Otherwise, the driver selects a lane from the available alternatives and assesses the adjacent gap in the target lane.

The lowest level of ovals in the decision tree shown in Figure 4-1 corresponds

to the gap acceptance process. When trying to perform a DLC, factors that affect drivers' gap acceptance behavior include the gap length, speed of the subject, speed of the vehicles ahead of and behind the subject in the target lane, and the type of the subject vehicle (heavy vehicle or not). For instance, a larger gap is required for merging at a higher travel speed. A heavy vehicle would require a larger gap length compared to a car due to lower maneuverability and the length of the heavy vehicle. In addition to the above factors, the gap acceptance process under the MLC conditions is influenced by factors such as remaining distance to the point at which lane change must be completed, delay (which captures the impatience factor that would make drivers more aggressive) etc.

Note that, delay cannot be used as an explanatory variable except for very specialized situations, for example, merging from an on–ramp. This is because the very inception of an MLC condition is usually unobserved. The specification of the complete model is presented next.

4.2.2 Model Formulation

The decisions in the hierarchy shown in Figure 4-1 can be modeled using the random utility approach (Ben-Akiva and Lerman 1985). The model formulation must explicitly capture the fact that, the available data for lane changing model estimation is panel data. Model formulation appropriate for panel data is presented in Appendix A.

The Lane Selection Model

As mentioned above, the lane selection process consists of the top four levels of the decision hierarchy shown in Figure 4-1. The top level, whether to respond to a mandatory lane change (MLC) condition or not ($\overline{MLC}$), can be modeled using a discrete choice model, for example, a binary logit model. Using the formulation of random term appropriate for panel data (see Appendix A), the probability that driver n at time t will respond to MLC, conditional on the individual specific random term,

ν_n, is given by:

$$\mathrm{P}_t(MLC \mid \nu_n) = \frac{1}{1 + \exp(-X_n^{MLC}(t)\beta^{MLC} - \alpha^{MLC}\nu_n)} \tag{4.1}$$

where,

$$\begin{aligned} X_n^{MLC}(t) &= \text{vector of explanatory variables affecting decision to respond to the } MLC \text{ conditions (discussed in Section 4.2.1),} \\ \beta^{MLC} &= \text{vector of parameters,} \\ \nu_n &= \text{individual specific random term assumed to be distributed standard normal,} \\ \alpha^{MLC} &= \text{parameter of } \nu_n. \end{aligned}$$

The individual specific random term, ν_n, is introduced to capture the correlation between different observations from a given driver. If the correlation is not captured it may introduce bias in the parameter estimates. The larger the product of the parameter α^{MLC} and the value of individual specific random variable, ν_n, the higher is the probability that the driver would respond to an MLC condition earlier.

If a driver decides not to respond to an MLC condition, or MLC conditions do not apply, a discretionary lane change (DLC) may be considered. The binary decision, whether the driving conditions are satisfactory or not, can be modeled using a binary logit model,

$$\mathrm{P}_t(DCNS \mid \nu_n) = \frac{1}{1 + \exp(-X_n^{DCNS}(t)\beta^{DCNS} - \alpha^{DCNS}\nu_n)} \tag{4.2}$$

where, superscript $DCNS$ denotes driving conditions not satisfactory. Generally, we expect α^{MLC} and α^{DCNS} to have opposite signs, or, the two corresponding utilities should have a negative correlation (see Equation A.4). This implies that, a driver postponing a response to an MLC condition to be an aggressive driver and hence, may have a higher propensity to perform a discretionary lane change.

If the driving conditions are not satisfactory, drivers are assumed to compare the driving condition of the current lane with the better among the left and right adjacent lanes. The utilities of perceiving the driving conditions unsatisfactory and selecting the other lanes over the current lane are expected to be positively correlated. Since there is an effort/hassle associated with changing lanes which is not explicitly captured, the utility of the adjacent two lanes are likely to be correlated. The nested logit model (Ben-Akiva and Lerman 1985) is a natural choice to capture such phenomenon. First, the utilities of the two adjacent lanes are compared (the 'left lane' versus 'right lane' decision under the 'other lanes' oval in Figure 4-1). Then, the utility of the 'other lanes' is compared to the utility of the 'current lane' to decide if the current lane is the desired lane.

The output from the lane selection model is the probability of selecting each of the three lanes in question. If the left or right lane is chosen, a driver seeks an acceptable gap in the target lane. The gap acceptance model is presented next.

The Gap Acceptance Model

The gap acceptance model captures drivers assessment of gaps as acceptable or unacceptable. Drivers are assumed to consider only the adjacent gap. An adjacent gap is defined as the gap in between the lead and lag vehicles in the target lane (see Figure 4-2). For merging into an adjacent lane, a gap is acceptable only when both

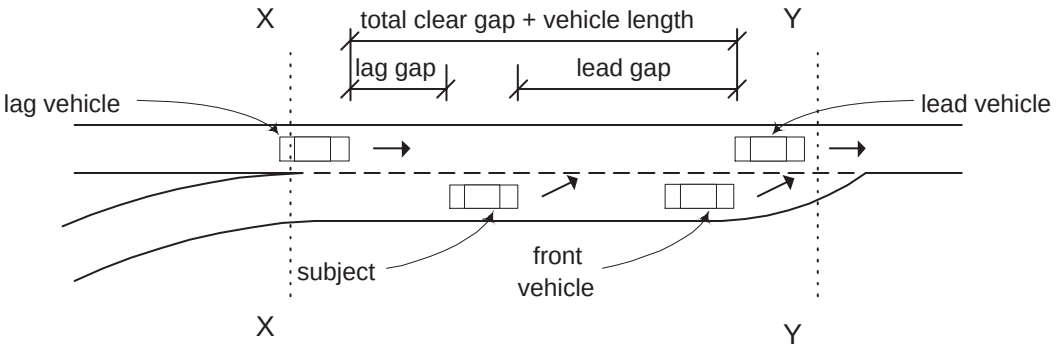

Figure 4-2: The subject, lead, lag, and front vehicles, and the lead and lag gaps.

lead and lag gaps are acceptable.

Drivers are assumed to have minimum acceptable lead and lag gap lengths which are termed as the lead and lag critical gaps respectively. These critical gaps vary not only among different individuals, but also for a given individual under different traffic conditions. The critical gap for driver n at time t is assumed to have the following functional form[3]:

$$G_n^{cr,g}(t) = \exp(X_n^g(t)\beta^g + \alpha^g \nu_n + \epsilon_n^g(t)) \tag{4.3}$$

where,

$$\begin{aligned} g &\in \{lead, lag\}, \\ \alpha^g &= \text{parameter of } \nu_n \text{ for } g \in \{lead, lag\}, \\ \epsilon_n^g(t) &= \text{generic random term that varies across all three dimensions, i.e., } g, t, \text{and } n. \end{aligned}$$

The exponential form of the critical gap guarantees that the estimated critical gap will always be non-negative. The individual specific random term, ν_n, and its parameter capture the correlation between the lead and lag critical gaps for a driver. This correlation, especially under MLC conditions, is expected to be positive.

A conservative driver is expected to have a larger lead/lag critical gaps compared to its aggressive counterpart. A larger product of α^g and ν_n, $g \in \{lead, lag\}$ implies a larger critical gap length requirement, and hence, represents a conservative driver. The lead/lag critical gaps are expected to be positively correlated with the utility of responding to an MLC condition and negatively correlated with the utilities of perceiving the driving conditions as unsatisfactory and selecting the other lanes over the current lane.

Assuming $\epsilon_n^g(t) \sim \mathcal{N}(0, \sigma_{\epsilon^g}^2)$, i.e., the critical gap lengths are lognormally distributed, the conditional probability of acceptance of a gap is given by:

[3]Adopted from Ahmed et al. (1996).

$$
\begin{aligned}
&\mathrm{P}_t(gapAcc \mid \nu_n) \\
&= \mathrm{P}_t(\text{lead gap acceptable}\mid \nu_n)\ \mathrm{P}_t(\text{lag gap acceptable}\mid \nu_n) \\
&= \mathrm{P}(G_n^{lead}(t) > G_n^{cr,lead}(t) \mid \nu_n)\ \mathrm{P}(G_n^{lag}(t) > G_n^{cr,lag}(t) \mid \nu_n) \\
&= \mathrm{P}(\ln(G_n^{lead}(t)) > \ln(G_n^{cr,lead}(t)) \mid \nu_n)\ \mathrm{P}(\ln(G_n^{lag}(t)) > \ln(G_n^{cr,lag}(t)) \mid \nu_n) \\
&= \Phi\left(\frac{\ln(G_n^{lead}(t)) - X_n^{lead}(t)\beta^{lead} - \alpha^{lead}\nu_n}{\sigma_{\epsilon^{lead}}}\right) \times \\
&\quad \Phi\left(\frac{\ln(G_n^{lag}(t)) - X_n^{lag}(t)\beta^{lag} - \alpha^{lag}\nu_n}{\sigma_{\epsilon^{lag}}}\right)
\end{aligned} \tag{4.4}
$$

where, $G_n^{lead}(t)$ and $G_n^{lag}(t)$ denote the lead and lag gaps (see Figure 4-2) respectively and Φ denotes the cumulative distribution function of a standard normal random variable. In addition to β's and α's, $\sigma_{\epsilon^{lead}}$ and $\sigma_{\epsilon^{lag}}$ are parameters that can be identified. Normalization of $\sigma_{\epsilon^{lead}}$ or $\sigma_{\epsilon^{lag}}$ is not necessary since the variables '$\ln(G_n^{lead}(t))$' and '$\ln(G_n^{lag}(t))$' in Equation 4.4 do not have any coefficient.

4.2.3 Likelihood Function Formulation

Drivers are assumed to consider the entire lane change decision process (Figure 4-1) at every discrete point in time, for example, every second. Let the sequence of lane changes performed by driver n be denoted as follows:

$$
[J_n(1), J_n(2), \ldots, J_n(T_n)] \tag{4.5}
$$

where,

$$
\begin{aligned}
J &\in \{L, R, C\} \\
L &= \text{change to the left lane,} \\
R &= \text{change to the right lane,} \\
C &= \text{continue in the current lane,} \\
T_n &= \text{number of time periods driver } n \text{ is observed.}
\end{aligned}
$$

As mentioned above, the individual specific random term captures the correlation between different decisions at different times for a given driver. Therefore, conditional on the individual specific random term, the probability of observing a pattern for a given driver can be expressed as the product of probabilities of observing each element of the pattern. Mathematically, this can be expressed as follows:

$$\begin{aligned} \mathrm{P}(J_{1n}, J_{2n}, \ldots, J_{T_n n} \mid \nu_n) &= \prod_{t=1}^{T_n} \mathrm{P}(J_{tn} \mid \nu_n) \\ &= \prod_{t=1}^{T_n} \mathrm{P}_t(L \mid \nu_n)^{\delta_{tn}^L} \ \mathrm{P}_t(R \mid \nu_n)^{\delta_{tn}^R} \ \mathrm{P}_t(C \mid \nu_n)^{1-\delta_{tn}^L-\delta_{tn}^R} \end{aligned} \tag{4.6}$$

where,

$$\delta_{tn}^J = \begin{cases} 1 & \text{if driver } n \text{ changes to } J \text{ at time } t \ (J \in \{L, R\}) \\ 0 & \text{otherwise.} \end{cases} \tag{4.7}$$

The unconditional probability of observing a pattern for a given driver is given by:

$$\mathrm{P}(J_{1n}, J_{2n}, \ldots, J_{T_n n}) = \int_{-\infty}^{\infty} \mathrm{P}(J_{1n}, J_{2n}, \ldots, J_{T_n n} \mid \nu) f(\nu) d\nu$$

where, $f(\nu)$ denotes the distribution of ν.

Assuming that the observations from different drivers in the sample are independent, the likelihood function for all drivers is:

$$\mathcal{L} = \sum_{n=1}^{N} \ln \mathrm{P}(J_{1n}, J_{2n}, \ldots, J_{T_n n}) \tag{4.8}$$

where, N denotes the number of drivers.

The probability of staying in the current lane or changing to the left or right lanes can be formulated using the decision tree of Figure 4-1. A driver may change to the left lane when he/she:

- responds to MLC conditions, the left lane is chosen, and the lead and lag gaps in the left lane are acceptable; or,

- does not respond to MLC conditions or MLC conditions do not apply, perceives the driving conditions as unsatisfactory, selects the other lanes over the current lane, selects the left lane, and the lead and lag gaps in the left lane are acceptable.

Therefore, the probability of an observation of *change to the left lane*, conditional on ν_n, is:

$$
\begin{aligned}
&\mathrm{P}_t(L \mid \nu_n) = \\
&\quad [\mathrm{P}_t(gap\ acceptable \mid left\ lane\ chosen, MLC, \nu_n) \\
&\quad \mathrm{P}_t(left\ lane\ chosen \mid MLC, \nu_n)\ \mathrm{P}_t(MLC \mid \nu_n)] + \\
&\quad [\mathrm{P}_t(gap\ acceptable \mid left\ lane\ chosen, other\ lanes, driving\ conditions\ not \\
&\qquad\qquad satisfactory, \overline{MLC}, \nu_n) \\
&\quad \mathrm{P}_t(left\ lane\ chosen \mid other\ lanes, driving\ conditions\ not\ satisfactory, \\
&\qquad\qquad \overline{MLC}, \nu_n) \\
&\quad \mathrm{P}_t(other\ lanes \mid driving\ conditions\ not\ satisfactory, \overline{MLC}, \nu_n) \\
&\quad \mathrm{P}_t(driving\ conditions\ not\ satisfactory \mid \overline{MLC}, \nu_n)\ \mathrm{P}_t(\overline{MLC} \mid \nu_n)]
\end{aligned}
$$

Similarly, the conditional probability of changing to the right lane or continuing in the current lane can be formulated.

4.2.4 Discussions

Complexities Associated with Capturing the Impact of Past Lane Changing Decisions in the Lane Changing Model

In this section, the complexities associated with modeling the impact of past lane changing decisions on the current lane changing decision are discussed with the help of a simple example. Consider a vehicle that is observed in a two lane roadway for three consecutive time periods during which time it did not change lanes and mandatory lane changing conditions do not apply. To simplify the discussion further, we combine

the two levels, 'driving conditions satisfactory or not' and 'other lane' or 'current lane', of the decision tree shown in Figure 4-1 into one level, DLC versus $\overline{DLC}$. Here, DLC implies that the driving conditions of the current lane is not satisfactory and another lane (the left lane) is better than the current lane. Therefore, for this driver, the lane changing decision tree shown in Figure 4-1 reduces to the one shown in Figure 4-3 (a). Since the driver did not change lanes, he/she may be in state 'DLC and gap reject given DLC' or in state '$\overline{DLC}$' during these three time periods (see Figure 4-3 (b)).

As shown in Figure 4-3 (b), there are $2^3 = 8$ possible state sequences that can explain the three observations from the driver. If the driver is observed for T_n time periods, the number of state sequences becomes 2^{T_n}, i.e., the number of possible state sequences increases exponentially with the number of times the driver is observed. Therefore, the number of state sequences to explain a particular pattern of lane

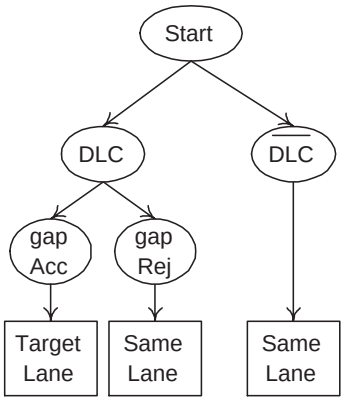

(a) decision tree at any instant of time

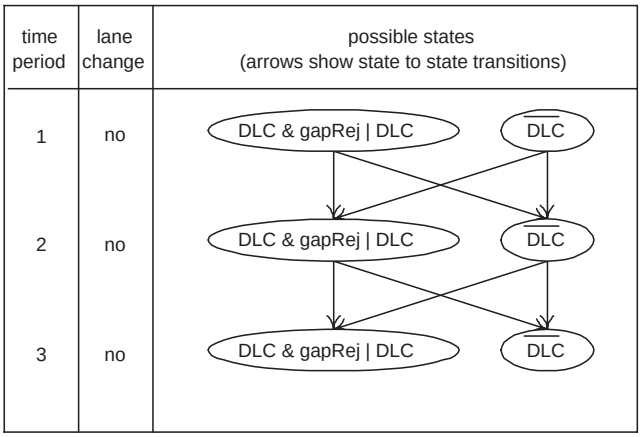

(b) possible states during the three successive time periods

Figure 4-3: The lane changing decision tree for a driver driving in a two lane roadway and possible states of the driver.

changing by a driver is prohibitively large from an estimation point of view. Further research with various modeling approaches and approximations is necessary to capture the impact of past lane changing decisions on the current lane changing decision.

Limitations of the Proposed MLC Model

Vehicles in heavily congested traffic travel at low speeds, with low space headways. In such situations, it is likely that a driver, trying to change lanes, will not find a gap that is larger than the driver's minimum acceptable gap length. In order to merge, gaps have to be created either through the lag vehicle's courtesy yielding or through the subject forcing the lag vehicle to slow down. The mandatory lane changing model presented above, however, assumes that drivers would ultimately find an acceptable gap. A forced merging model that captures driver decisions leading to a gap creation is proposed in the following section.

4.3 The Forced Merging Model

We assume that a driver has decided to change to the adjacent lane (see Figure 4-4). The merging process involves the driver's decision as to whether he/she *intends to merge into the adjacent gap* and perception as to whether his/her *right of way is established*, and finally moving into the target lane. An adjacent gap is defined as the gap behind the lead vehicle in the target lane. Establishment of right of way means that an understanding between the subject and the lag vehicle in the target lane has

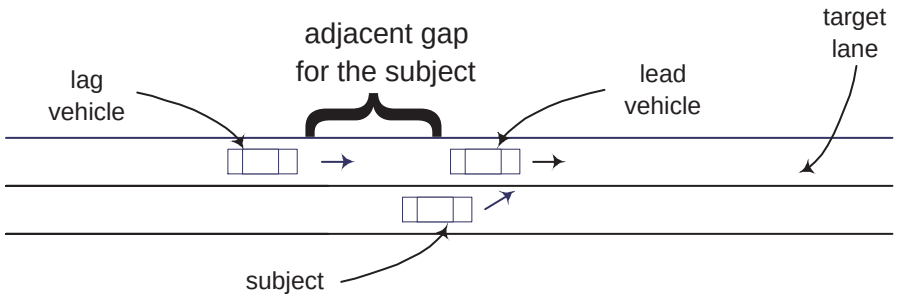

Figure 4-4: Definition of the adjacent gap.

been reached such that the lag vehicle would allow the subject to be in front of it. The conceptual framework of the proposed model is presented next.

4.3.1 Conceptual Framework

The tree diagram in Figure 4-5 summarizes the proposed structure of the forced merging model. As before, the ovals correspond to the latent part of the process that involves decisions and the rectangles correspond to the events that are directly observable.

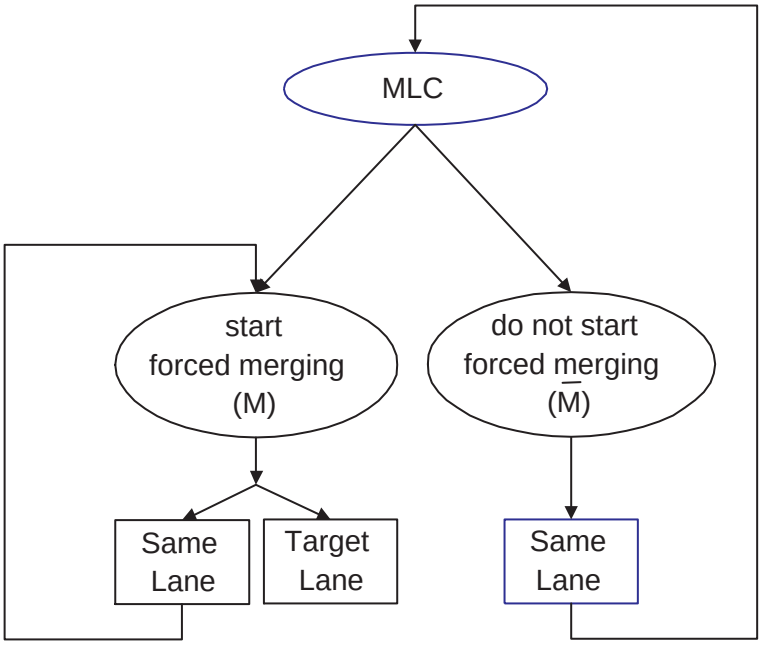

Figure 4-5: The forced merging model structure.

At every discrete point in time, a driver is assumed to (a) evaluate the traffic environment in the target lane to decide whether the driver *intends to merge in front of the lag vehicle in the target lane* and (b) try to communicate with the lag vehicle to understand whether the driver's *right of way is established*. If a driver *intends to merge in front of the lag vehicle* and *right of way is established*, the decision process ends and the driver gradually moves into the target lane. We characterize this instant by state M, where M denotes *start forced merging*. This process may last from less than a second to a few seconds. This is shown by the arrow below the left 'same lane' box. If right of way is not established, the subject continues the evaluation/communication process (i.e., remains in state $\overline{M}$) during the next time instant.

4.3.2 Model Formulation

Let, $S_n(t)$ denote the state of driver n at time t. Using a binary logit model and the random utility specification appropriate for panel data (see Appendix A), the probability of switching to state M from state $\overline{M}$, conditional on ν_n, is given by:

$$\mathrm{P}\{S_n(t) = M \mid S_n(t-1) = \overline{M}, \nu_n\} = \frac{1}{1 + e^{-X_n^{FM}(t)\beta^{FM} - \alpha^{FM}\nu_n}} \tag{4.9}$$

where, superscript FM implies forced merging. Important explanatory variables include:

- lead relative speed only when the lead vehicle is slower: when the lead vehicle is slower, the subject is more likely to slow down to match its speed with the speed of the lead vehicle first so as to focus exclusively on the interaction with the lag vehicle; this reduces the probability of being in state M;
- lag relative speed: when the lag vehicle is faster, the subject is more likely to speed up before attempting to establish right of way and hence this reduces the probability of being in state M;
- remaining distance to the point at which lane change must be completed by: as the remaining distance decreases, drivers become more concerned about merging and hence more aggressive. As a result, the probability of being in state M also increases;
- delay (time elapsed since the mandatory lane change conditions apply): higher delay makes a driver more frustrated and hence more aggressive, i.e., the probability of being in state M increases with additional delays[4].
- total clear gap (equal to the sum of the lead and lag gaps, see Figure 4-2): a large clear gap makes merging relatively easier and hence increases the probability of being in state M;

[4]As explained in Section 4.2.1, delay can be used as an explanatory variable only when the starting point is well defined, for example, merging from an on–ramp to the freeway.

- indicator for heavy vehicles (for example, bus, truck, semi–trailer): due to lower maneuverability and larger gap length requirement of heavy vehicles as compared to their non–heavy counterparts, they have a higher probability of being in state M under similar conditions.

The likelihood function formulation is presented next.

4.3.3 Likelihood Function Formulation

At any discrete point in time, a driver may be in state M or $\overline{M}$ (see Figure 4-5). Once a vehicle is in state M, by definition, the decision process ends and the remaining process is placing the vehicle in front of the lag vehicle, and the state of the driver cannot return to $\overline{M}$. The time taken in placing the vehicle in front of the lag vehicle is captured by the arrow below the left 'same lane' rectangle in Figure 4-5. This implies the following:

$$\mathrm{P}\{S_n(t') = M \mid S_n(t) = M, \nu_n\} = 1 \quad \forall\ t' > t \tag{4.10}$$

$$\mathrm{P}\{S_n(t') = \overline{M} \mid S_n(t) = M, \nu_n\} = 0 \quad \forall\ t' > t \tag{4.11}$$

We also assume that the initial state of the driver is $\overline{M}$. Different cases in which forced merging can occur are shown in Figure 4-6. Time period 1 denotes the first time period considered in the forced merging model and time period 0 denotes the preceding time period. In the first two cases (Figures 4-6 (a) and (b)), i.e., merging from an on–ramp and exiting, at time period 0 it is practically impossible to start merging. Therefore, the initial state is $\overline{M}$. On the other hand, in the last two cases (Figures 4-6 (c) and (d)), the driver could be in state M or $\overline{M}$ at time 0. If a driver is already in state M, then the sequence observed for the driver does not involve any decision and therefore, the probability of the observing the sequence is not a function of the model parameters to be estimated. In such cases, assuming drivers' state to be $\overline{M}$ would be reasonable only if the length of the section (measured from the diverging point toward the upstream direction) is large enough. A reasonable way to define a section large enough is 200 meters or more. Note that, in the last two cases delay

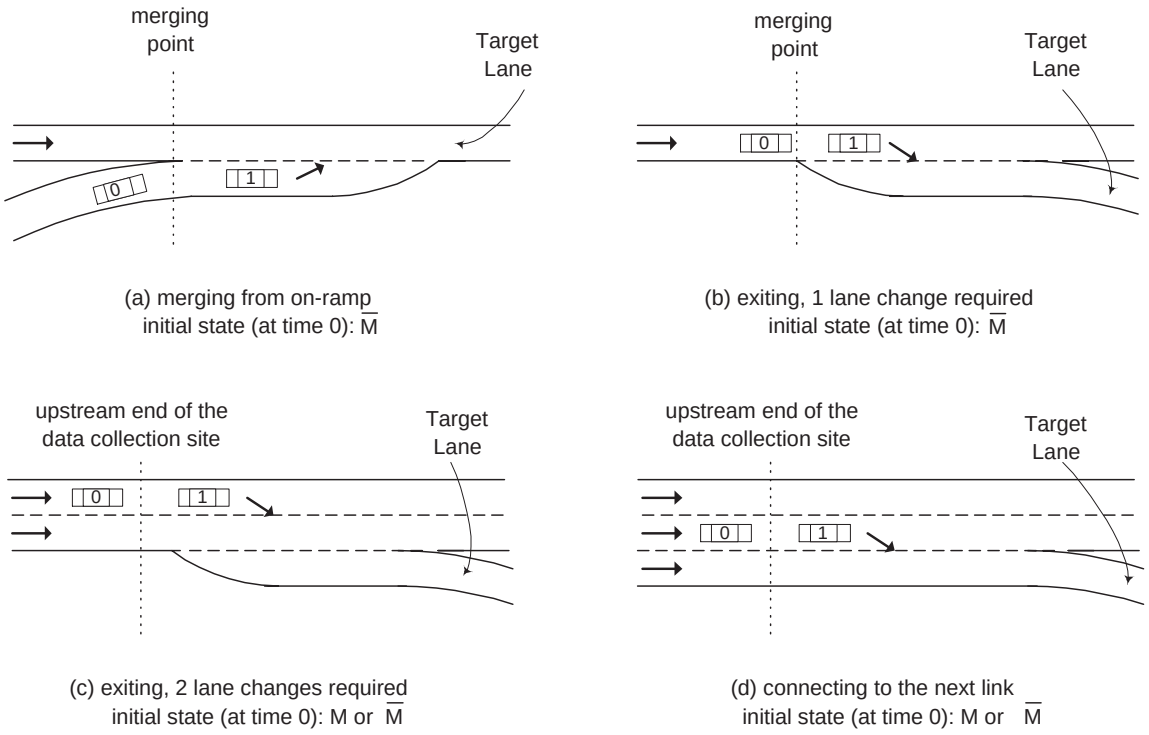

Figure 4-6: Initial state of the driver for the forced merging model for different cases.

cannot be used as an explanatory variable since the time instant at which the driver's state became $\overline{M}$ for the first time cannot be observed.

Since, ν_n is assumed to capture the correlation between the utilities of different states at different times, conditional on ν_n, the probability of being in state M at time t, given all earlier states were $\overline{M}$, is also given by Equation 4.9. Mathematically,

$$\mathrm{P}\{S_n(t) = M \mid S_n(t') = \overline{M}, t' = 0, 1, \ldots, (t-1), \nu_n\} = \frac{1}{1 + e^{-X_n^{FM}(t)\beta^{FM} - \alpha^{FM}\nu_n}} \tag{4.12}$$

The impact of being in state $\overline{M}$ during the earlier time periods on the probability of being in state M at time t is captured through the explanatory variable delay.

Let, T_n be the number of time periods driver n was observed in the original lane. There are T_n possible state sequences that may lead to observing driver n in the target lane at time $(T_n + 1)$. These sequences are listed in Table 4.1. *Sequence 1* in Table 4.1 implies that driver n reached state M at time period 1 and it took another

Table 4.1: Possible decision state sequences of observing a lane change by forced merging.

Time Period	Observed lane	Possible state sequences						
		1	2	3	...	t	...	T_n
1	SL	M	$\overline{M}$	$\overline{M}$		$\overline{M}$		$\overline{M}$
2	SL	M	M	$\overline{M}$		$\overline{M}$		$\overline{M}$
3	SL	M	M	M		$\overline{M}$		$\overline{M}$
$\vdots$	$\vdots$	$\vdots$	$\vdots$	$\vdots$		$\vdots$		$\vdots$
$t-1$	SL	M	M	M		$\overline{M}$		$\overline{M}$
t	SL	M	M	M		M		$\overline{M}$
$\vdots$	$\vdots$	$\vdots$	$\vdots$	$\vdots$		$\vdots$		$\vdots$
T_n-1	SL	M	M	M		M		$\overline{M}$
T_n	SL	M	M	M		M		M
T_n+1	TL							

Note: SL = same lane, TL = target lane

$(T_n - 1)$ seconds to execute the lane changing process. *Sequence 2* corresponds to the case where driver n was in state $\overline{M}$ at time period 1, and in state M during the time interval 2 to T_n. Similarly, *Sequence* t corresponds to the case that the driver was in state $\overline{M}$ during the time interval 1 to $(t-1)$, and in state M during the time interval t to T_n. Note that, these sequences are mutually exclusive.

As mentioned above, the individual specific random term, ν_n, captures the correlation between different decision elements at different times for a given driver. Therefore, conditional on ν_n, the probability of observing a particular state sequence for a given driver can be expressed as the product of probabilities of observing each state of the sequence. The conditional probability of observing the t^{th} state sequence for driver n is,

$$
\begin{aligned}
&\mathrm{P}_n\{\text{state sequence}_t \mid \nu_n\} = \\
&\quad \mathrm{P}\{S_n(T_n) = M \mid S_n(t') = M, \forall t' = t, \ldots, T_n - 1, \\
&\qquad\qquad S_n(t'') = \overline{M}, \forall t'' = 0, 1, \ldots, t-1, \nu_n\} \\
&\quad \mathrm{P}\{S_n(T_n - 1) = M \mid S_n(t') = M, \forall t' = t, \ldots, T_n - 2, \\
&\qquad\qquad S_n(t'') = \overline{M}, \forall t'' = 0, 1, \ldots, t-1, \nu_n\} \ldots \\
&\quad \mathrm{P}\{S_n(t) = M \mid S_n(t') = \overline{M}, \forall t' = 0, 1, \ldots, t-1, \nu_n\} \ldots \\
&\quad \mathrm{P}\{S_n(2) = \overline{M} \mid S_n(1) = \overline{M}, S_n(0) = \overline{M}, \nu_n\} \\
&\quad \mathrm{P}\{S_n(1) = \overline{M} \mid S_n(0) = \overline{M}, \nu_n\} \qquad (4.13)
\end{aligned}
$$

Using Equations 4.11 and 4.12,

$$
\begin{aligned}
&\mathrm{P}_n\{\text{state sequence}_t \mid \nu_n\} \\
&= \mathrm{P}\{S_n(t) = M \mid S_n(t') = \overline{M}, \forall t' = 0, 1, \ldots, t-1, \nu_n\} \ldots \\
&\quad \mathrm{P}\{S_n(2) = \overline{M} \mid S_n(1) = \overline{M}, S_n(0) = \overline{M}, \nu_n\} \\
&\quad \mathrm{P}\{S_n(1) = \overline{M} \mid S_n(0) = \overline{M}, \nu_n\} \\
&= \mathrm{P}\{S_n(t) = M \mid S_n(t') = \overline{M}, \forall t' = 0, 1, \ldots, t-1, \nu_n\} \times \\
&\quad \prod_{t'=1}^{t-1} \mathrm{P}\{S_n(t') = \overline{M} \mid S_n(t'') = \overline{M}, \forall t'' = 1, \ldots, t'-1, \nu_n\} \qquad (4.14)
\end{aligned}
$$

Since, an observed lane change by a driver can be explained by any one of the mutually exclusive state sequences listed in Table 4.1, the conditional likelihood function is the sum of the probabilities of observing all the sequences. This is given by:

$$
\begin{aligned}
&\mathcal{L}_n(\beta^{FM}, \alpha^{FM} \mid \nu_n) \\
&= \sum_{t=1}^{T_n} \mathrm{P}_n\{\text{state sequence}_t \mid \nu_n\} \\
&= \mathrm{P}_n\{\text{state sequence}_1 \mid \nu_n\} + \mathrm{P}_n\{\text{state sequence}_2 \mid \nu_n\} + \ldots + \\
&\quad \mathrm{P}_n\{\text{state sequence}_{T_n} \mid \nu_n\} \\
&= [\mathrm{P}\{S_n(1) = M \mid S_n(0) = \overline{M}, \nu_n\}] + \\
&\quad [\mathrm{P}\{S_n(2) = M \mid S_n(1) = \overline{M}, S_n(0) = \overline{M}, \nu_n\}\mathrm{P}\{S_n(1) = \overline{M} \mid S_n(0) = \overline{M}, \nu_n\}] + \\
&\quad \ldots + [\mathrm{P}\{S_n(T_n) = M \mid S_n(t') = \overline{M}, \forall t' = 0, 1, \ldots, T_n - 1, \nu_n\} \\
&\qquad \prod_{t'=1}^{T_n - 1} \mathrm{P}\{S_n(t') = \overline{M} \mid S_n(t'') = \overline{M}, \forall t'' = 1, \ldots, t' - 1, \nu_n\}]
\end{aligned} \tag{4.15}
$$

Let us now introduce variable δ_{tn}^{FM} defined as:

$$
\delta_n^{FM}(t) = \begin{cases} 1 & \text{if the adjacent gap at time } t \text{ is the same gap} \\ & \text{driver } n \text{ ultimately merged into} \\ 0 & \text{otherwise} \end{cases} \tag{4.16}
$$

Figure 4-7 illustrates the meaning of the variable $\delta_n^{FM}(t)$ with the help of an example. The subject (vehicle C) was observed for 4 time periods in the original lane (the right lane). Only during the 3^{rd} and 4^{th} time periods, vehicle C was adjacent to the gap between vehicles A and B that it ultimately merged into. Therefore, the sequence of δ^{FM} for this driver is {0,0,1,1}. Since, the driver was not adjacent to the gap between vehicles A and B during the first two time periods, communication with vehicle B cannot be established during these time intervals. Therefore, the driver cannot be in state M during time periods 1 and 2. This implies that, the first two sequences listed in Table 4.1 do not apply to this driver. While forming the likelihood function for this driver, the first two sequences must be taken out of the likelihood function (Equation 4.15). A convenient way of incorporating this into the likelihood function for a general case is as follows:

$$
\mathcal{L}_n(\beta^{FM}, \alpha^{FM} \mid \nu_n) = \sum_{t=1}^{T_n} \mathrm{P}_n\{\text{state sequence}_t \mid \nu_n\} \times \delta_n^{FM}(t) \tag{4.17}
$$

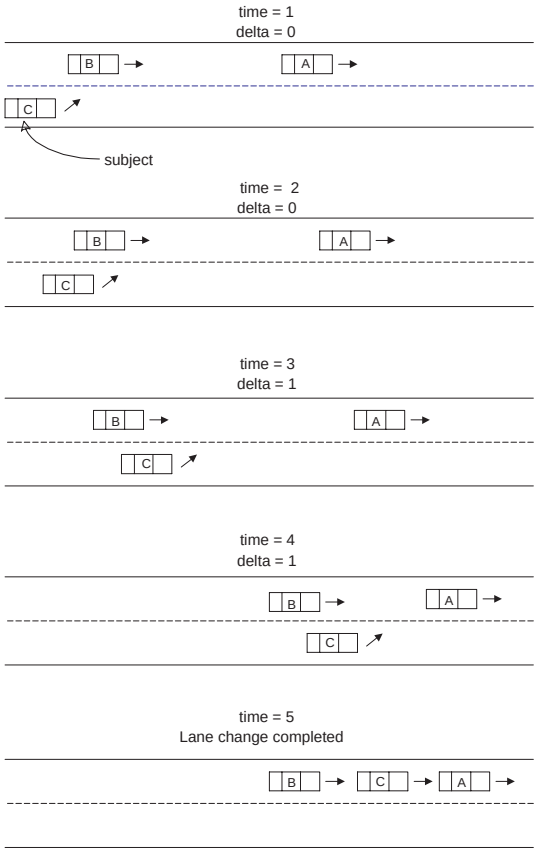

Figure 4-7: Definition of $\delta_n^{FM}(t)$ for the forced merging model.

The unconditional likelihood function for driver n is

$$\mathcal{L}_n(\beta^{FM}, \alpha^{FM}) = \int_{-\infty}^{\infty} \left(\sum_{t=1}^{T_n} \mathrm{P}_n\{\text{state sequence}_t \mid \nu\} \times \delta_n^{FM}(t) \right) f(\nu) d\nu \qquad (4.18)$$

where, $f(\nu)$ denotes, as before, the probability density function of the random variable ν.

Assuming that the observations from different drivers in the sample are independent, the log–likelihood function for all observations is given by:

$$\mathcal{L}(\beta^{FM}, \alpha^{FM}) = \sum_{n=1}^{N} \ln \left\{ \int_{-\infty}^{\infty} \left(\sum_{t=1}^{T_n} \mathrm{P}_n\{\text{state sequence}_t \mid \nu\} \times \delta_n^{FM}(t) \right) f(\nu) d\nu \right\} \qquad (4.19)$$

4.3.4 Discussion

As mentioned above, in order to merge in heavily congested traffic, drivers must create gaps either through force or through courtesy yielding. A reasonable way to define heavy traffic congestion is level of service F defined by the Highway Capacity Manual (HCM 1985). The HCM characterizes this level of service as traffic conditions in which a breakdown of flow occurs and queues form behind breakdown points. At this level of congestion, the probability of finding acceptable gaps is very low and in order to merge gaps have to be created. For level of services A through E, drivers are assumed to merge by the gap acceptance process presented in Section 4.2.2.

The boundary (level of services F versus A through E) that is used to determine whether to apply the usual gap acceptance process or the forced merging process is rather arbitrary. Although the boundary can also be estimated formally (e.g. like the headway threshold in the acceleration model), the process the drivers actually follow may be different. For example, drivers first search for acceptable gaps and consider forced merging only when they perceive the probability of finding acceptable gaps to be very low. Further research is necessary to combine the mandatory lane changing and forced merging models into a single framework which would apply to all level of services. We leave this as a subject for future research.

4.4 Conclusions

In this chapter, a framework for modeling drivers' lane changing behavior was developed. A significant enhancement to the state of the art is the development of the forced merging model that captures merging behavior under heavy traffic congestion. This model is based on the assumption that in heavily congested traffic, gaps of acceptable lengths are rare, and therefore, for a vehicle to merge, gaps must be created either through courtesy yielding of the lag vehicle in the target lane or through the subject forcing the lag vehicle to slow down.

Chapter 5

Data Requirements for Estimating Driver Behavior Models

In this chapter, the data required to estimate the acceleration and lane changing models and the data that was obtained from real traffic are presented. In addition, a methodology for estimating instantaneous speed and acceleration that are required for model estimation from discrete trajectory data that can be obtained from the field is developed.

Data required to estimate the acceleration and lane changing models include the position, speed, acceleration, and length of a subject vehicle and the vehicles ahead of and behind the subject in the current lane as well as in adjacent lanes. Data on gap lengths, headways, density of traffic, etc. can be extracted from the above mentioned data by simple addition and subtraction operations. In addition, to capture the impact of site specific factors, such as the speed limit of a section, geometry (curvature, grade, and lane configuration) and whether the roadway section is a tunnel or not, data from different sites is required.

Typically, such data is collected using photographic and video equipment (see, for example, Smith (1985)). The raw data collected through such devices is processed to obtain useful information such as vehicle location at discrete points in time. Instantaneous speed and acceleration data, that is required for estimation of the models, have to be inferred from the trajectory data.

This chapter begins with a description of the method that is used to estimate instantaneous speed and acceleration from discrete trajectory data. Then the data collection strategy and the actual processing of the data is presented.

5.1 Methodology for Estimating Instantaneous Speed and Acceleration from Discrete Trajectory Data

As mentioned above, the data usually available includes discrete measurements of vehicle positions over time. A continuous function describing the vehicle trajectory can be estimated from the discrete position observations using the local regression procedure developed by Cleveland and Devlin (1988). Once the trajectory function, $X(t)$, is estimated, the first and second derivatives of the estimated trajectory function at time t, provide estimates of the speed and acceleration at time t respectively. Mathematically,

$$\begin{aligned} V(t) &= \frac{dX(t)}{dt} \\ a(t) &= \frac{d^2X(t)}{dt^2} \end{aligned} \tag{5.1}$$

where,

$$\begin{aligned} V(t) &= \text{speed at time } t, \\ a(t) &= \text{acceleration at time } t. \end{aligned}$$

In general, vehicles frequently stop in congested traffic, often for significant durations. Whether a vehicle is stopped or not, cannot be ascertained from the observed trajectory, as there are measurement errors while collecting and processing the data. A very high order polynomial would be necessary to fit a curve to the trajectories of such vehicles. This gives rise to computational problems as the objective function of

such problems becomes nearly singular[1]. Furthermore, even a high order polynomial may not fit the data well during the instances when a vehicle is stopped. The local regression procedure addresses some of these problems by fitting local curves using the observations around the time period of interest which is described in more detail in Section 5.1.1.

Local regression can be used to estimate a wide class of functions. Three major uses of local regression were listed by Cleveland and Devlin (1988). First, a local regression estimate can be used as a graphical exploratory tool to study the structure of the data. This would help in choosing an appropriate functional form that fits the data. Second, it can be used to validate an already estimated model that used a parametric class of models. And finally, local regression estimates can be used instead of regular regression estimates when dealing with data that require very flexible functional form. The application in this research falls in the third category.

5.1.1 The Local Regression Procedure

The local regression procedure has three basic elements: weight assignment, function specification, and neighborhood or window size. A unit weight is assigned to the trajectory observation at the time period of interest (t) and a gradually decreasing weight is assigned to the other points, depending on their distance from the t^{th} observation. The window size around time t determines the number of points that are used for fitting a polynomial curve of a suitable degree.

Weight Assignment. A tricube weight function with the following functional form is used:

$$w(t_o, t) = (1 - u(t_o, t)^3)^3 \tag{5.2}$$

[1]For polynomials of order 10 or above, the hessian of the objective function becomes nearly singular as the independent variables (polynomial of time) vary from tens and twenties to billions. This also depends on the precision of the computer. Nearly singular hessian makes the estimation process computationally intensive and time consuming as the convergence rate reduces significantly.

where,

$$
\begin{aligned}
t &= \text{time period at which speed/acceleration estimates are desired,} \\
w(t_o, t) &= \text{weight for observation at time } t_o,\ t_o \in \{1, 2, \ldots, t, \ldots\}, \\
u(t_o, t) &= \text{distance function for an observation at } t_o \\
&= \frac{\mid t - t_o \mid}{d}, \\
d(t) &= \text{distance from } t \text{ to the farthest point + constant.}
\end{aligned}
$$

A small constant is added to d so that the distance function, u, is less than one for the observation farthest from t. This guarantees a non-zero weight for that observation. Note that, $0 \leq u(t_o, t) < 1$ and $0 < w(t_o, t) \leq 1\ \forall t_o$.

Function specification. As mentioned above, the trajectory function, $X(t)$, is assumed to be a polynomial of time. The parameters of a polynomial are uniquely identified if the order of the polynomial is at most one less than the number of observations (trajectory points). A perfect fit is obtained when the order of the polynomial is one less than the number of points.

Window Size. The window size determines the number of points used in each local regression. For example, a window size of 7 implies that the 7 closest (in terms of time of observation) position measurements including the measurement at the time period of interest (t) are considered for local fitting of data. The bias (variance) of the estimated position increases (decreases) with increasing window size (Cleveland et al. 1988). Depending on the type of application, the window size should be selected such that either the bias or the variance or the mean square error of the estimates is minimized. Note that, the mean square error is the sum of the bias squared and the variance. Since the proposed curve fit algorithm uses inequality constraints (discussed below), a close form solution for estimating the bias (or variance) does not exist. Instead, a sensitivity analysis can be conducted to evaluate the impact of the window size on the quality of the results (e.g. magnitude of the position estimation errors, the speed and acceleration profiles etc.).

Mathematically, the curve fit problem using the local regression can be stated as:

$$\min_{\gamma^{t,s} \in \Re^m} \quad [X(t,s) - T(t,s)\ \gamma^{t,s}]'\ \ W(t,s)\ \ [X(t,s) - T(t,s)\ \gamma^{t,s}] \tag{5.3}$$

where,

$$\begin{aligned}
t &= \text{time period at which speed/acceleration estimates are desired,} \\
s &= \text{window size,} \\
X(t,s) &= \text{vector of discrete trajectory observations corresponding to time} \\
&\quad \text{period } t \text{ and window size } s, \\
T(t,s) &= \text{matrix of independent variables, } constant, time, time^2, \ldots, time^m, \\
\gamma^{t,s} &= \text{vector of parameters corresponding the } t^{th} \text{ time period and window} \\
&\quad \text{size } s, \\
m &= \text{order of the polynomial,} \\
W(t,s) &= \text{weight function, a diagonal matrix.}
\end{aligned}$$

The i^{th} diagonal element of $W(t,s)$ corresponds to the weight assigned to the i^{th} trajectory observation obtained by using Equation 5.2.

However, it is very common that in the data due to measurement errors, the measured position of a vehicle at two successive time periods may be decreasing. Hence, a curve fitted to these points may yield an unrealistic (negative) speed and/or acceleration estimates. To guarantee that the speed estimates are non–negative and acceleration estimates are within the acceleration and deceleration capacities, Equation 5.3 has to be minimized subjected to the following set of constraints over the range of time periods considered in a particular local regression:

$$\begin{aligned}
\text{speed} &\geq 0 \\
\text{acceleration} &\geq \text{maximum deceleration} \\
\text{acceleration} &\leq \text{maximum acceleration}
\end{aligned} \tag{5.4}$$

The curve fit algorithm (Equation 5.3 subjected to constraints 5.4) is repeated for each driver for each instant of time at which position, instantaneous speed and/or acceleration are desired. Then for each instant of time, the fitted value of the polynomial is used as an estimate of position and the first and second derivatives of the polynomial as the speed and acceleration respectively.

Figure 5-1 shows an example of estimating the speed and acceleration at time

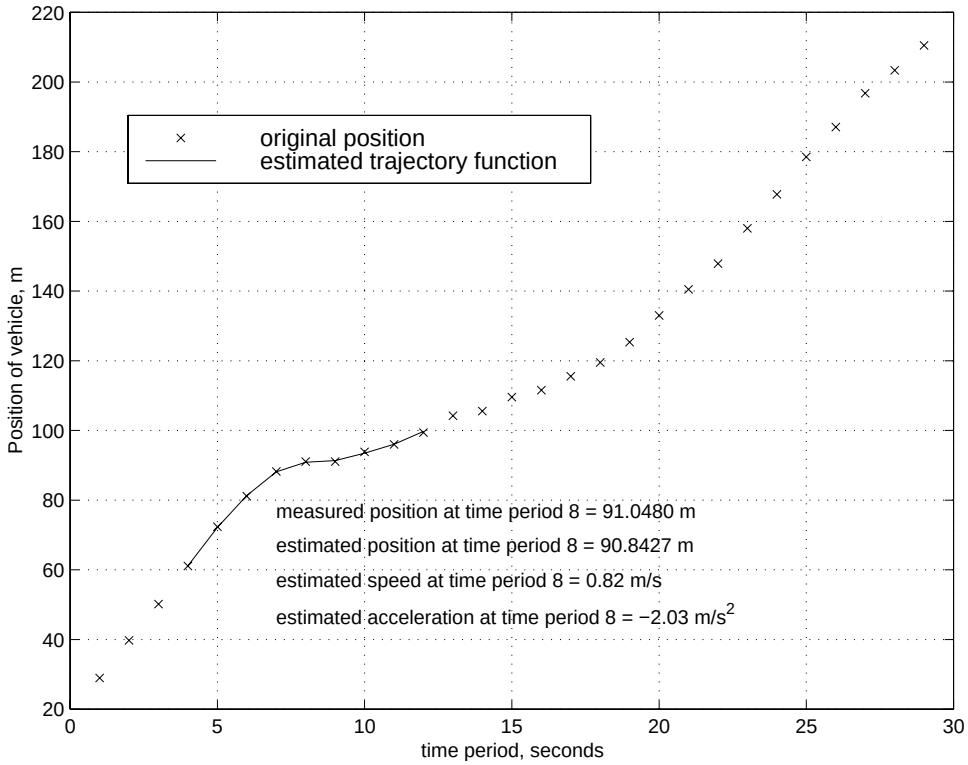

Figure 5-1: An example of estimation of instantaneous speed and acceleration from discrete position measurements.

period 8 from discrete position measurements of a vehicle using the local regression methodology. A window of size 9 was used in this exercise. Figure 5-2 shows the weight function used in this exercise and fitted curve. The trajectory function was fitted from the discrete position measurements around time period 8 (time periods 4 to 12). As shown Figure 5-2, a very good fit of the data was obtained except for time periods 8 and 9. Vehicle position at time periods 8 and 9 was measured at 91.05 and 91.04 meters respectively. Since, vehicle position cannot decrease (which implies an unrealistic negative average speed), the position measurement either at time period

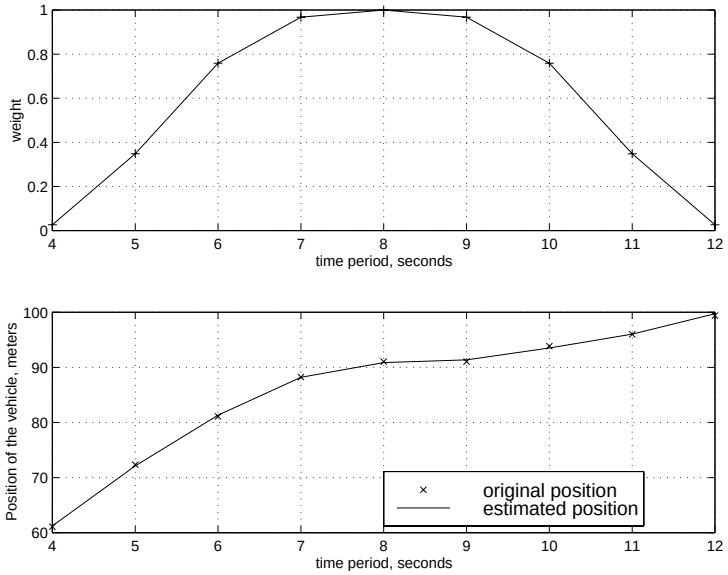

Figure 5-2: The weight function and the fitted curve for an observation at time period 8.

8 or at time period 9 must be erroneous. When the local regression procedure is used, the speed non–negativity constraint (Equation 5.4) takes care of this problem. Using the local regression procedure, the position at time period 8 was estimated to be 90.84 meters. Observe that, fitting a single curve to the observations in Figure 5-1 would require a polynomial of a very high degree.

5.2 Data Collection

Data was collected using standard video equipment. The video tapes were analyzed using VIVA, an image processing software specially designed for traffic application (described in Section 5.2.2).

5.2.1 Description of the Data Collection Site

Video data of traffic flow was collected on Interstate 93 at the Central Artery, located in downtown Boston (the rectangle area in Figure 5-3). The video was processed using the VIVA software package (described in Section 5.2.2). The manual and automatic features of VIVA were used to process congested and uncongested to semi congested

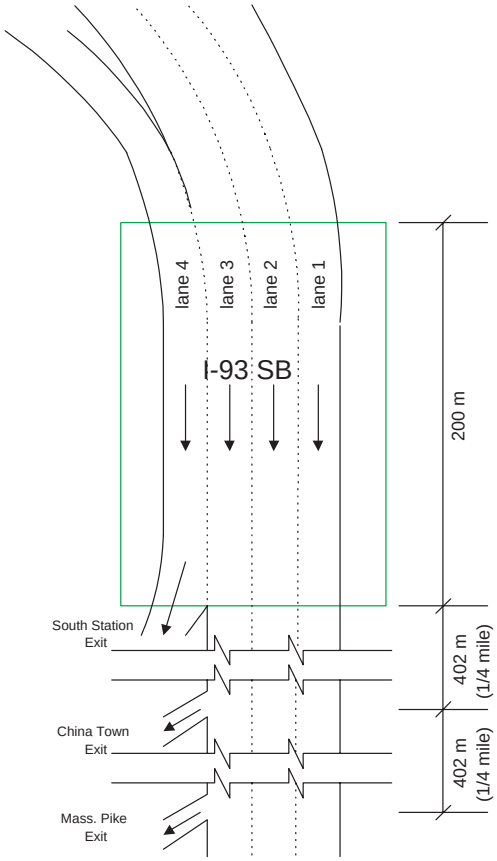

Figure 5-3: Schematic diagram of the I–93 southbound data collection site (figure not drawn to scale).

traffic respectively to obtain discrete measurements of vehicle lengths and positions over time. The processed data was then used to obtain vehicle trajectories.

The section has a three lane mainline (lanes 1 to 3) and a weaving lane (lane 4). The mainline lanes continue into an underground tunnel. The weaving section leads to Exit 22 (The South Station Exit). There are two more exits further downstream from this section. The first exit is 1/4 mile away (Exit 21, The Kneeland Street and Chinatown Exit) and the second exit is 1/2 mile away (Exit 20, The Massachusetts Turnpike and Albany Street Exit).

Trajectory and vehicle length data was extracted for vehicles only when they were within the rectangular area shown in Figure 5-3. The length of the recorded section varied from 150 to 200 meters as different zooms were used during the filming process (see Table 5.1). Data was collected for 2 hours starting at 10:26 a.m. (tape 1) on

Table 5.1: Description of the collected traffic video.

	Date	Time (hrs)	Length of the Section (meters)
tape 1	8/9/95	10:26 to 12:26	200
tape 2	12/10/97	12:30 to 13:00	165
tape 3	12/10/97	13:09 to 13:39	190
tape 4	12/10/97	13:47 to 14:17	150
tape 5	12/10/97	14:25 to 14:55	180

August 9, 1995, and for 30 minutes each starting at 12:30 p.m. (tape 2), 1:09 p.m. (tape 3), 1:47 p.m. (tape 4), and 2:25 p.m. (tape 5) on December 10, 1997. On both days of recording, the sky was overcast with periodical sunshine.

Vehicles that traveled in the mainline lanes and made no lane changes provide samples for estimating the acceleration model. Vehicles from lanes 2 or 3, that changed to the left adjacent lane or did not change lanes within the data collection site, provide samples for estimating the discretionary lane change model (see discussion on page 121). Vehicles that traveled from the on–ramp and merged with the mainline provide samples for estimating the mandatory lane change and forced merging models.

5.2.2 Video Processing Software

VIVA[2] (Video Traffic Analysis System) is an image processing software developed at Universitat Kaiserslautern, Germany. It is capable of measuring positions of vehicles from video images. It has both an automatic and a manual feature. The automatic feature extracts positions of all vehicles within the video image in real time. However, in heavily congested traffic, due to lack of spacing between vehicles, the software runs into difficulty in identifying front and rear bumpers of closely spaced vehicles and hence the position estimates become unreliable. In such situations, the manual feature can be used to identify vehicle positions (by clicking on the screen) and the software generates the coordinates of vehicle positions. The manual process, however,

[2]Information about this software package may be found in the World Wide Web at the URL http://transport.arubi.uni–kl.de/ViVAtraffic/English.

is very time consuming. An initial testing indicated that the manual feature requires approximately 30 person–hours to process one minute of video data.

The accuracy associated with the position measurements from the video images depends on the sharpness of the images and the scale of the images. In the automatic feature, VIVA uses the contrast between the image of a vehicle and that of the underlying pavement to identify the vehicle. In the manual process, the user identifies the vehicle. Therefore, a sharper image compared to a blurred image and a larger scale[3] compared to a smaller scale would increase the accuracy with which the bumpers of the vehicles can be identified on which the accuracy of position measurement depends. The position measurement error for the video that we collected was estimated to be ± 1 meter.

5.2.3 Processing the Traffic Data

Description of the Trajectory Data

The trajectory data obtained from processing the video data with VIVA included vehicle position recorded at discrete time points. The methodology described in Section 5.1 was used to develop vehicle trajectories and subsequently speed and acceleration profiles for each vehicle.

The first row of plots in Figure 5-4 shows minute by minute traffic flow at the upstream end of the data collection site, and the second and the third row of plots show second by second density and average speed of all vehicles of the mainline (lanes 1 to 3) respectively. The first column of plots corresponds to tape 1 data, the second column of plots corresponds to tape 2 data and so on.

Nine minutes of trajectory data was extracted from tape 1 using the manual feature of VIVA as traffic was extremely congested and at times stopped and the software's automatic data extraction feature would not work in such traffic conditions. Using the automatic feature, for the other four tapes that had less congestion, 30, 30, 21, and 18 minutes of trajectory data were extracted.

[3] A larger scale compared to a smaller scale implies that a vehicle would appear larger.

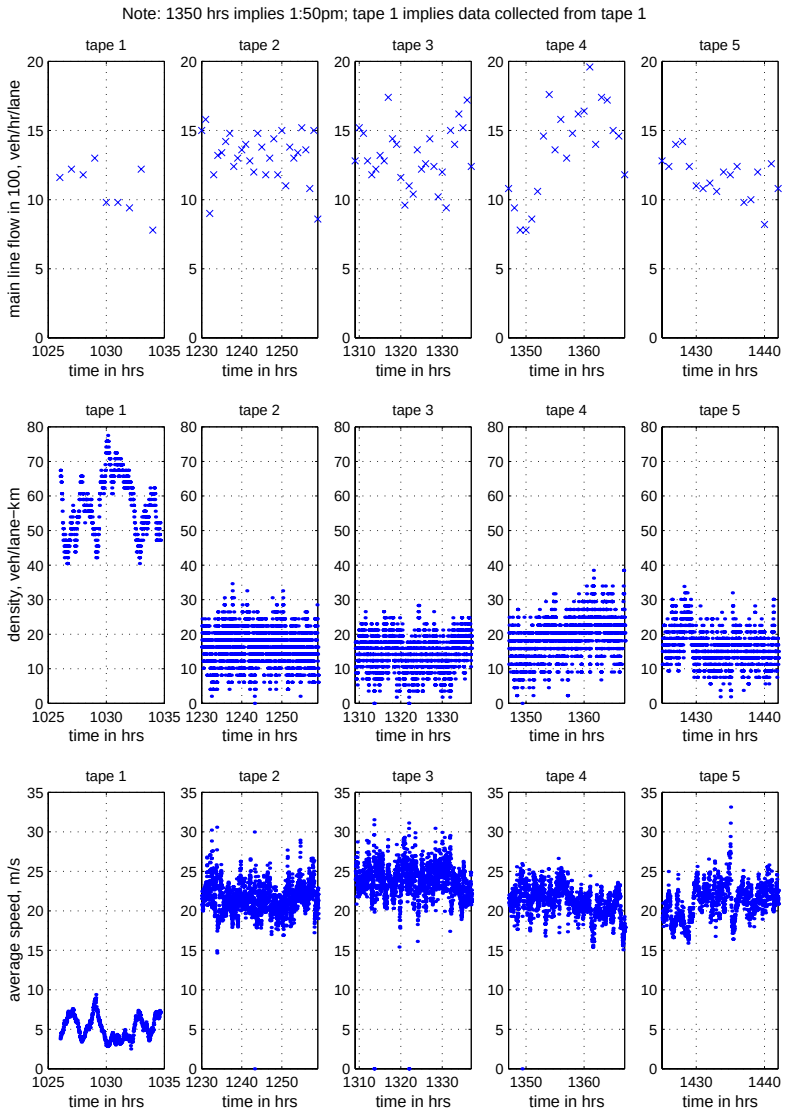

Figure 5-4: Flow, density, and average speed of the I–93 southbound trajectory data.

Although in the first 9 minutes of data, flow was in the order of 800 to 1300 vehicles/hr/lane (compared to a capacity of approximately 2000 vehicles/hr/lane), due to conditions downstream of the data collection site, traffic moved very slowly. This may have been in part due to a high volume of traffic trying to perform a lane change to take the two exits a quarter mile and a half mile downstream. The density, as shown in the 1st plot of row 2 in Figure 5-4, was always above 41 vehicles/km/lane which corresponds to level of service F (HCM 1985). The average speed of traffic across the mainline lanes varied from 3 to 10 m/s (meters per second) which is also

indicative of the heavy congestion.

Traffic in the last four tapes varied from free flow to semi congested with level of service between A and E. The last four columns of the first row of plots in Figure 5-4 show that the flow varied from 1000 to almost 2000 vehicles/hr/lane. Density, shown in the last four plots of the second row, varied from 0 to 40 vehicles/km/lane and never exceeded 41 vehicles/km/lane. The average speed of the mainline traffic varied from 15 to 33 m/s.

Estimation Results using the Local Regression Procedure

Window Size Selection

As mentioned above, depending on the type of application, the window size should be selected such that either the bias or the variance or the mean square error of the estimates is minimized. However, a close form solution for estimating the bias (or variance) does not exist since the curve fit algorithm uses inequality constraints (Equation 5.4). We, instead, conducted a sensitivity analysis to evaluate the impact of window size on the quality of the results. For this analysis we have used odd number of window sizes (e.g. 7, 9, 11 etc.) to make the number of observations before and after the time period of interest equal. The minimum window selected was 7. The reason for this choice is the following: with window size equal to 5, the order of the polynomial cannot exceed 4. As a result, the order of the polynomial representing the acceleration profile would be 2 (since the acceleration is obtained by taking the second derivative of the trajectory function). This implies that, the curvature of the acceleration profile (i.e., its second derivative) is restricted to be a constant. Windows of size 7 and above do not suffer from such a limitation.

The curve fit procedure was repeated for a subset of vehicles using window sizes 7, 9, 11, 13, and 15. Figure 5-5 shows the histograms of the absolute values of the position estimation error corresponding to the measured position of a driver using different window sizes. Although, in this case the mean of the absolute errors increased with the window size, such phenomenon was not observed when the sensitivity analysis was performed on the trajectories of other vehicles. Considering the ± 1 meter

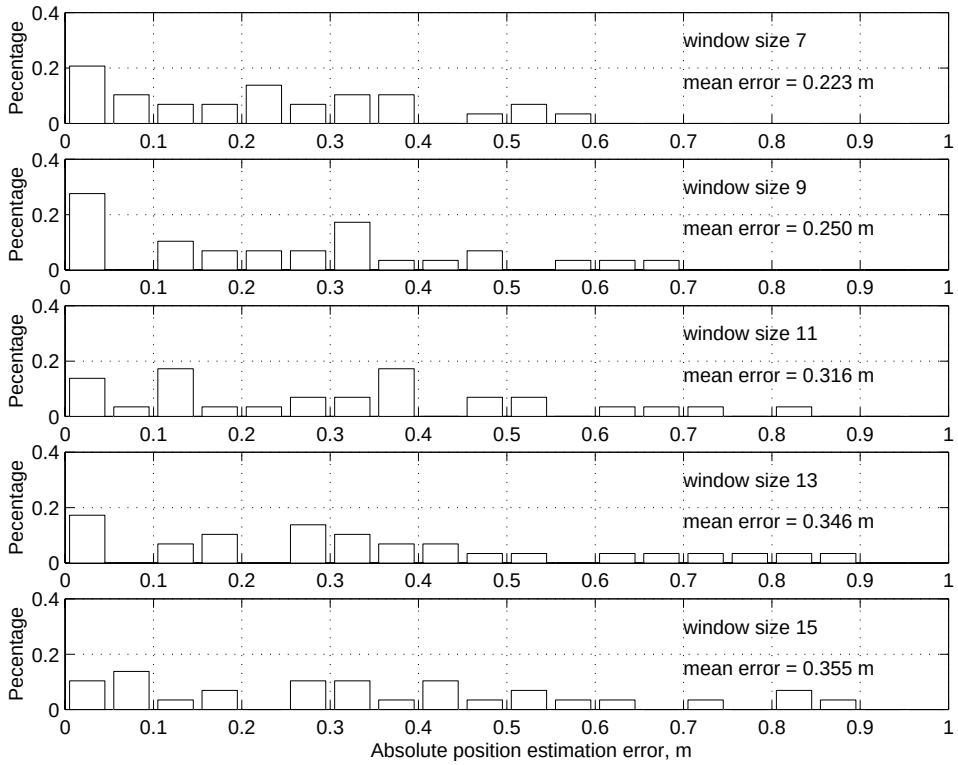

Figure 5-5: Histograms of the absolute values of the position estimation error using different window sizes.

accuracy associated with recording vehicle trajectories, the magnitude of errors for different window sizes is within a reasonable range.

The estimated speed and acceleration profiles of the vehicle for different window sizes are shown in Figure 5-6. Except for the first and last time periods, the speed and acceleration estimates do not differ significantly. Therefore, speed and acceleration estimates at these boundary points should not be used in estimating different driver behavior models. On the basis of these plots, any window size between 7 to 15 can be considered acceptable. Of these sizes, 9 was chosen since it strikes the best balance between accuracy and computational effort. Errors for window size greater than or equal to 9 were very similar (especially for the case of stopped vehicles).

Examples

Figure 5-7 shows two examples of curve fitting to the whole trajectory by applying the local regression procedure described above. In the second example (second plot of Figure 5-7), the vehicle was stopped for a few seconds. As shown in the figure, a

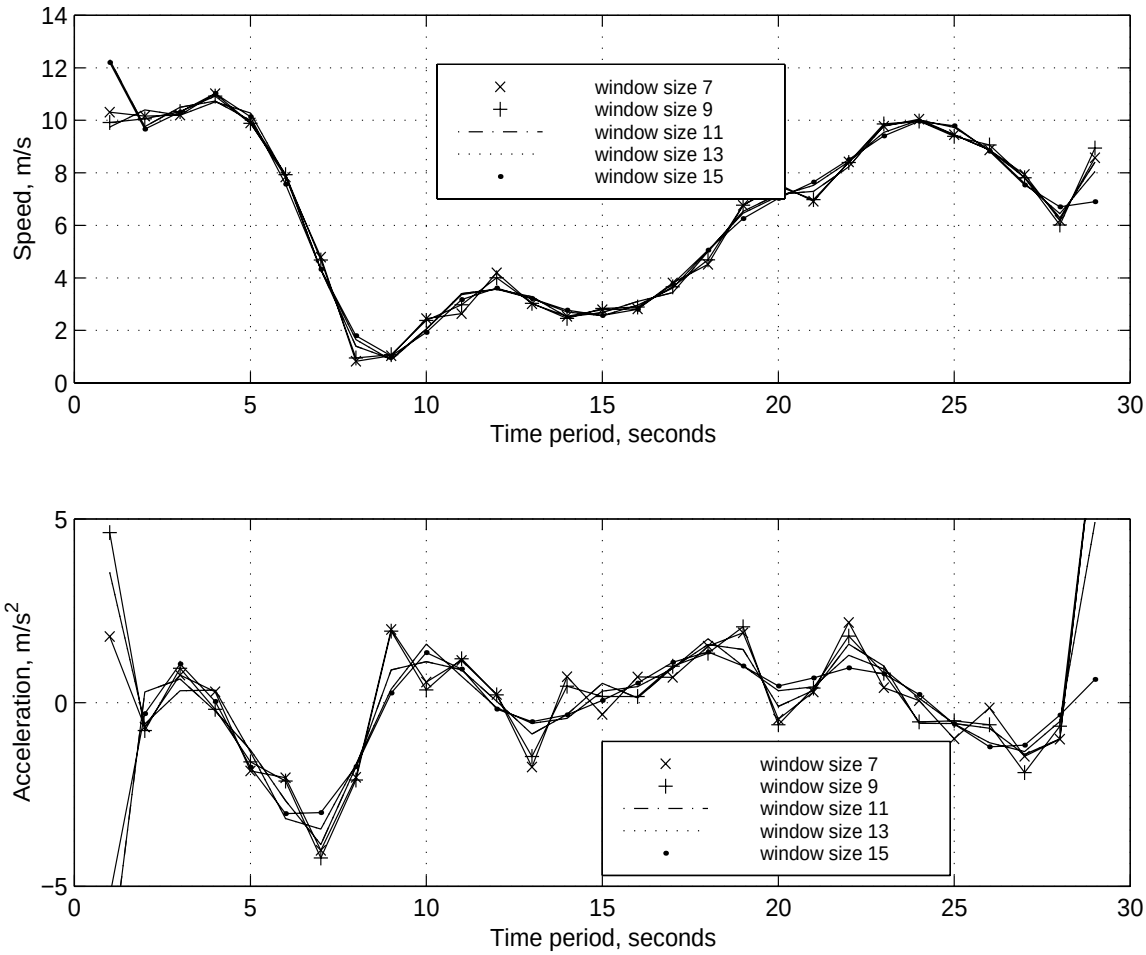

Figure 5-6: Estimated speed and acceleration profiles using different window sizes.

very good fit of the model was obtained in both cases.

Data for Estimating the Acceleration Model

The data required for estimating the acceleration model includes acceleration, speed, headway, and type of the subject vehicle, speed and type of its leader's vehicle, density ahead[4] of the subject, roadway curvature, grade, speed limit of the roadway section, and pavement surface quality.

The trajectory information described above was used to estimate acceleration,

[4]Although the data collection section is fairly straight, a visibility distance of 100 meters ahead of the driver was used while computing the explanatory variable density ahead. If, however, the distance from a vehicle' current position to the downstream end of the data collection site is less than 100 meters, the density of traffic ahead computed while this distance was greater than 100 meters is used as the density for this case.

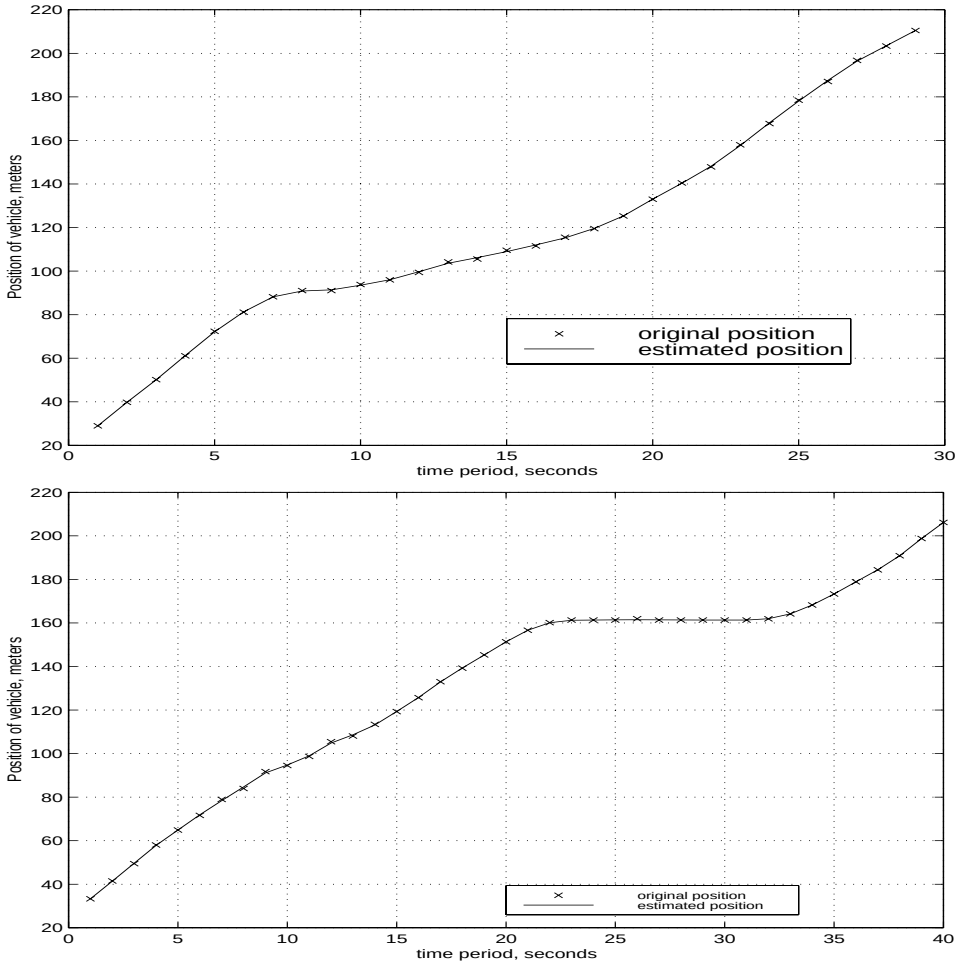

Figure 5-7: Examples of curve fitting by local regression.

speed, and space headways. The tapes were also used to collect data on vehicle length. Since the data was collected only from one site, site specific explanatory variables (for example, geometric characteristics) cannot be used. Observations for a driver were recorded from the instant the driver reached the upstream end of the data collection site. A sample of 1647 observations from 402 drivers was used for estimation.

An acceleration observation was recorded at a time instant such that the data on the traffic conditions τ_{max} seconds (the maximum reaction time) earlier can be obtained. We adopted the maximum of the range of τ_{max} to be considered while estimating the model equal to 4 seconds. This is because, 4 seconds is the most conservative value suggested in the literature (see, for example, Johansson and Rumer

(1971), Lerner et al. (1995), and Homburger and Kell (1988)). Therefore, the first acceleration observation was recorded at the 5^{th} second. Furthermore, since reaction time cannot vary for a given driver observed over a short period of time, explanatory variables for the reaction time model (for example, average front vehicle speed to be used as a proxy for vehicle travel speed) were obtained by averaging the observations recorded during the first five seconds, i.e., before the first acceleration observation recorded for the driver.

Figure 5-8 shows the histograms of the acceleration, subject speed, front relative

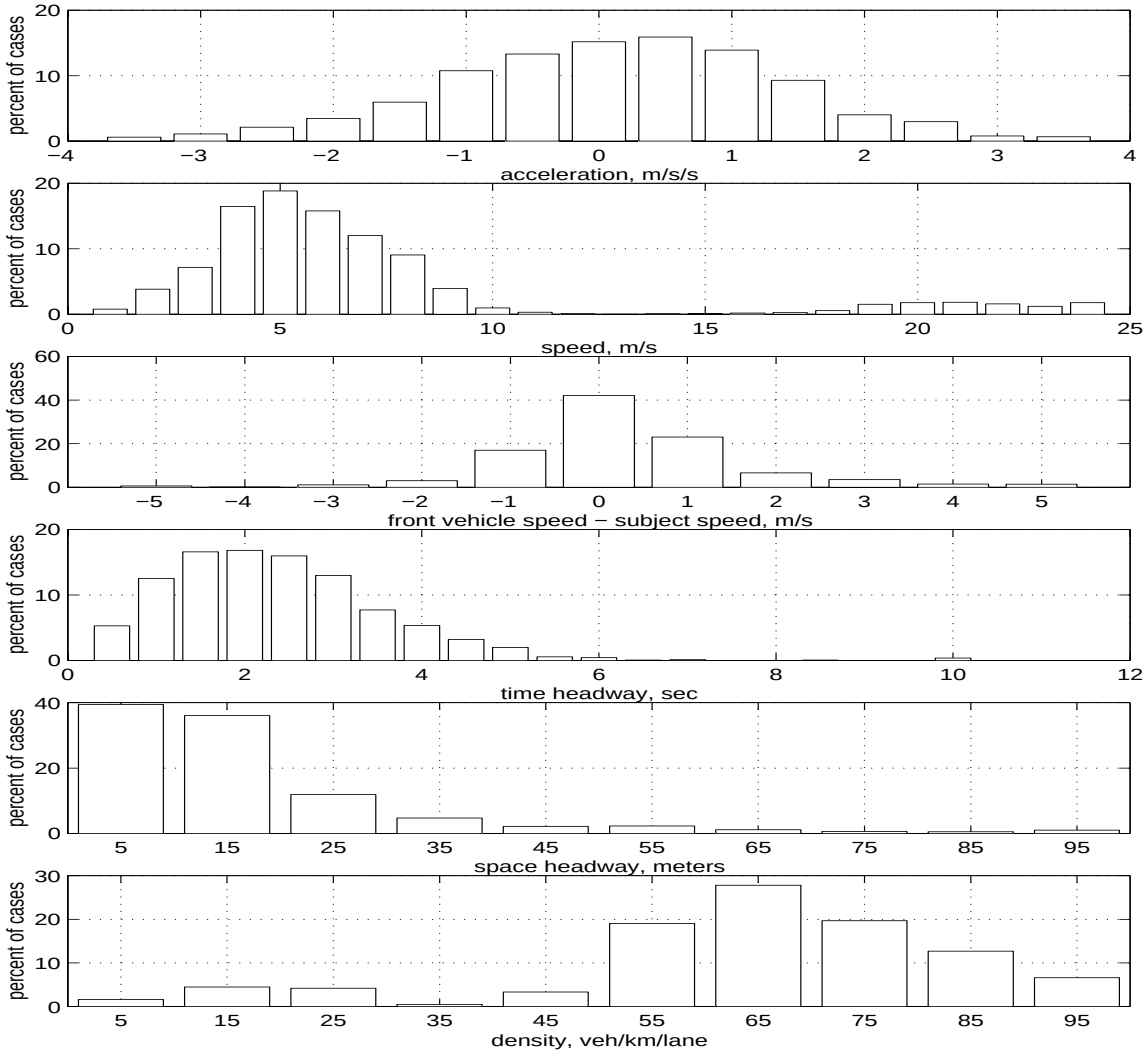

Figure 5-8: Histograms of the acceleration, subject speed, relative speed, time and space headway, and density in the data used for estimating the acceleration model.

speed, time and space headways, and density of traffic ahead of the subject of all

vehicles in the data. The second plot of Figure 5-8 shows two regimes: regime one represents heavily congested traffic with speeds varying between 0 and 12 m/s and the traffic density varying between 40 and 102 veh/km/lane, and regime two represents semi congested to uncongested traffic with speeds varying between 12 and 32 m/s and density below 40 veh/km/lane. Table 5.2 shows more statistics of the data.

Table 5.2: Statistics of the data used for estimating the acceleration model.

	acce-leration (m/s/s)	speed (m/s)	front Vehicle speed (m/s)	time headway (sec)	space headway (m)	density ahead (veh/km/lane)
maximum	7.28	27.1	32.3	15.1	152.1	102.0
minimum	-5.73	1.01	0.4	0.1	0.1	0.0
mean	0.12	7.2	7.5	2.4	17.2	64.4
median	0.19	5.7	5.8	2.2	12.1	66.7
std. dev.	1.29	5.2	6.0	1.3	17.2	19.8
number of drivers = 402						
number of observations = 1647						
percent of acceleration observations = 56.0 %						
mean and standard deviation of all acceleration observations: 1.02, 0.78						
mean and standard deviation of all deceleration observations: -1.02, 0.81						
percent of heavy vehicle = 19%						

The speed of the subject vehicle varied from 1 to 27 m/s. The traffic density varied between 7 and 103 vehicles/km/lane. The time headway varied from a fraction of a second to 15 seconds while the space headway varied from less than 5 meters to 152 meters. 54.0% of the observations were acceleration observations while the rest were deceleration observations. 19% of the vehicles were heavy vehicles (length greater than 9.14 meters or 30 feet). The data, therefore, represents a wide range of traffic conditions.

Data for Estimating the Discretionary Lane Changing Model

The data used for estimating the discretionary lane changing model consists of observations from 843 drivers. The total number of gaps observed was 4335, and the number of discretionary lane changes was 75

For each gap and driver, the data provides information on the lead, lag, and front gaps, vehicle length, speed, and acceleration of the subject, front, lead and lag vehicles (see Figure 5-9 for definition of different vehicles and gaps), density of traffic in the

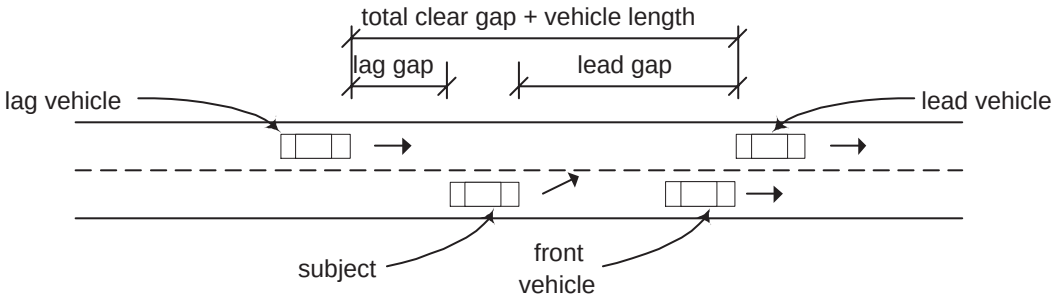

Figure 5-9: The subject and the front, lead, and lag vehicles.

current and target lanes, and whether the driver merged into this gap.

In some cases, there was no lead vehicle within the data collection site (rectangle area in Figure 5-3). To obtain the lead gap, the trajectory data from earlier time periods was searched to find the last vehicle that crossed the downstream boundary of the site from the target lane. Assuming that the vehicle continued in the same lane with the same speed, the lead vehicle's position was extrapolated to the time period in question to calculate the lead gap. Similarly, when there was no lag vehicle in the target lane, trajectory data from later time periods was searched to find the first vehicle that entered the upstream end of the target lane. Again, assuming that the lag vehicle traveled with the speed of its first appearance during this time span, the lag vehicle's position was extrapolated backwards to the time period in question to calculate the lag gap.

Statistics corresponding to the gaps that the drivers merged into (i.e., the gaps that were acceptable to the drivers) are shown in Table 5.3. The density of traffic in the target lane varied from 0 to 85 vehicles/km/lane. Vehicle speeds varied from 2 to 38 m/s with a mean around 18 m/s. As before, this represents a wide range of traffic conditions.

Table 5.3: Statistics of the discretionary lane changing model data corresponding to the gaps that the drivers merged into.

	lead gap (m)	lag gap (m)	front gap (m)	current lane density (veh/km)	target lane density (veh/km)	speed (m/s)	lead veh. speed (m/s)	lag veh. speed (m/s)	front veh. speed (m/s)
max.	192.5	232.5	166.6	84.9	75.8	28.1	37.9	25.7	37.3
min.	1.7	2.5	0.1	0.0	0.0	3.5	5.4	1.9	2.0
mean	35.1	36.1	29.5	24.8	22.3	16.9	20.1	16.8	17.4
median	22.3	26.9	16.2	18.2	16.9	18.5	22.8	19.4	19.3
std. dev.	41.8	34.5	35.0	21.4	16.1	7.0	8.1	6.5	7.9
number of drivers = 843									
number of observations = 4335									
number of lane change observations = 75									
percent of heavy vehicle (vehicle longer than 9.14 m) = 22%									

Data for Estimating the Mandatory Lane Changing Model

This data consists of observations from vehicles merging from the on–ramp to the mainline. As mentioned in Section 4.3.4, we assumed that drivers merge by gap acceptance when the level of service of the roadway section is between A and E and by gap creation (i.e., forced merging) when level of service is F. Therefore, to estimate the mandatory lane changing model, observations were recorded only when the level of service was between A and E, i.e., density was less than 41 vehicles/km/lane. A total of 500 observations was recorded from 202 drivers. For each driver, the observation includes a series of gaps. The last gap observed by each driver before he/she changed lanes, was considered acceptable, since at the next time period the driver was observed in the target lane.

The variables of interest for each gap and driver include the lead, lag, and front gaps, vehicle length, speed, and acceleration of the subject, front, lead and lag vehicles, delay or time elapsed since the subject crossed the merging point between the on–ramp and the freeway (section X–X in Figure 5-10), remaining distance to point at which the lane change must be completed (section Y–Y in Figure 5-10), and density of traffic in the target lane.

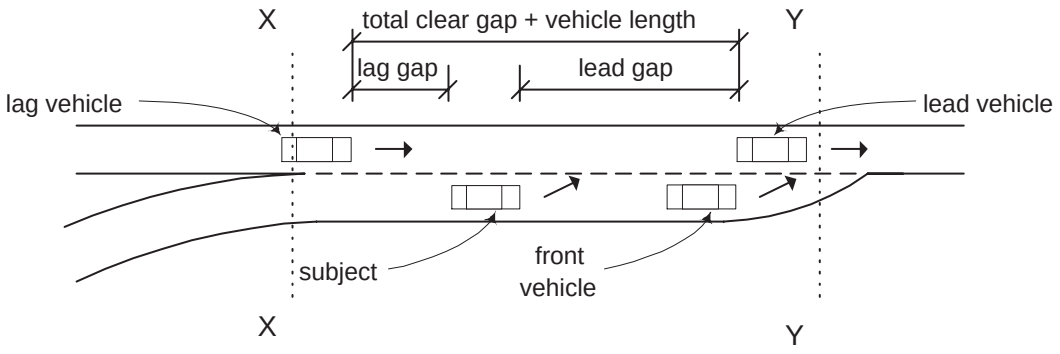

Figure 5-10: The subject, lead, lag, and front vehicles, and the lead and lag gaps.

Similar to the discretionary lane change data, in some cases there was no lead and/or lag vehicle within the data collection site. The technique described in Section 5.2.3 was applied here as well to infer the lead/lag gaps for such cases.

Statistics corresponding to the gaps that the drivers merged into (i.e., the gaps that were acceptable to the drivers) are shown in Table 5.4. The maximum and minimum delays in merging were 5 and 0 seconds respectively with a mean and

Table 5.4: Statistics of the mandatory lane changing model data corresponding to the gaps that the drivers merged into.

	lead gap (m)	lag gap (m)	delay (sec.)	rem. dis-tance (m)	adjac. lane density (veh/km)	speed (m/s)	lead veh. speed (m/s)	lag veh. speed (m/s)	front veh. speed (m/s)
max.	302.7	188.1	5.0	179.9	33.96	25.90	35.92	29.03	30.95
min	1.2	2.1	0.0	47.6	0.00	9.09	6.52	7.49	9.07
mean	44.8	36.2	1.8	129.5	15.83	18.48	20.86	18.10	20.78
median	28.3	27.4	2.0	135.4	15.92	18.75	20.36	18.23	20.94
std. dev.	44.6	31.4	1.2	26.4	8.36	3.14	4.71	3.11	4.43
number of drivers = 202 number of observations = 500 percent of heavy vehicle (vehicle longer than 9.14 m) = 4.5%									

standard deviation of 1.8 and 1.2 seconds respectively. The density of traffic in the target lane varied from 0 to 34 vehicles/km/lane—which is rather low and explains why the drivers experienced lower delay in merging. Vehicle speeds varied from 7 to

36 m/s with a mean around 20 m/s. The remaining distance to the point at which lane change must be completed varied from 48 to 180m with a mean, median, and standard deviation of 130, 135, and 26 meters respectively. This implies that, for a majority of the drivers in this data, remaining distance may not have significant influence on the merging process.

Data for Estimating the Forced Merging Model

The data consists of observations from vehicles merging from the on–ramp to the adjacent mainline. As mentioned in Section 4.3.4, we assumed that drivers merge by gap creation (i.e., forced merging) when the level of service of the roadway section is F. Therefore, observations were recorded only when the level of service was F, i.e., the traffic density was more than 41 vehicles/km/lane. A total of 998 observations was recorded from 79 drivers. Descriptive statistics of the data corresponding to the observations for the forced merging model are presented in Table 5.5.

Table 5.5: Statistics of the data used for estimating the forced merging model.

	lead gap (m)	lag gap (m)	delay (sec.)	rem. dis-tance (m)	mainline lane density (veh/km)	target lane density (veh/km)	speed (m/s)	lead veh. speed (m/s)	lag veh. speed (m/s)
max.	31.8	56.9	28.0	154	72.5	75.8	15.1	12.8	11.6
min	-13.2	-12.2	0.0	23	41.0	20.2	0.0	0.0	0.0
mean	4.3	7.8	9.5	103	57.9	58.8	5.1	5.2	5.0
median	3.7	3.6	8.0	102	59.0	60.7	4.8	5.1	4.8
std. dev.	6.0	11.9	6.3	27	7.9	10.1	2.8	2.5	2.6
number of drivers = 79									
number of observations = 566									
percent of heavy vehicle (vehicle longer than 9.14 m) = 5.1%									

The variables in the data, for each gap and driver, are the lead and lag gaps, vehicle length, speed, and acceleration of the subject, lead and lag vehicles, time elapsed since the subject crossed the merging point between the on–ramp and the freeway (section X–X in Figure 5-10), remaining distance to point at which the lane

change must be completed (section Y–Y in Figure 5-10), and density of traffic in the mainline lanes and the target lane.

The lead gap varied from -13.2[5] to 32 meters with a mean of 4.3 meters. The lag gap varied from -12 to 57 meters with a mean of 8 meters. The mean delay experienced by the drivers was 9.5 seconds compared to 1.8 seconds observed in the mandatory lane changing data (Table 5.4). The mainline traffic density varied from 40 to 73 vehicles/km/lane with a mean of 58 vehicles/km/lane representing a very congested traffic. The average speed of vehicles was around 5 m/s.

5.3 Conclusions

In this chapter, a methodology to estimate instantaneous speed and acceleration that are required for model estimation from trajectory data that can be obtained from the field using video technology is described. The methodology is based on the local regression procedure of Cleveland and Devlin (1988). The main advantage of this procedure, over the conventional regression, is that it allows for estimating position, speed, and acceleration profiles that, otherwise, would require fitting polynomials of a very high order. Although local regression estimates are less efficient, the flexibility of the method outweighs this disadvantage.

The characteristics of the freeway trajectory data (collected in the Central Artery, Boston) are also described. The data represents a wide range of traffic conditions, from very congested stop–and–go traffic to free flow. The traffic density varied from no vehicles within the data collection site to 90 vehicles/km/lane. In addition to the length of each vehicle that traveled in the section, the data contains position, speed, and acceleration of every vehicle for every second. Finally, descriptive statistics of the data used to estimate the acceleration model, the discretionary and mandatory lane changing models, and the forced merging model are presented.

[5]In this case, the lead vehicle and the subject were overlapping and the lead vehicle was a heavy vehicle.

Chapter 6

Estimation Results

In this chapter, estimation results of the acceleration and lane changing models, using the data described in Chapter 5, are presented. Along with the estimation results, assessment of the parameter estimates from statistical and behavioral standpoints are also presented.

In addition, parameter estimates of the car–following model, the headway threshold and reaction time distributions, and the gap acceptance model under mandatory lane changing situations are compared to those estimated by other researchers. No such comparison can be made for parameters of the free–flow acceleration model, the discretionary lane changing model, and the forced merging model since these have not been estimated before.

6.1 Estimation Results of the Acceleration Model

Given the complexity of the likelihood function, the estimation of the parameters was simplified by estimating the values of h^*_{min}, h^*_{max}, and τ_{max} non–parametrically. The overall estimation approach was based on the following algorithm:

1. Set $\{h^*_{min}, h^*_{max}, \tau_{max}\}$ to reasonable initial values.

2. Using the current values of $\{h^*_{min}, h^*_{max}, \tau_{max}\}$ specify and estimate the model using the maximum likelihood method (Equation 3.25).

3. Estimate the parameters of the model specification in step 2 for different set of values of $\{h^*_{min}, h^*_{max}, \tau_{max}\}$. Through this grid search procedure obtain the best $\{h^*_{min}, h^*_{max}, \tau_{max}\}$, i.e., the one with the highest likelihood value.

4. Iterate between steps 2 and 3 until the same set of $\{h^*_{min}, h^*_{max}, \tau_{max}\}$ is obtained.

The parameters h^*_{min}, h^*_{max}, and τ_{max} were initially set to 0, 8, and 3 seconds respectively. Using these values, step two was executed. In this step, we investigated different model specifications and simultaneously varied the parameter ξ (Equation 3.7) between the 0 to 1 range. The likelihood function attained its maximum at $\xi = 0$. Step three was performed next by varying h^*_{min}, h^*_{max}, and τ_{max}. Table 6.1 shows the values of the maximized likelihood function at different values of h^*_{min}, h^*_{max}, and

Table 6.1: Estimated likelihood function for different values of h^*_{min}, h^*_{max}, and τ_{max}.

$h^*_{max} = 6$			
	$h^*_{min} = 0$	$h^*_{min} = 0.5$	$h^*_{min} = 1$
$\tau_{max} = 3$	-2255.24	-2252.17	-2257.69
$\tau_{max} = 3.5$	-2256.00	-2257.49	-2256.25
$\tau_{max} = 4$	-2263.95	-2266.09	-2259.95
$h^*_{max} = 8$			
	$h^*_{min} = 0$	$h^*_{min} = 0.5$	$h^*_{min} = 1$
$\tau_{max} = 3$	-2254.61	-2258.63	-2257.69
$\tau_{max} = 3.5$	-2257.50	-2256.41	-2262.38
$\tau_{max} = 4$	-2263.47	-2274.23	-2265.05

τ_{max}. The likelihood function attained the maximum value for $\tau_{max} = 3$ seconds, $h^*_{min} = 0.5$ second, and $h^*_{max} = 6$ seconds. In the next iteration of step two, the same model specification was obtained as was used while executing step three. The parameter ξ was varied again between the range 0 to 1. Figure 6-1 shows the value of the likelihood function as a function of ξ. As before, the likelihood function attained its maximum value at $\xi = 0$. Since, experience with the model estimation indicated that the likelihood function may not be globally concave, we reestimated the model using different starting values of the parameters to obtain the best possible local maxima. We obtained the same solution for different starting values of the parameters.

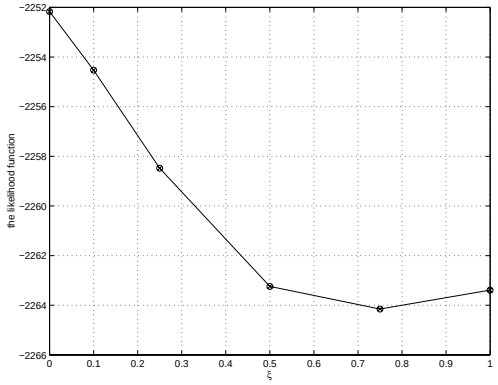

Figure 6-1: The likelihood function as a function of ξ.

Table 6.2 summarizes the estimation results. All the parameters, with the exception of the car–following acceleration sensitivity parameters, have the expected signs. Note that, a positive sign of the parameters of speed and headway in the car–following acceleration or deceleration model (Equations 3.2 and 3.7) implies that the variables are in the numerator and denominator respectively. The signs of the explanatory variables speed and density of the car–following acceleration model are not what we anticipated. Their t–statistics are highly significant. This indicates that Boston drivers may behave differently than the way we anticipated (see Section 3.2.1). The high acceleration sensitivity at high speeds and high densities indicate that drivers are more aggressive in this situations. This may be in part due to the drivers effort not to let anyone infront of them from an adjacent lane. The positive sign of the space headway parameter for the car–following acceleration model indicates that drivers tend to follow the speed of the lead vehicle less as the space headway increases.

In the car–following acceleration and deceleration models, except the constants, all the parameters have significant t-statistics at the 1% level of significance. The speed parameter for the car–following deceleration model had counterintuitive sign with a t–statistic of 0.64, and therefore, was dropped from the specification. The explanatory variable density has significant t-statistic for both the acceleration and deceleration models. Therefore, the proposed enhancement of the sensitivity term was supported by the data for both the acceleration and deceleration models.

Table 6.2: Estimation results of the acceleration model.

Variable	Parameter	t–stat.
Car–following acceleration		
constant	0.0225	1.08
speed (m/s)	0.722	4.67
space headway (m)	0.242	6.31
density (veh/km/lane)	0.682	4.20
relative speed (m/s)	0.600	7.20
$\ln(\sigma_{\epsilon^{cf,acc}})$	-0.193	-2.64
Car–following deceleration		
constant	-0.0418	-1.20
space headway (m)	0.151	5.32
density (veh/km/lane)	0.804	4.21
relative speed (m/s)	0.682	10.71
$\ln(\sigma_{\epsilon^{cf,dec}})$	-0.221	-5.44
Free–flow acceleration		
sensitivity constant	0.309	7.37
constant	3.28	6.83
front veh. speed (m/s)	0.618	10.04
heavy veh. dummy	-0.670	-1.54
indicator for density $\leq$ 19 (veh/km/lane)	7.60	5.51
$\ln(\sigma_{\epsilon^{ff}})$	0.126	1.99
Headway threshold distribution, $0.5 < h^* \leq 6$		
mean (sec)	3.17	13.90
σ_{ϵ^h}	0.870	3.82
Reaction time distribution, $0 < \tau \leq 3$		
constant	0.272	7.62
$\ln(\sigma_{\epsilon^\tau})$	-1.55	-9.59
number of drivers = 402		
number of observations = 1647		
$\mathcal{L}(0)$ = -2727.75		
$\mathcal{L}$(c) = -2561.26		
$\mathcal{L}(\hat{\beta})$ = -2252.17		
$\overline{\rho}^2 = 0.167$		

Note: Density $\leq$ 19 veh/km/lane implies level of services A through C (HCM 1985).

The test statistic for the null hypothesis that the stimulus is a linear function of the lead relative speed for the car–following acceleration model (i.e., $\lambda^{acc} = 1$) is given by:

$$\frac{\hat{\lambda}^{acc} - 1}{\sqrt{\text{var}(\hat{\lambda}^{acc})}} = \frac{0.600 - 1}{0.0834} = -4.79 \tag{6.1}$$

Therefore, the null hypothesis can be rejected at the 1% level of significance. Similar null hypothesis for the car–following deceleration model (i.e., $\lambda^{dec} = 1$) can also be rejected at the 1% level of significance (the t-statistic is equal to -4.99). These imply that the proposed extension of the the stimulus term to be a nonlinear function of the lead relative speed is supported by the data.

The free–flow acceleration model parameters with one exception have significant t–statistics at the 1% level of significance. The parameter for the heavy vehicle dummy does not have a significant t–statistic. Both the headway threshold distribution parameters are statistically significant at the 1% level of significance. The mean and standard deviation of the reaction time distribution are statistically significant at the 1% level of significance. The adjusted fit of the model[1] was 0.167.

The acceleration model estimation results for the case of $\xi = 1$ is presented in Table 6.3. $\xi = 1$ implies that the sensitivity is a function of the traffic conditions at the moment the driver perceives the stimulus and decides that he/she should respond to it. Hence, the explanatory variables affecting the acceleration sensitivity are observed at the time instant at which the stimulus is observed. As shown in Figure 6-1, this model has a significantly lower fit than the one in which has the best fit. By relaxing ξ to be a parameter to be estimated, the likelihood function improved by 11.2 units (for the $\xi = 0$ case) over this model (the $\xi = 1$ case). It is interesting to note that, although the car–following acceleration and deceleration model parameters are of different orders of magnitude, the free–flow acceleration model and the headway threshold and reaction time distribution parameters are of

[1] $\overline{\rho^2} = 1 - \frac{\mathcal{L}(\hat{\beta}) - \text{no. of parameters}}{\mathcal{L}(0)}$.

Table 6.3: Estimation results of the acceleration model for $\xi = 1$.

Variable	Parameter	t–stat.
Car–following acceleration		
constant	0.468	1.56
speed (m/s)	0.129	1.11
space headway (m)	0.194	5.44
density (veh/km/lane)	0.188	1.57
relative speed (m/s)	0.670	10.48
$\ln(\sigma_{\epsilon^{cf,acc}})$	-0.253	-5.48
Car–following deceleration		
constant	-0.0470	-1.25
space headway (m)	0.179	5.68
density (veh/km/lane)	0.791	4.31
relative speed (m/s)	0.749	11.12
$\ln(\sigma_{\epsilon^{cf,dec}})$	-0.235	-6.32
Free–flow acceleration		
sensitivity constant	0.316	8.31
constant	3.12	7.50
front veh. speed (m/s)	0.611	10.80
heavy veh. dummy	-0.638	-1.57
indicator for density $\leq$ 19 (veh/km/lane)	7.58	5.96
$\ln(\sigma_{\epsilon^{ff}})$	0.170	3.59
Headway threshold distribution, $0.5 < h^* \leq 6$		
mean (sec)	3.28	13.11
σ_{ϵ^h}	1.08	5.00
Reaction time distribution, $0 < \tau \leq 3$		
constant	0.307	8.89
$\ln(\sigma_{\epsilon^\tau})$	-1.34	-13.68
number of drivers = 402		
number of observations = 1647		
$\mathcal{L}(0)$ = -2727.75		
$\mathcal{L}$(c) = -2561.26		
$\mathcal{L}(\hat{\beta})$ = -2263.39		
$\overline{\rho}^2 = 0.163$		

Note: Density $\leq$ 19 veh/km/lane implies level of services A through C (HCM 1985).

the same order of magnitude. We adopt the model presented in Table 6.2 which has a significantly higher fit.

6.1.1 Discussion

The Car–Following Models

The estimated car–following acceleration model is

$$a_n^{cf,acc}(t) = 0.0225 \frac{V_n(t)^{0.722}}{\Delta X_n(t)^{0.242}} \; k_n(t)^{0.682} \, |\Delta V_n(t-\tau_n)|^{0.600} + \epsilon_n^{cf,acc}(t) \qquad (6.2)$$

where,

$$\begin{aligned}
t &= \text{current time period,} \\
\tau_n &= \text{reaction time for driver } n, \\
V_n(t) &= \text{subject speed at time } t \text{ (m/s)}, \\
\Delta X_n(t) &= \text{space headway at time } t \text{ (m)}, \\
k_n(t) &= \text{density of traffic ahead of the subject (veh/km/lane)}, \\
\Delta V_n(t-\tau_n) &= \text{front vehicle speed – subject speed (m/s)}, \\
\epsilon_n^{cf,acc}(t) &\sim \mathcal{N}(0, 0.825^2).
\end{aligned}$$

The estimated car–following deceleration model is

$$a_n^{cf,dec}(t) = -0.0418 \frac{1}{\Delta X_n(t)^{0.151}} \; k_n(t)^{0.804} \, |\Delta V_n(t-\tau_n)|^{0.682} + \epsilon_n^{cf,dec}(t) \qquad (6.3)$$

where, $\epsilon_n^{cf,dec}(t) \sim \mathcal{N}(0, 0.802^2)$.

Figure 6-2 shows the sensitivity of different factors on the car–following acceleration and deceleration. Acceleration increases with speed, density, and relative speed, and decreases with space headway. On the other hand, deceleration (in absolute term) increases with density and relative speed (in absolute term), and decreases with headway.

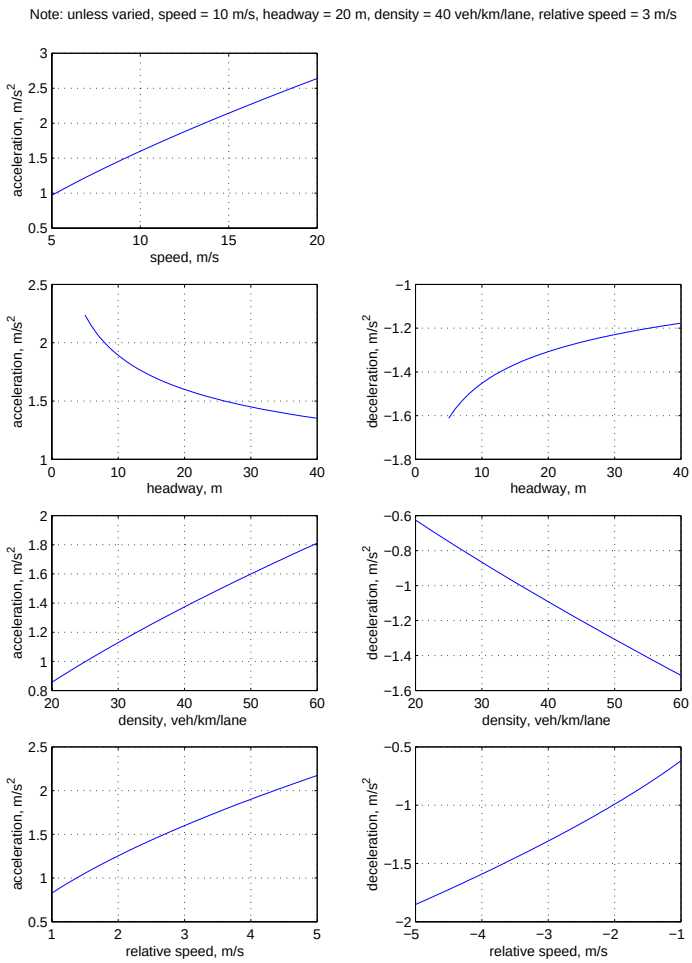

Figure 6-2: Sensitivity of different factors on the car–following acceleration and deceleration decisions.

At low speeds the mean acceleration is lower compared to those for higher speeds. Traffic conditions ahead of the subject and its leader are likely to change more rapidly at high densities than at low densities. Due to this, higher uncertainty is involved in predicting the position and speed of the leader in the near future. As a result, drivers are expected to be more conservative at high densities than at low densities. Although the mean deceleration increases with density, the mean acceleration does not decrease with density as we had expected.

The slopes of the acceleration and deceleration curves with respect to the relative speed are decreasing. This captures the fact that, the acceleration (deceleration) applied by a driver is limited by the acceleration (deceleration) capacity of the vehicle and acceleration (deceleration) gradually reaches the capacity as the relative speed

increases.

Figure 6-3 shows a comparison between the estimated car–following acceleration and deceleration at different front gaps as a function of subject speed using the models proposed in this thesis with those obtained by Subramanian (1996)[2]. The acceleration

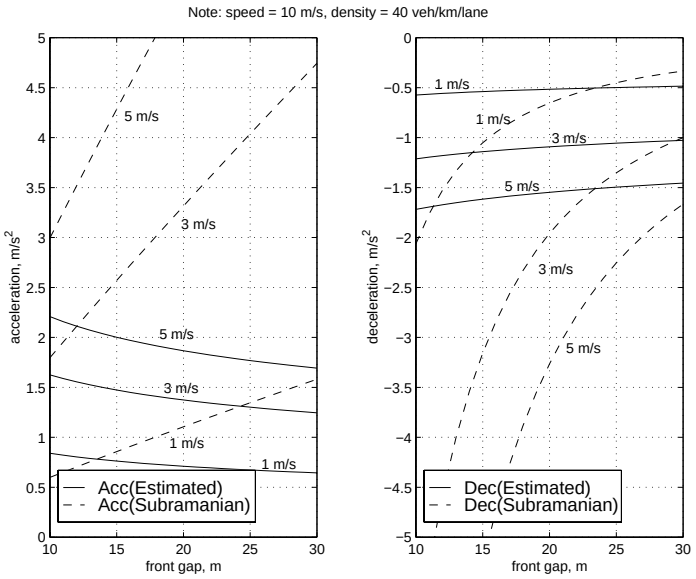

Figure 6-3: Comparison between the car–following acceleration and deceleration estimated in this thesis with those obtained by Subramanian (1996).

and deceleration estimated in this thesis are generally smaller in magnitude compared to those estimated by Subramanian. At low speeds, his acceleration and deceleration estimates are too high. The acceleration estimated by the model proposed in this thesis is smaller than expected, while the estimated deceleration is reasonable. This may be due to lack of variability in the data with acceleration observations or may be due to the influence of the geometric characteristics of the Boston data collection site.

The difference between the two models may be due to several reasons. First, Subramanian used data that was collected in 1983 from a section of Interstate 10 Westbound near Los Angeles, whereas, this research used data that was collected in 1995 and 1997 from a section of Interstate 93 Southbound in Boston. The different data collection years and sites may have contributed to the differences in the estimates.

[2]The parameters estimated by Subramanian (1996) are presented in Table 2.3.

Second, the LA data collection site is a fairly straight section without any ramps, whereas, the Boston data collection site has a weaving section adjacent to the freeway. The geometry of the freeway and the number of lane changes taking place in the Boston data may have an effect on the estimates obtained in this research. Finally, Subramanian assumed that all the drivers in the data were car–following even at large space headways. He further investigated the implication of this assumption and concluded that the assumption on the headway threshold has significant impact on the car–following model estimates. The estimation results presented in this thesis do not suffer from such a limitation.

The Free–Flow Acceleration Model

The estimated free–flow acceleration model is

$$\begin{aligned} a_n^{ff}(t) &= 0.309\ [3.28 + 0.618\ V_n^{front}(t-\tau_n) - 0.670\ \delta_n^{heavy} \\ &\quad +7.60\ \delta[k_n(t-\tau_n)] - V_n(t-\tau_n)] + \epsilon_n^{ff}(t) \end{aligned} \tag{6.4}$$

where,

$$\begin{aligned} V_n^{front}(t-\tau_n) &= \text{front vehicle speed at time } (t-\tau_n) \text{ (m/s)}, \\ \delta_n^{heavy} &= \begin{cases} 1 & \text{if the subject vehicle is a heavy vehicle} \\ & \text{(vehicle length} \geq 9.14 \text{ m or 30 ft)} \\ 0 & \text{otherwise} \end{cases} \\ \delta[k_n(t-\tau_n)] &= \begin{cases} 1 & \text{if } k_n(t-\tau_n) \leq 19 \text{ veh/km/lane} \\ 0 & \text{otherwise} \end{cases} \\ \epsilon_n^{ff}(t) &\sim \mathcal{N}(0, 1.13^2). \end{aligned}$$

The estimated free–flow acceleration increases with front vehicle (leader) speed. A higher acceleration for level of services A through C captures the effect of higher maneuverability at low densities compared to high densities. The impact of lower maneuverability for the heavy vehicles compared its non–heavy counterparts is cap-

tured by an indicator whether the subject vehicle is heavy. The standard deviation of the free–flow acceleration is high compared to its car–following acceleration and deceleration counterparts.

The Headway Threshold Distribution

The headway threshold (seconds), that defines whether a driver is in the car–following regime or in the free–flow regime, is distributed as follows (see Figure 6-4):

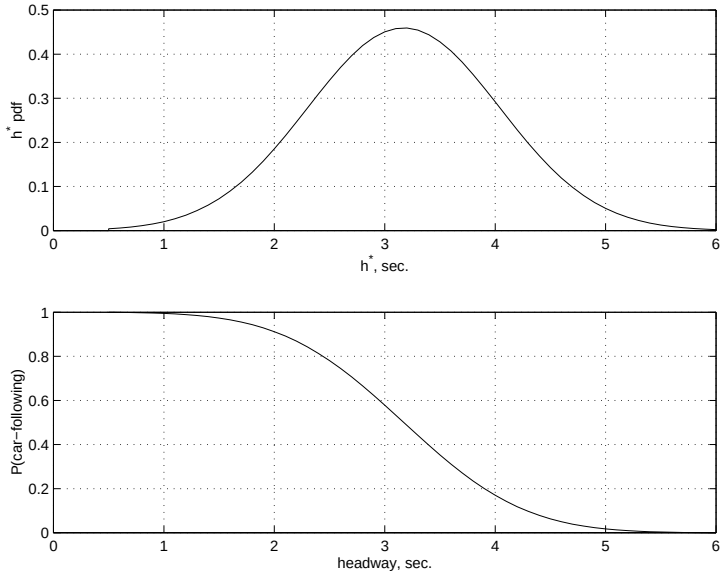

Figure 6-4: The headway threshold distribution and the probability of car–following as a function of time headway.

$$f(h^*) = \begin{cases} \frac{1}{0.868}\phi\left(\frac{h^*-3.17}{0.870}\right) & \text{if } 0.5 < h^* \leq 6 \\ 0 & \text{otherwise} \end{cases} \tag{6.5}$$

For a given headway, $h_n(t)$, the probability that driver n is in the car–following regime is given by:

$$\text{P(car–following at time } t) = \begin{cases} 1 & \text{if } h_n(t) \leq 0.5 \\ 1.00 - \frac{1}{0.998}\Phi\left(\frac{h_n(t)-3.17}{0.870}\right) & \text{if } 0.5 < h_n(t) \leq 6 \\ 0 & \text{otherwise} \end{cases} \tag{6.6}$$

The 5, 50, and 95 percentile values of the headway threshold are 1.75, 3.17, and 4.60 seconds respectively. These values are reasonable.

Figure 6-5 shows the mean of the headway threshold as a function of subject

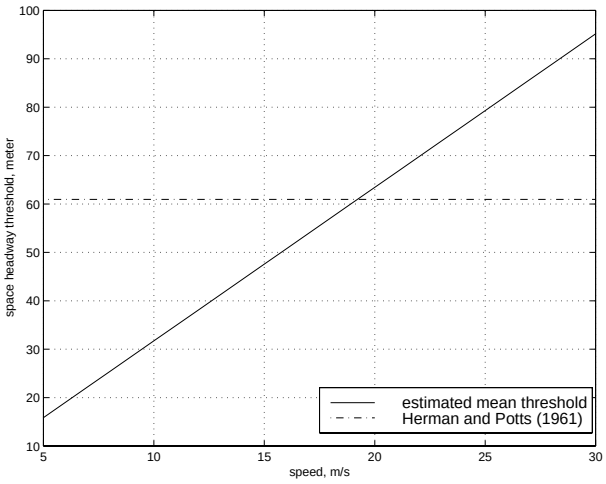

Figure 6-5: Comparison between the estimated mean headway threshold and the 61 meters threshold suggested by Herman and Potts (1961).

speed. In the Traffic Engineering Literature (Herman and Potts 1961)[3] a threshold of 61 meters (200 ft) is usually used to distinguish the free–flow regime. As shown in Figure 6-5, the 61 meters threshold is too high at low speeds while the threshold estimated in this thesis is high at high speeds. The two estimates are in close agreement in the 15 to 23 m/s speed range.

The Reaction Time Distribution

The estimated distribution of reaction time is

$$f(\tau) = \begin{cases} \dfrac{1}{0.212\ \tau\ \sqrt{2\pi}}\ \mathrm{e}^{-\frac{1}{2}\left(\frac{\ln(\tau)-0.272}{0.212}\right)^2} & \text{if } 0 < \tau \leq 3 \\ 0 & \text{otherwise} \end{cases} \tag{6.7}$$

[3]Herman and Potts (1961) estimated this 61 meters thresholds based on an observation that, the correlation between the observed accelerations and the accelerations estimated by the car–following model was low when the space headways were greater than 61 meters.

Figure 6-6 shows the probability density function and the cumulative distribution function of the reaction time. The median, mean, and standard deviation of the

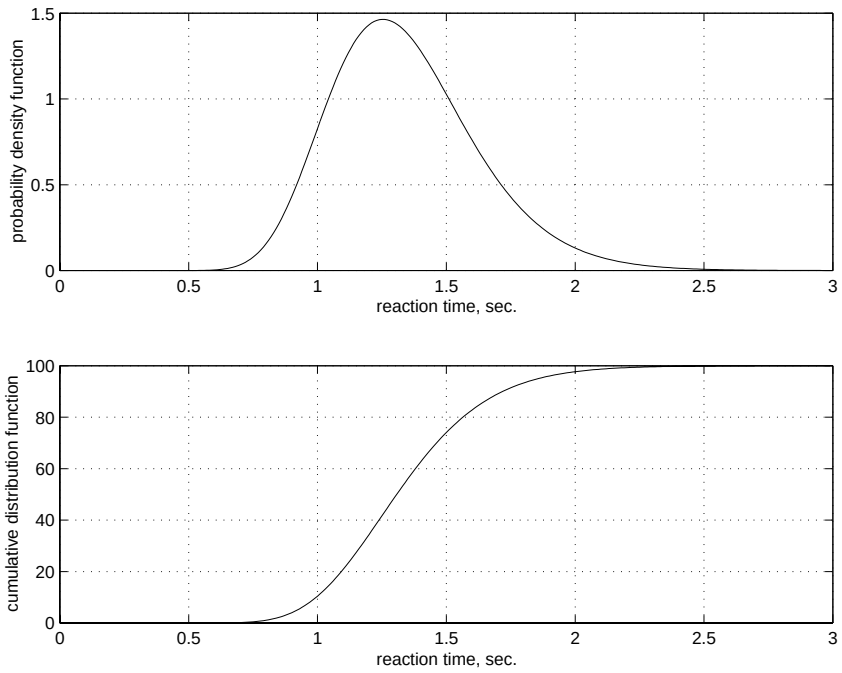

Figure 6-6: The probability density function and the cumulative distribution function of the reaction time.

reaction time distribution are 1.31, 1.34, and 0.31 seconds respectively.

As discussed in Section 3.2.4, we apriori expect the surrounding traffic conditions to affect the reaction time of a driver. Explanatory variables capturing traffic conditions include the density of traffic ahead of the driver, the average front vehicle speed (that was used as a proxy for average travel speed of the subject), whether the subject vehicle is a heavy vehicle, and an indicator for free–flow traffic conditions (density $\leq$ 19 veh/km/lane). However, the t–statistics of these explanatory variables indicated that their impact on the reaction time were not significant and in some cases the parameters had counterintuitive signs. Therefore, the model with only the constant as an explanatory variable for the mean of the reaction time distribution was adopted.

Finally, a comparison between the estimates of the reaction time distribution parameters obtained in this thesis and those obtained by Johansson and Rumer (1971) and Lerner et al. (1995) is presented in Table 6.4. The median and mean estimated in

Table 6.4: Comparison between the reaction time distribution parameters obtained from different sources.

source	sample size	stimulus	median (sec)	mean (sec)	std. dev. (sec)
this thesis	402	speed difference	1.31	1.34	0.31
Johansson and Rumer (1971)	321	sound	0.89	1.01	0.37
Lerner et al. (1995)	56	unexpected object	1.44	1.51	0.39

Note: Speed difference implies difference between the target speed and the current speed.

this research are higher than those obtained by Johansson and Rumer (1971)[4], while, they are lower than those obtained by Lerner et al. (1995). The standard deviation estimated in this research is smaller than those obtained by others.

The differences between the reaction time estimates from different studies may be due to the differences in the time period of study, data collection site, or procedures used in different studies. The acceleration and deceleration capacity of vehicles have increased over the past 27 years which may have increased the reaction time of drivers as better vehicle performance may have made driving more relaxing. Driving habits at different locations may have also contributed to different reaction time estimates. Finally, different stimulus were used in different studies. In the Johansson and Rumer (1971) study drivers responded to sound, in the Lerner et al. (1995) study drivers responded to visualizing a rolling drum, while in this thesis, drivers responded to the difference between their target speeds (desired speeds or the leaders' speeds depending on the headways) and the current speeds. Overall, the parameters of the reaction time distribution estimated in this research are well within the typical range of other studies.

In summary, the empirical work suggests that, the sensitivity term of the car–following acceleration is a function of the subject speed, the space headway, and the

[4]As mentioned in Chapter 2, drivers responded to sound indicating them to press the brake pedal. This may have reduced the perception time, and hence the reaction time.

density, while the sensitivity term of the car–following deceleration is a function of the space headway and the density of traffic. Furthermore, the sensitivity term comprises of explanatory variables observed at the time of applying acceleration/deceleration while the stimulus term is lagged by the reaction time of the drivers. The impact of the reaction time on the sensitivity was not supported by the data. The stimulus is a nonlinear function of the front relative speed. The free–flow acceleration is a function of the subject's speed, the leader's speed, an indicator whether the subject vehicle is a heavy vehicle, and an indicator whether the density of traffic is low.

6.2 Estimation Results of the Lane Changing Model

The discretionary and mandatory lane change models were estimated separately due to lack of data over a long stretch of roadway (approximately 1500 to 3000 meters long). The data collection site, shown in Figure 6-7, used in this study has a length of approximately 200m. If a driver in this site changes to the right lane and takes the exit, it is unlikely that the driver is also performing a discretionary lane change. However, if the remaining distance to the exit is 2000 meters as opposed to 200 meters, the probability of performing a discretionary lane change may not be negligible. Therefore, a model that captures discretionary lane changing decision when the driver is in a mandatory lane change situation cannot be estimated using this data.

Estimation results of the discretionary and the mandatory lane changing models are presented first. Then, estimation results of the forced merging model are presented.

6.2.1 Estimation Results of the Discretionary Lane Changing Model

The discretionary lane changing model was estimated using observations from drivers in the following two cases (see Figure 6-7 for definition of lanes 1 to 4):

- drivers that changed from lanes 2 or 3 to the left, and

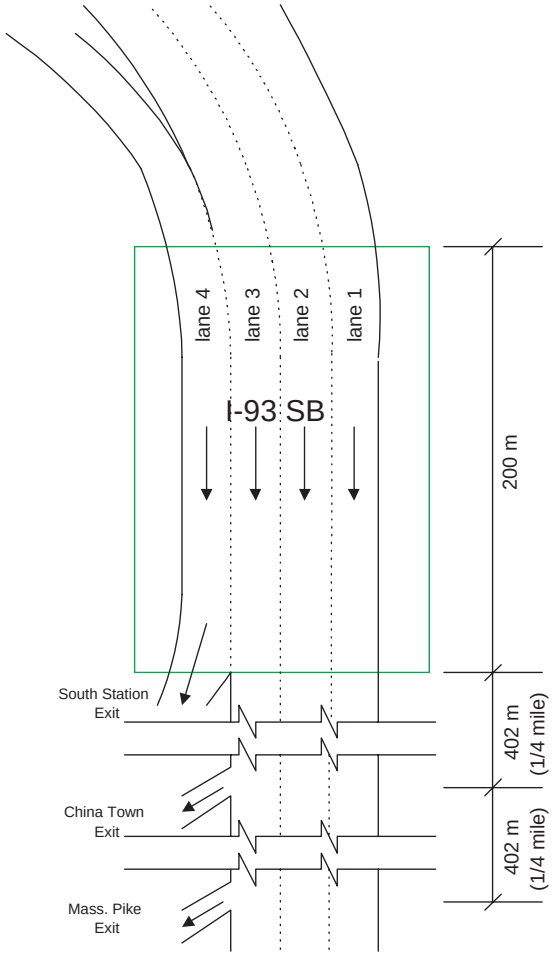

Figure 6-7: Schematic diagram of the I–93 southbound data collection site (figure not drawn to scale).

- drivers that traveled in lanes 2 or 3 without changing lanes.

If drivers from lanes 1 to 3 change to the right and take the exit at the downstream end of the data collection site, the lane changes would be mandatory. Even if they do not take this exit, since there are two exits a quarter mile and a half mile downstream, it is likely that drivers would be changing lanes to take these exits. Since drivers are not observed downstream of the data collection site, the upstream lane changes towards lane 4 cannot be categorized with certainty as discretionary lane changes. Therefore, the choice set for the discretionary lane change subjects includes the left adjacent and the current lanes.

Thus, there are two observable states: *change to the left lane* and *continue in the current lane*. The discretionary lane changing decision tree then reduces to the decision tree shown in Figure 6-8. For this decision tree, the likelihood function given by Equation 4.8 reduces to:

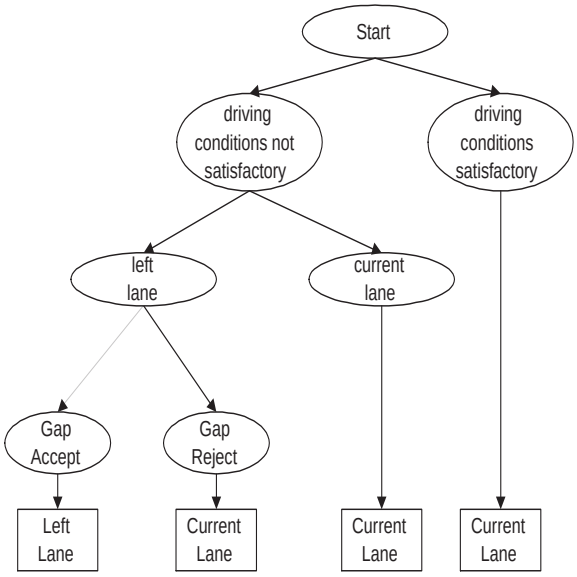

Figure 6-8: The decision tree for a driver considering a discretionary lane change with the current and the left lanes as choice set.

$$\mathcal{L} = \sum_{n=1}^{N} \ln \left\{ \int_{-\infty}^{\infty} \left(\prod_{t=1}^{T_n} \mathrm{P}_t(L \mid \nu)^{\delta_{tn}^L} \, \mathrm{P}_t(C \mid \nu)^{1-\delta_{tn}^L} \right) f_\nu(\nu) d\nu \right\} \tag{6.8}$$

where,

$$\delta_{tn}^L = \begin{cases} 1 & \text{if driver } n \text{ changes to the left lane at time } t \\ 0 & \text{otherwise.} \end{cases} \tag{6.9}$$

$$\begin{aligned} \mathrm{P}_t(L \mid \nu_n) = & \\ & \mathrm{P}_t(gap\ acceptable \mid left\ lane, driving\ conditions\ not\ satisfactory, \nu_n) \times \\ & \mathrm{P}_t(left\ lane \mid driving\ conditions\ not\ satisfactory, \nu_n) \times \\ & \mathrm{P}_t(driving\ conditions\ not\ satisfactory \mid \nu_n) \end{aligned} \tag{6.10}$$

$$\mathrm{P}_t(C \mid \nu_n) = 1 - \mathrm{P}_t(L \mid \nu_n) \tag{6.11}$$

The expression for the gap acceptance probability is given by Equation 4.4. The conditional probability that the left lane is chosen is given by:

$$\mathrm{P}_t(left\ lane \mid driving\ conditions\ not\ satisfactory, \nu_n) = \frac{1}{1+\exp(-X_n^{LL}(t)\beta^{LL} - \alpha^{LL}\nu_n)} \tag{6.12}$$

where, superscript 'LL' denotes $left\ lane$. Finally, the conditional probability that the driver is not satisfied with the driving condition of the current lane is given by:

$$\mathrm{P}_t(driving\ conditions\ not\ satisfactory \mid \nu_n) = \frac{1}{1+\exp(-X_n^{DCNS}(t)\beta^{DCNS} - \alpha^{DCNS}\nu_n)} \tag{6.13}$$

where, superscript 'DCNS' denotes $driving\ conditions\ not\ satisfactory$.

Estimation Results

Table 6.5 shows the estimation results of the discretionary lane changing model. At convergence, the hessian of the the likelihood function did not invert since it was nearly singular. The estimates of the standard deviation of the generic random terms of the lead and lag critical gaps ($\sigma_\epsilon^{lead,dlc}$, $\sigma_\epsilon^{lag,dlc}$) were close to zero. Nearly singular hessian and zero estimates of the standard deviations indicate identification problems of the model. Next, we estimated a restricted version of the likelihood function in which the serial correlation between different observations from a given driver is not modeled. In this case, the likelihood function converged with a negative definite hessian at convergence (as desired) and the estimates of the standard deviation of the generic random terms were reasonable. Further research is required to address the identification problem mentioned above and this is left as a topic for future research.

The restriction of no serial correlation implies that, α^{DCNS} in Equation 6.13, α^{LL} in Equation 6.12, and $\alpha^g,\ g \in \{lead, lag\}$ in Equation 4.3 are restricted to be zero, and the model formulation becomes a cross–sectional one. The test statistic

Table 6.5: Estimation results of the discretionary lane changing model.

Variable	Parameter
Desired Speed Model	
average speed, m/s	0.727
Utility of Driving Conditions not Satisfactory	
constant	0.0343
(subject speed – desired speed), m/s	-0.0757
heavy vehicle dummy	-3.56
tailgate dummy	0.486
α^{DCNS}	-1.11
Utility of the Left Lane	
constant	-1.87
(lead veh. speed – desired speed), m/s	0.0328
(front veh. speed – desired speed), m/s	-0.158
lag veh. speed – subject speed, m/s	-0.0960
α^{LL}	-0.246
Lead Critical Gap	
constant	0.665
min(0, lead veh. speed – subject speed), m/s	-0.412
α^{lead}	0.727
$\ln(\sigma_{\epsilon}^{lead,dlc})$	-7.16
Lag Critical Gap	
constant	1.69
min(0, lag veh. speed – subject speed), m/s	0.172
max(0, lag veh. speed – subject speed), m/s	0.177
α^{lag}	-0.653
$\ln(\sigma_{\epsilon}^{lag,dlc})$	-15.5
number of drivers = 843	
number of observations = 4335	
number of discretionary lane change observations = 75	
$\mathcal{L}(0)$ = -482.92	
$\mathcal{L}$(c) = -360.05	
$\mathcal{L}(\hat{\beta})$ = -326.51	
$\overline{\rho}^2$ = 0.282	

Note: different vehicles and gaps are defined in Figure 6-9.

$-2(\mathcal{L}(restricted) - \mathcal{L}(unrestricted))$ is distributed χ^2 with degrees of freedom equal to the number of restrictions.

The test statistic for the null hypothesis of no serial correlation, i.e.,

$$\alpha^{DCNS} = \alpha^{LL} = \alpha^{lead} = \alpha^{lag} = 0, \tag{6.14}$$

is given by:

$$\begin{aligned} -2(\mathcal{L}(restricted) - \mathcal{L}(unrestricted)) &= -2 \times [-330.57 - (-326.51)] \\ &= 8.12 \end{aligned} \tag{6.15}$$

The critical value of the χ^2 distribution with 4 degrees of freedom at the 5% level of significance is 9.49. Therefore, the null hypothesis of no serial correlation cannot be rejected and we adopt the model with no serial correlation.

Table 6.6 shows the parameter estimates obtained by maximizing the restricted likelihood function. The factors affecting a driver's decision whether the driving conditions are satisfactory are the difference between the subject speed and their desired speed, an indicator whether the subject vehicle is a heavy vehicle, and an indicator whether the subject is tailgated. See Figure 6-9 for definition of different vehicles and gaps.

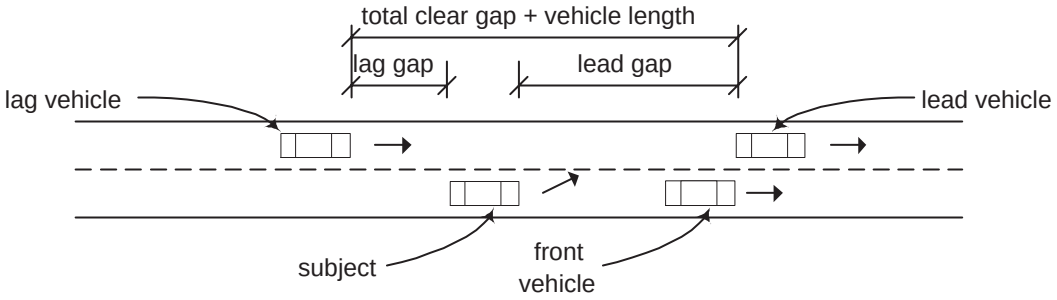

Figure 6-9: The subject and the front, lead, and lag vehicles.

The desired speed model is assumed to have the following functional form:

$$V_n^*(t) = X_n^{DS}(t)\beta^{DS} \tag{6.16}$$

Table 6.6: Estimation results of the discretionary lane changing model.

Variable	Parameter	t–stat.
Desired Speed Model		
average speed, m/s	0.768	5.37
Utility of Driving Conditions not Satisfactory		
constant	0.225	0.17
(subject speed – desired speed), m/s	-0.0658	-0.62
heavy vehicle dummy	-3.15	-3.18
tailgate dummy	0.423	1.71
Utility of the Left Lane		
constant	-2.08	-2.53
(lead veh. speed – desired speed), m/s	0.0337	0.76
(front veh. speed – desired speed), m/s	-0.152	-3.12
lag veh. speed – subject speed, m/s	-0.0971	-1.84
Lead Critical Gap		
constant	0.508	1.53
min(0, lead veh. speed – subject speed), m/s	-0.420	-3.73
$\ln(\sigma_\epsilon^{lead,dlc})$	-0.717	-1.45
Lag Critical Gap		
constant	2.02	5.00
min(0, lag veh. speed – subject speed), m/s	0.153	1.29
max(0, lag veh. speed – subject speed), m/s	0.188	1.69
$\ln(\sigma_\epsilon^{lag,dlc})$	-0.642	-1.67
number of drivers = 843		
number of observations = 4335		
number of discretionary lane change observations = 75		
$\mathcal{L}(0)$ = -482.92		
$\mathcal{L}(c)$ = -360.05		
$\mathcal{L}(\hat{\beta})$ = -330.57		
$\overline{\rho}^2$ = 0.282		

Note: different vehicles and gaps are defined in Figure 6-9.

where,

$$\begin{aligned} X_n^{DS}(t) &= \text{explanatory variables affecting the desired speed } (DS), \\ \beta^{DS} &= \text{model parameters.} \end{aligned}$$

Note that, a constant for the desired speed cannot be estimated since it is absorbed into the constants of the utilities of the decisions 'driving conditions not satisfactory' and 'left lane'. The explanatory variables used for the desired speed model include the average speed of the vehicles ahead of the subject, the speed of the front vehicle, the density of traffic ahead of the subject, and an indicator whether the subject vehicle is a heavy vehicle. A higher average speed of the vehicles ahead or the front vehicle speed and a lower density of traffic are expected to increase the desired speed of the driver. Due to lack of maneuverability and safety concern, driver of a heavy vehicle is expected to have lower desired speed than its non heavy counterpart. However, except for the average speed, the t–statistics of the other explanatory variables were insignificant and some of parameters had counterintuitive signs. In the final model only the average speed of the vehicles ahead of the subject was used which had a significant t–statistic. To capture the effect of tailgating which cannot be observed from the data, a proxy variable tailgate dummy is defined as follows:

$$\delta_n^{tailgate}(t) = \begin{cases} 1 & \text{if gap behind the subject's rear bumper} \leq 10 \text{ m and} \\ & \text{traffic level of service is A, B, or C} \\ 0 & \text{otherwise} \end{cases} \tag{6.17}$$

where, $\delta_n^{tailgate}(t)$ denotes the tailgate dummy.

A speed above the desired speed implies satisfaction with the current lane, since in this situation a driver has the flexibility to adjust its speed. On the other hand, a speed below the desired speed would motivate a driver to perform a discretionary lane change. The corresponding parameter has the desired negative sign. Although, its t–statistic is not significant, it is included in the model due to its importance from a behavioral standpoint. Due to lack of maneuverability, heavier vehicles are

hesitant toward changing lanes and the corresponding parameter has a significant t–statistic. Finally, when tailgated, drivers tend to seek discretionary lane change and the corresponding parameter has the desired positive sign and its t–statistic is significant at the 10% level of significance.

Factors affecting the decision whether the left lane is more desirable than the current lane include the difference between the lead vehicle's speed and the subject's desired speed, the difference between the front vehicle's speed and the subject's desired speed, and the difference between the subject speed and the speed of the lag vehicle. A higher lead or front vehicle's speed implies higher flexibility for the subject in the corresponding lanes. The lag relative speed captures the effect of safety concern to perform a lane changing decision and its parameter has a significant t–statistic at the 10% level of significance.

The only factor affecting the discretionary lead critical gap is the lead relative speed only when the lead vehicle is slower. Its parameter is statistically significant at the 1% level of significance. For the lag critical gap, the lag relative speed is the only important factor. To capture the different impact of the lag relative speed depending on whether the lag vehicle is faster or not, a piecewise linear approximation of the lag relative speed with a breakpoint at 0 m/s is used. The variable max(0, lag vehicle speed - subject speed) has a significant t–statistic at the 10% level of significance while the variable min(0, lag vehicle speed - subject speed) does not have a significant t–statistic. In spite this, the latter variable is included in the model due to its importance from a behavioral standpoint. Higher sensitivity of the lag critical gap when the lag vehicle is faster is captured by the higher parameter estimates of the variable max(0, lag vehicle speed – subject speed) compared to the variable min(0, lag vehicle speed – subject speed).

The adjusted fit of the model was 0.282. To test the null hypothesis that all the parameters except the constants and standard deviations are zero, the likelihood ratio test was used. The test statistic is given by:

$$
\begin{aligned}
-2(\mathcal{L}(\hat{C}) - \mathcal{L}(\hat{\beta})) &= -2(-330.57 - (-360.05)) \\
&= 58.96 \qquad (6.18)
\end{aligned}
$$

The critical value of the χ^2 distribution with 9 degrees of freedom at the 5% level of significance is 16.92. Hence, the null hypothesis can be rejected.

The estimated probability that driver n is not satisfied with the current lane (driving conditions not satisfactory) at time t is given by:

$$
\mathrm{P}_t(\textit{driving conditions not satisfactory}) = \frac{1}{1 + e^{[-0.225 + 0.0658\ (V_n(t) - V_n^*(t)) + 3.15\ \delta_n^{heavy} - 0.423\ \delta_n^{tailgate}(t)]}} \qquad (6.19)
$$

The conditional probability of choosing the left lane over the current lane is given by:

$$
\mathrm{P}_t(\textit{left lane} \mid \textit{driving conditions not satisfactory}) = \frac{1}{1 + e^{[2.08 - 0.0337\ (V_n^{lead}(t) - V_n^*(t)) + 0.152\ (V_n^{front}(t) - V_n^*(t)) + 0.0971\ \Delta V_n^{lag}(t)]}} \qquad (6.20)
$$

where, $\Delta V_n^{lag}(t)$ denotes the lag vehicle speed minus the subject speed (m/s).

The estimated lead and lag critical gaps (in meters) for the discretionary lane change case are

$$
\begin{aligned}
G_{cr,n}^{lead,dlc}(t) &= \exp[0.508 - 0.420\ \min(0, \Delta V_n^{lead}(t)) + \epsilon_n^{lead,dlc}(t)] \qquad (6.21) \\
G_{cr,n}^{lag,dlc}(t) &= \exp[2.02 + 0.153\ \min(0, \Delta V_n^{lag}(t)) + \\
&\qquad 0.188\ \max(0, \Delta V_n^{lag}(t)) + \epsilon_n^{lag,dlc}(t)] \qquad (6.22)
\end{aligned}
$$

where,

$$
\begin{aligned}
\Delta V_n^{lead}(t) &= \text{lead vehicle speed – subject speed (m/s)}, \\
\epsilon_n^{lead,dlc}(t) &\sim \mathcal{N}(0, 0.488^2),
\end{aligned}
$$

$$\epsilon_n^{lag,dlc}(t) \quad \sim \quad \mathcal{N}(0, 0.526^2).$$

Another way of assessing the estimated parameters is to compute the probability of acceptance of gaps that drivers merged into and hence were acceptable to them. There were 75 such cases. These estimates should be higher than 0.5 and close to 1.0. The estimated probability had a mean of 0.83 and a standard deviation of 0.25. Figure 6-10 shows the histogram and cumulative distribution of the estimated probabilities. For

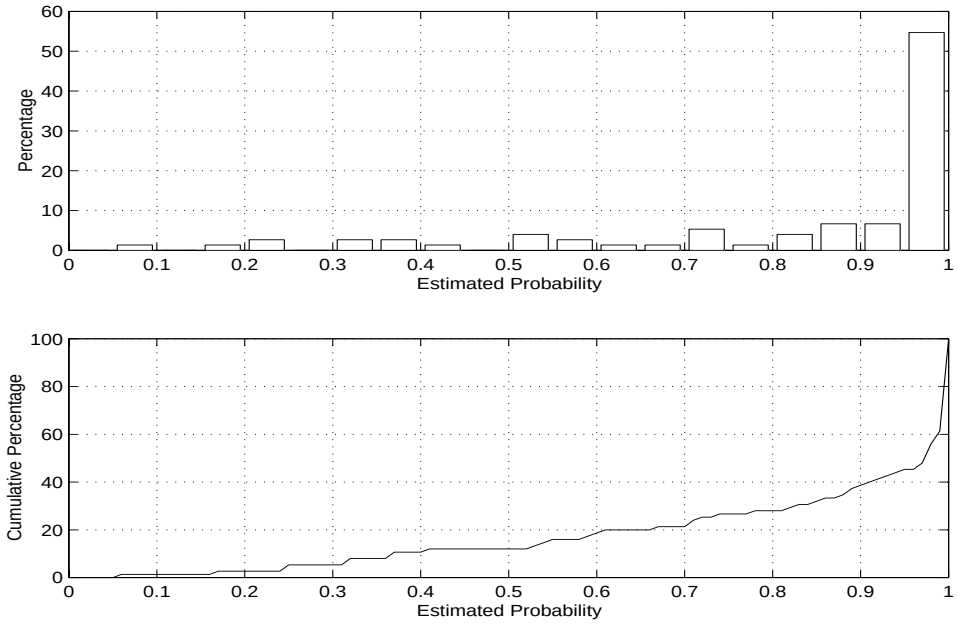

Figure 6-10: The estimated probability of acceptance of gaps that were acceptable and merging were completed.

the majority of the gaps actually accepted, the estimated probability of acceptance was close to one. On 88% of the cases, the estimated probabilities were greater than 0.5.

Finally, Figure 6-11 shows the median lead and lag critical gaps (for DLC situations) as a function of the lead and lag relative speeds. When both the lead and lag relative speeds are zero, the median lead and lag critical gaps are 1.7 and 7.5 meters respectively. This is intuitive since the lag gap acceptance process is more critical than the lead gap acceptance process. The median lead critical gap decreases from 13.5 to 1.7 meters as the lead relative speed increases from -5 m/s to 0 m/s. As the

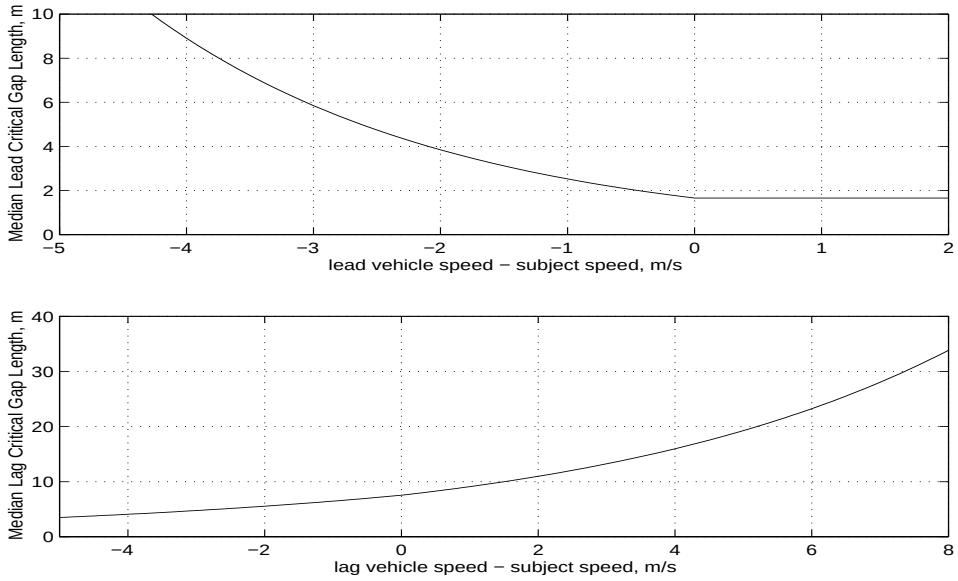

Figure 6-11: The median lead and lag critical gaps for discretionary lane change as a function of relative speed.

lag relative speed increases from -5 to 8 m/s, the median lag critical gap increases from 3.5 to 49.2 meters. These numbers are realistic from a behavioral standpoint.

In summary, drivers' decision to perform a discretionary lane change is modeled as a two step decision process. First, drivers examine their satisfaction with the driving conditions of the current lane. Important factors affecting such decision include the difference between the current speed and the driver's desired speed, an indicator whether the subject vehicle is a heavy vehicle, and an indicator whether the subject is tailgated. If the driver is not satisfied with the the driving conditions of current lane, he/she compares the driving conditions of the current lane with those of the other lanes. Such a decision is influenced by the the speeds of the vehicles ahead in different lanes compared to the subject's desired speed and the lag relative speed. The lead critical gap is a function of the lead relative speed only when the leader is slower while the lag critical gap is a function of the lag relative speed. The importance on the decision to perform a discretionary lane change of other explanatory variables, such as the relative density of traffic in different lanes, whether the lead or the lag vehicle is heavy, and whether the lane is adjacent to an on–ramp, was not supported by the data.

6.2.2 Estimation Results of the Mandatory Lane Changing Model

The mandatory lane changing model parameters are estimated using observations from the drivers who merged from the on–ramp (lane 4 in Figure 6-7) to the adjacent mainline lane (lane 3). The data consists of observations from drivers when the level of service of the roadway section was between A and E. For such drivers, the decision tree shown in Figure 4-1 reduces to the decision tree shown in Figure 6-12.

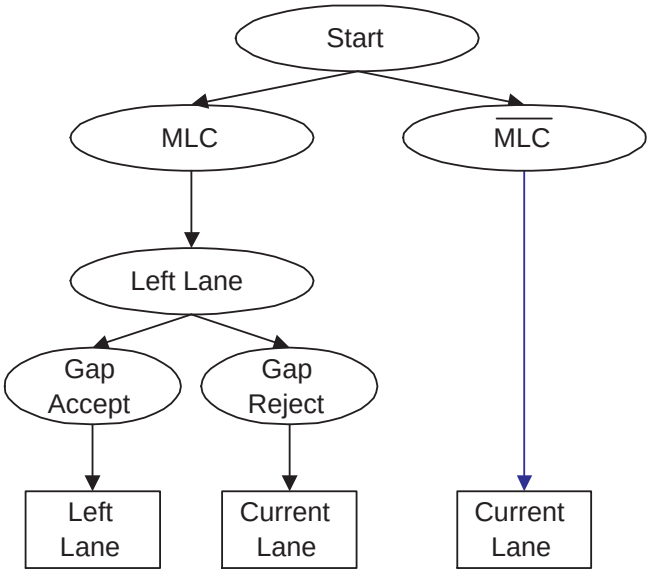

Figure 6-12: The decision tree for a driver merging from an on–ramp to the adjacent mainline lane.

In this case, the left and the current lanes are the two choices. Thus, there are two observable states: *change to the left lane* and *continue in the current lane*. For this decision tree, the likelihood function given by Equation 4.8 reduces to:

$$\mathcal{L} = \sum_{n=1}^{N} \ln \left\{ \int_{-\infty}^{\infty} \left(\prod_{t=1}^{T_n} \mathrm{P}_t(L \mid \nu)^{\delta_{tn}^L} \, \mathrm{P}_t(C \mid \nu)^{1-\delta_{tn}^L} \right) f_\nu(\nu) d\nu \right\} \tag{6.23}$$

where, δ_{tn}^L is defined in Equation 6.9 and the conditional probability of an observation of driver n changing to the left lane is given by:

$$\mathrm{P}_t(L \mid \nu_n) = \mathrm{P}_t(gap\ acceptable \mid MLC, \nu_n)\mathrm{P}_t(MLC \mid \nu_n) \tag{6.24}$$

The probabilities on the right hand side of Equation 6.24 are given by Equations 4.4 and 4.1 respectively. The probability of staying in the current lane is given by:

$$\mathrm{P}_t(C \mid \nu_n) = 1 - \mathrm{P}_t(L \mid \nu_n) \tag{6.25}$$

Estimation Results

The maximum likelihood estimation results of the mandatory lane changing model are given in Table 6.7. All the parameters that capture the correlation between different

Table 6.7: Estimation results of the mandatory lane changing model.

Variable	Parameter	t–stat.
Mandatory Lane Change Utility		
constant	-0.740	-1.75
first gap dummy	-0.884	-2.36
delay (sec)	0.749	1.36
α^{MLC}	0.685	0.65
Lead Critical Gap		
constant	0.414	0.79
α^{lead}	0.676	1.21
$\ln(\sigma_\epsilon^{lead,mlc})$	-1.07	-0.26
Lag Critical Gap		
constant	0.663	0.97
min[0, lag veh. speed – subject speed] (m/s)	0.0457	0.24
max[0, lag veh. speed – subject speed] (m/s)	0.363	2.59
α^{lag}	0.330	0.69
$\ln(\sigma_\epsilon^{lag,mlc})$	0.0101	0.03
number of drivers = 202		
number of observations = 500		
$\mathcal{L}(0)$ = -336.16		
$\mathcal{L}(c)$ = -334.83		
$\mathcal{L}(\hat{\beta})$ = -288.19		
$\overline{\rho}^2$ = 0.107		

observations from a given driver (i.e., α^{MLC} in Equation 4.1, and $\alpha^{g},\ g \in \{lead, lag\}$ in Equation 4.3) are statistically insignificant. To test the null hypothesis of no serial correlation, i.e.,

$$\alpha^{MLC} = \alpha^{lead} = \alpha^{lag} = 0, \tag{6.26}$$

a restricted version of the likelihood function with no serial correlation was estimated. These restrictions make the model formulation a cross–sectional one. The test statistic is

$$\begin{aligned} -2(\mathcal{L}(restricted) - \mathcal{L}(unrestricted)) &= -2 \times [-288.45 - (-288.19)] \\ &= 0.53 \end{aligned} \tag{6.27}$$

The critical value of the χ^2 distribution with 3 degrees of freedom at the 5% level of significance is 7.81. Therefore, the null hypothesis of no serial correlation cannot be rejected.

The parameters obtained by maximizing the restricted likelihood function are shown in Table 6.8. Note that, except for the parameters that correspond to standard deviation of the random terms, the parameter estimates of the unrestricted and restricted models are of the same order of magnitude. Factors affecting a driver's decision to respond to mandatory lane change situation (MLC) are delay (time since the driver crossed the merging point, section X–X in Figure 6-13) and the indicator for the first gap (when delay is equal to zero)[5]. The parameters have the expected signs and significant t–statistics at the 5% level of significance.

The lead critical gap was found to be insensitive to the traffic conditions, whereas, the lag critical gap length is sensitive only to the lag relative speed. Similar to the discretionary lag critical gap model, a piecewise linear lag relative speed variable was used with a breakpoint at 0 m/s was used. As expected, the parameter for the

[5]As explained in Section 4.2.1, delay or the first gap dummy cannot be defined for general mandatory lane changing cases unless the time at which the driver is in MLC state is well defined.

Table 6.8: Estimation results of the mandatory lane changing model.

Variable	Parameter	t–stat.
Mandatory Lane Change Utility		
constant	-0.654	-2.27
first gap dummy	-0.874	-2.50
delay (sec)	0.577	3.85
Lead Critical Gap		
constant	0.384	0.63
$\ln(\sigma_{\epsilon}^{lead,mlc})$	-0.152	-0.29
Lag Critical Gap		
constant	0.587	0.79
min[0, lag veh. speed – subject speed] (m/s)	0.0483	0.23
max[0, lag veh. speed – subject speed] (m/s)	0.356	2.39
$\ln(\sigma_{\epsilon}^{lag,mlc})$	0.0706	0.14
number of drivers = 202		
number of observations = 500		
$\mathcal{L}(0)$ = -336.16		
$\mathcal{L}(c)$ = -334.83		
$\mathcal{L}(\hat{\beta})$ = -288.45		
$\overline{\rho}^2$ = 0.115		

explanatory variable max(0, lag vehicle speed – subject speed) was higher than that for min(0, lag vehicle speed – subject speed). The remaining distance did not affect a driver's decision process—not an intuitive result. This may be due to the fact that, in the data the mean and median remaining distances were 130 and 135 meters respectively and level of service (HCM 1985) varied between A and C. As a result, the remaining distance may not have a significant impact on the merging behavior of the sample drivers in the data. The lead and lag critical gap parameters have low t–statistics except for the lag relative speed when the lag vehicle is faster.

The adjusted fit of the model was 0.115. A likelihood ratio test was conducted to test the null hypothesis that all the parameters except the constants and standard deviations are zero. The test statistic, $-2(\mathcal{L}(\hat{C}) - \mathcal{L}(\hat{\beta}))$, is equal to 92.76 and the critical value with 4 degrees of freedom at the 5% level of significance is 9.49. Hence, the null hypothesis can be rejected.

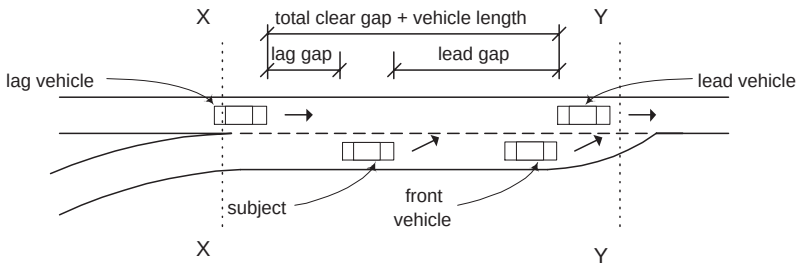

Figure 6-13: The subject, lead, lag, and front vehicles, and the lead and lag gaps.

The estimated probability that a driver would respond to an MLC situation is

$$\mathrm{P}_t(MLC) = \frac{1}{1+\exp(0.654 - 0.577\ delay_n(t) + 0.874\ \delta_n^{1stGap}(t))} \quad (6.28)$$

where,

$$delay_n(t) = \text{time elapsed since an } MLC \text{ situation arises (sec)},$$

$$\delta_n^{1stGap}(t) = \begin{cases} 1 & \text{if delay} = 0 \\ 0 & \text{otherwise.} \end{cases}$$

Figure 6-14 shows the probability of responding to MLC as a function of delay. The

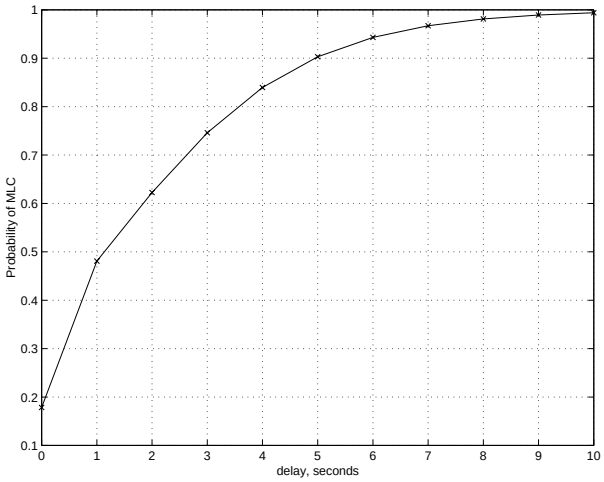

Figure 6-14: The probability of responding to MLC as a function of delay.

estimated probability approaches one as delay increases beyond 10 seconds and is

higher than expected. This may be due to lack of data with larger delay experienced by the drivers in the data set (the median and the maximum delay experienced by the drivers in the data were 2 and 5 seconds respectively).

The estimated lead and lag critical gaps (in meter) for mandatory lane change situations are

$$G_{cr,n}^{lead,mlc}(t) = \exp(0.384 + \epsilon_n^{lead,mlc}(t)) \quad (6.29)$$

$$G_{cr,n}^{lag,mlc}(t) = \exp(0.587 + 0.0483\ \min(0, \Delta V_n^{lag}(t)) + 0.356\ \max(0, \Delta V_n^{lag}(t)) + \epsilon_n^{lag,mlc}(t)) \quad (6.30)$$

where, $\Delta V_n^{lag}(t)$ denotes the lag relative speed (m/s), $\epsilon_n^{lead,mlc}(t) \sim \mathcal{N}(0, 0.859^2)$, and $\epsilon_n^{lag,mlc}(t) \sim \mathcal{N}(0, 1.07^2)$.

The probability of acceptance of gaps that drivers merged into and hence were acceptable to them was calculated using the estimated parameters. On 72% of the cases, the estimated probabilities were greater than 0.9. Figure 6-15 shows the histogram and cumulative distribution of the estimated probabilities. The estimated

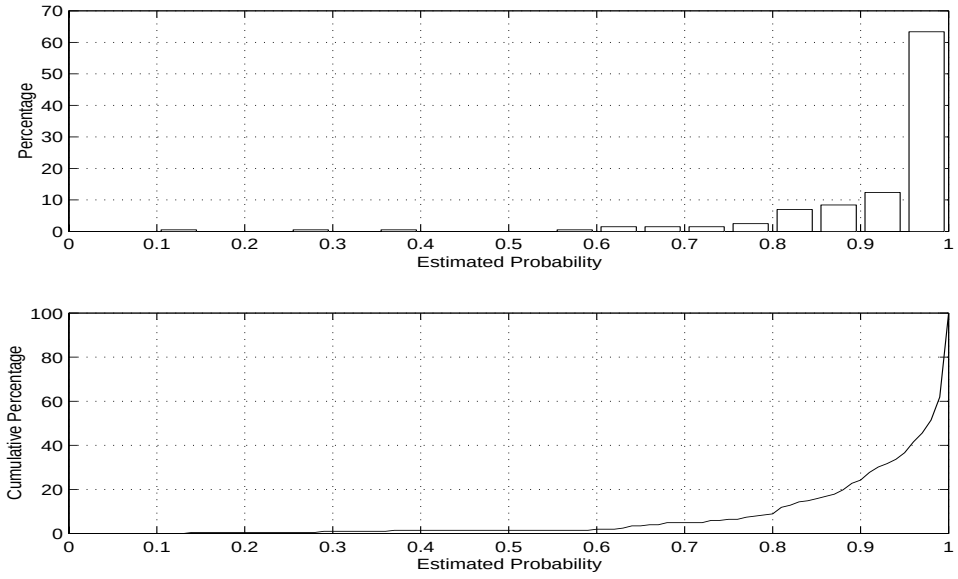

Figure 6-15: The estimated probability of acceptance of gaps that were acceptable and merging were completed.

probability had a mean of 0.93 and a standard deviation of 0.12. These results are satisfactory.

The median value of the lag critical gap (for the mandatory lane change situation) was calculated for different values of lag relative speed, and the variation is shown in Figure 6-16. When the subject is faster than the lag vehicle in the target lane, the

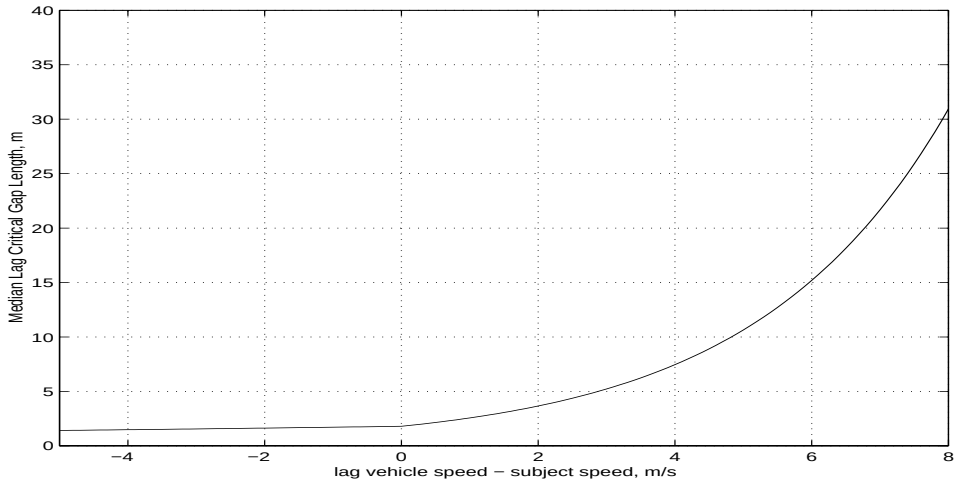

Figure 6-16: The mean lag critical gap for mandatory lane change as a function of lag relative speed.

median lag critical gap is less than 2 meters. The median lag critical gap increases at an exponential rate to 32 meters as the lag relative speed increases to 8 m/s. The median lead critical gap was 1.5 meters.

Ahmed et al. (1996) estimated the median lead and lag critical gaps to be 4.7 and 15.6 meters respectively (assuming a 152 meters remaining distance and the gap is the first gap observed by the driver)[6]. Although, this research and Ahmed et al. (1996) used the same methodology to estimate the gap acceptance model, the differences in the estimates may be due to the differences in the data collection years or sites. From 1983 to 1995 vehicle characteristics have improved (KBB 1998) and driving habits of the drivers of these two areas may be different which may have contributed to the

[6]Ahmed et al. (1996) used a data collected in 1983 from a site at Interstate 95 Northbound near the Baltimore Washington Parkway (Smith 1985). The site is a two lane freeway with an adjacent weaving section on the right. Density of traffic varied from 3 veh/km/lane to 56 veh/km/lane with a mean of 27 veh/km/lane. The median length of the lead and lag gaps corresponding to the gaps that the drivers found acceptable and completed the merge were 21 and 25 meters respectively.

differences in the critical gap length estimates.

The estimated median critical gap lengths under MLC situations are also compared to their DLC counterparts as shown in Figure 6-17. As expected, the median critical lead/lag gaps under MLC situations are smaller than their DLC counterparts.

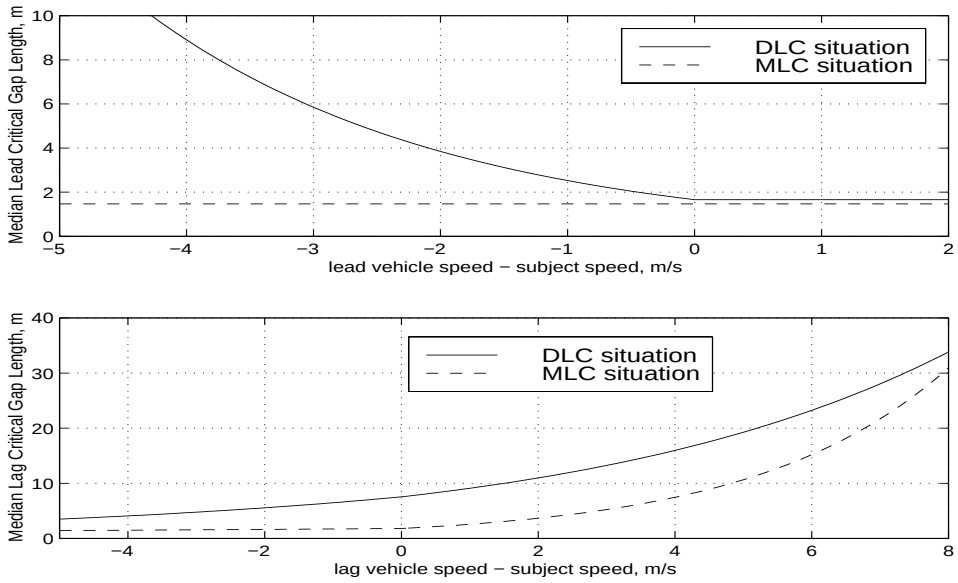

Figure 6-17: Comparison between the estimated critical gap lengths under DLC and MLC situations.

6.2.3 Estimation Results of the Forced Merging Model

The forced merging model was estimated for the case of merging from an on–ramp. Since, the forced merging model is assumed to be applicable only in heavily congested traffic, the data consisted of observations from drivers when the level of service of the roadway section was F.

The estimation results are shown in Table 6.9. The parameter α^{FM} (in Equation 4.9) that captures the correlation between different observations from the same driver, was estimated to be 0.0012, which is very small. Its t–statistic was 0.001. This implies that, the dynamic aspect of driver behavior may be adequately captured by state dependence and that the random term of the utility specification is independent over time, even for the same driver. The estimation results presented in Table 6.10 correspond to the parameter estimates obtained by maximizing the

Table 6.9: Estimation results of the forced merging model.

Variable	Parameter	t–stat.
constant	-3.16	-10.59
min(0, lead veh. speed – subject speed) (m/s)	0.313	2.66
remaining distance impact $\times 10$	2.05	5.33
total clear gap/10 (meters)	0.285	2.85
α^{FM}	0.0012	0.001
number of drivers = 79		
number of observations = 566		
$\mathcal{L}(0)$ = -306.5		
$\mathcal{L}(c)$ = -112.3		
$\mathcal{L}(\hat{\gamma})$ = -88.5		
$\overline{\rho}^2 = 0.695$		

likelihood function with no serial correlation.

The probability that the n^{th} driver will switch from state $\overline{M}$ to state M at time t is given by:

$$\mathrm{P}(S_n(t) = M \mid S_n(t-1) = \overline{M}) = \frac{1}{1 + \exp[3.16 - 0.303\ f(\Delta V_n^{ld}(t)) - 2.05\ f(L_n^{rem}(t)) - 0.285\ G_n(t)]} \quad (6.31)$$

where,

$$\begin{aligned}
S_n(t) &= \text{state of driver } n \text{ at time } t, \\
f(\Delta V_n^{ld}(t)) &= \min(0, \Delta V_n^{ld}(t)), \\
\Delta V_n^{ld}(t) &= \text{lead vehicle speed – subject speed (m/s)}, \\
f(L_n^{rem}(t)) &= \textit{remaining distance impact}, \\
L_n^{rem}(t) &= \text{remaining distance to the point at which lane change must be completed by}, \\
G_n(t) &= \text{lead gap plus lag gap (m)}.
\end{aligned}$$

Table 6.10: Estimation results of the forced merging model.

Variable	Parameter	t–stat.
constant	-3.16	-10.59
min(0, lead veh. speed – subject speed) (m/s)	0.313	2.66
remaining distance impact ×10	2.05	5.33
total clear gap divided by 10 (meters)	0.285	2.85
number of drivers = 79		
number of observations = 566		
$\mathcal{L}(0)$ = -306.5		
$\mathcal{L}(c)$ = -112.3		
$\mathcal{L}(\hat{\gamma})$ = -88.5		
$\overline{\rho}^2$ = 0.698		

State M is defined as the situation in which a driver intends to merge into the adjacent gap in the adjacent lane and perceives that his/her right of way has been established and thus starts merging.

The explanatory variable min(0, lead vehicle speed – subject speed) captures the fact that, if the subject is interested in merging into the adjacent gap, it would slow down to match the leader's speed to better focus on the interaction with the lag vehicle. The variable should always be non-positive and its estimate reflects such behavior. The explanatory variable total clear gap has the desired positive sign.

The variable remaining distance impact, a function of the remaining distance, is used to capture the fact that the remaining distance does not impact a driver's merging behavior when it is greater than a certain threshold, while at small values, drivers become more concerned and hence more aggressive. The variable remaining distance impact for driver n at time t is assumed to have the following functional form:

$$remaining\ distance\ impact = 1 - \frac{1}{1 + e^{\lambda^{FM}\ L_n^{rem}(t)}} \tag{6.32}$$

where, λ^{FM} is parameter. For different values of λ^{FM} the likelihood function (Equation 4.19) was maximized and the value of λ^{FM} that corresponds to the highest

maximum likelihood value was adopted. λ^{FM} was estimated to be -0.027.

Figure 6-18 shows how the explanatory variable remaining distance impact, the

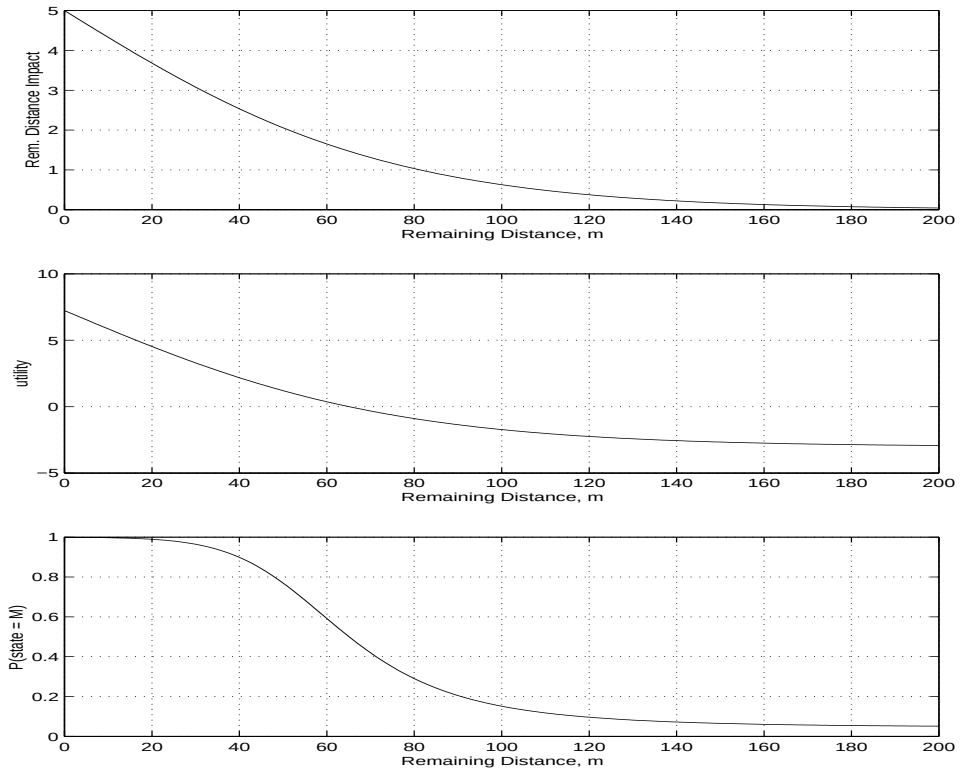

Figure 6-18: Remaining distance versus explanatory variable remaining distance impact, the utility function, and the estimated probability of being in state M.

utility, and the estimated probability of being in state M change as a function of the remaining distance (assuming a zero lead relative speed and a 5m clear gap). Drivers' increasing desperation to complete the merge as remaining distance decreases is shown in the middle plot of Figure 6-18—the utility increases at an increasing rate as a driver approaches the end of the acceleration lane and the probability of being in state M approaches unity. The variable remaining distance impact, as shown in the first plot of Figure 6-18, increases from 0 to 5 as the remaining distance decreases from greater than 150 to 0 meters.

All parameters have significant t-statistics. The adjusted fit of the model was 0.698. In addition, a likelihood ratio test was used to test the null hypothesis that the parameters of all the explanatory variables except the constant are zero. The statistic, $-2(\mathcal{L}(c) - \mathcal{L}(\hat{\gamma}))$, is equal to 47.54. The chi–square critical value for 3 degrees

of freedom at the 5% level of significance is 7.81. Hence, the null hypothesis can be rejected.

Note that, the variable lag relative speed was not included in the model since the sign of the corresponding parameter was counter intuitive. The use of the explanatory variable delay (time elapsed since crossing the merging point between the on–ramp and the freeway) was also not supported by the data may be because the effect is captured by the explanatory variable remaining distance impact. In addition, the vehicle type (heavy vehicle or not) did not have any impact on the forced merging behavior. This may be due to lack of observations since only 4 vehicles out of the 79 samples were heavy vehicles.

6.3 Conclusions

The estimation work presented in this chapter shows that, the sensitivity term of the car–following acceleration is a function of the subject speed, the space headway, and the density of traffic, and the sensitivity term of the car–following deceleration is a function of the space headway and the density of traffic. The sensitivity lag was estimated to be zero. In other words, the sensitivity is a function of traffic conditions observed at the time instant at which acceleration is applied. In both cases, the stimulus is a nonlinear function of the front relative speed. Enhancements of the car–following sensitivity and stimulus proposed in this thesis were supported by the data. The mean of estimated free–flow acceleration increases with front vehicle speeds. Heavier vehicles tend to apply slower acceleration due to physical limitations. In free–flow traffic conditions (i.e., density $\leq$ 19 veh/km/lane or level of service A through C), drivers are expected to apply a higher acceleration and the parameter of the indicator for free–flow traffic conditions has the desired sign and a significant t–statistic.

The headway threshold distribution has a mean and standard deviation of 3.17 and 0.87 seconds respectively. The median, mean, and standard deviation of the reaction time distribution are estimated to be 1.31, 1.34 and 0.31 seconds respectively.

The parameters of the discretionary and mandatory lane changing models were estimated separately due to lack of appropriate data. The estimated median lead and lag critical gap lengths under mandatory lane changing situations were lower their discretionary lane changing situation counterparts.

Important factors that affect forced merging behavior include the lead relative speed only when the lead vehicle is slower, remaining distance to the point at which the lane change must be completed by, and total clear gap (reduced by the subject vehicle length).

Finally, it must be stated that the estimation results presented in this section were obtained using data from a particular freeway segment. Due to the curvature of the roadway upstream of the data collection site, presence of the weaving section, and two exits downstream, the behavior of drivers, while driving in this area, may be influenced by these conditions. This can be addressed by estimating the models using data from different sites with different geometrical configurations. This will also address the issue of applicability of the estimation results to general networks.

Chapter 7

Model Validation Using a Microscopic Traffic Simulator

In this chapter, the acceleration and lane changing models are evaluated through their use in a microscopic traffic simulator, MITSIM[1]. Some basic information about MITSIM is given in Section 7.1. Two new versions of MITSIM were created: MITSIM with only the acceleration model replaced (MITSIM ONE), and MITSIM with both the acceleration and lane changing models replaced (MITSIM TWO). Traffic in a small network in Boston was simulated using the original version of MITSIM and MITSIM ONE and TWO. Actual traffic counts at different locations of the network were collected during the morning peak hours. The actual counts, aggregated over five minute intervals, were compared to their simulated counterparts to assess the performance of the estimated models.

This chapter begins with a brief description of MITSIM with emphasis on the acceleration and lane changing models implemented in the original version. The validation methodology and the case study are presented next.

[1]A detailed description of MITSIM can be found in the World Wide Web at the URL http://its.mit.edu/products/mitsim/mitsim.html, or in Yang and Koutsopoulos (1996) or Yang (1997).

7.1 MITSIM: a Microscopic Traffic Simulator

MITSIM is a microscopic traffic simulation model that represents the road network, surveillance system, traffic signs and signals, and the control logic in detail. Each lane is represented with its geometric characteristics (for example, curvature, grade, connectivity), its functional classification (for example, freeway, ramp, local street, tunnel or at–grade), speed limit, and lane use regulations. Loop detectors, lane use signals, and variable message signs are simulated in MITSIM. The control logic supported by MITSIM includes ramp metering, mainline metering, urban control, etc.

In addition to the network, a time dependent origin–destination trip table and the traffic control and route guidance logic are input to the simulator. Vehicles travel through the network between their origins and destinations. The simulator collects the sensor readings, individual vehicle specific trajectory and trip information, and average link and path travel times to provide measures of effectiveness required for system evaluation. The sensor readings include traffic counts, occupancies, and speeds at a given frequency (e.g. every 5 or 10 minutes).

The travel behavior of the driver is captured by a route choice model. The route choice model captures drivers' route selection process which is influenced by traffic information through variable message signs, highway advisory radio, on–board navigation systems, etc. In the route selection process, drivers take lane use regulations into consideration.

Two main driving behavior models are used to simulate vehicle movements in a network:

- the acceleration model, and
- the lane changing model.

The acceleration model calculates the acceleration that drivers apply in response to various situations and factors. The most restrictive acceleration is implemented. The factors that trigger acceleration include:

- car–following,
- desired speed,
- signs and signals,
- connection to appropriate downstream link,
- speed limit,
- incidents, and
- courtesy yielding.

The lane changing model captures lane selection and gap acceptance behavior. A driver first checks for the necessity/desirability of changing lanes. Subsequently, the driver selects a lane from the available choices and assesses the adjacent gap in the target lane. Lane change takes place when the driver perceives the gap in the target lane as acceptable.

Description of the acceleration and the lane changing models implemented in the original version of MITSIM that are replaced in the case study with the corresponding models estimated in this thesis are presented next.

7.1.1 The Acceleration Model

Based on time headway, a driver is categorized to be in one of the three regimes:

emergency regime: if the current headway is less than a lower threshold;

car–following regime: if the current headway is greater than the lower threshold but less than an upper threshold; and finally,

free–flow regime: if the current headway is greater than the upper threshold.

The default thresholds are 0.5 and 1.36 seconds respectively. They were estimated by using engineering judgment in combination with a sensitivity analysis of these parameters on the simulator performance.

In the emergency regime, drivers apply the minimum of the deceleration necessary to avoid collisions with the leader and a "normal" deceleration. The normal deceleration depends on the speed of the vehicle and was adopted from ITE (1982). The value is 2.38 m/s^2 for speeds up to 6.1 m/s, 2.0 m/s^2 for speeds within the range 6.1 to 12.2 m/s, and 1.5 m/s^2 for speeds greater than 12.2 m/s.

The acceleration in the car–following regime is calculated using the *GM Model* (Equation 2.7). Different sets of parameters are allowed for positive and negative relative speed cases. These parameters (α, β, and γ) were adopted from Subramanian (1996) and are presented in Table 2.3.

In the free–flow regime, a driver does not accelerate/decelerate if the current speed is equal to its "desired" speed (Table 7.1). If the current speed is less than the desired speed , he/she applies "maximum" acceleration (Table 7.2), otherwise, he/she applies a normal deceleration.

Table 7.1: The cumulative distribution of speed that is added to the posted speed limit to obtain the desired speed.

Percentile	speed above the speed limit (m/s)
5	-4.67
15	-1.73
25	-0.20
35	0.97
45	1.98
55	3.05
65	4.06
75	5.33
85	6.71
95	8.94

7.1.2 The Lane Changing Model

In MITSIM, lane changes are classified as either discretionary (DLC) or mandatory (MLC). The implementation is as follows:

Table 7.2: Maximum acceleration (m/s^2).

vehicle class	Speed (m/s) < 6.1	6.1–12.2	12.2–18.3	18.3–24.4	> 24.4
high performance car	3.05	2.41	1.71	1.22	1.22
low performance car	2.65	1.58	1.35	0.88	0.61
bus	2.13	1.52	1.22	0.46	0.30
heavy single unit truck	0.85	0.76	0.46	0.30	0.15
trailer trucks	0.49	0.44	0.27	0.14	0.12

Source: adjusted based on FHWA (1980), FHWA (1994), and Pline (1992).

1. check if a lane change is desired/required and define the type of lane change,
2. select a target lane, and
3. check if the gap in the target lane is acceptable.

To capture different driver behavior under DLC and MLC situations, different gap acceptance model parameters are allowed under DLC and MLC situations. The models are presented next.

The Discretionary Lane Changing Model

As mentioned in Section 2.2, MITSIM (Yang and Koutsopoulos 1996) uses a rule–based discretionary lane changing model. A driver considers a discretionary lane change (DLC) only if the driver cannot accelerate more than 85% of the maximum acceleration (Table 7.2) or if the current speed is less than an impatience factor times the driver's desired speed (Table 7.1). The impatience factor varies from 0.8 to 1.0.

Once a driver decides to to perform a DLC, he/she selects a desired lane by comparing the speeds of the left and right adjacent lanes with that of the current lane. A parameter *speed indifference factor* (10%) is used to check whether the current speed is low enough and the speeds in the adjacent lanes are high enough to consider a lane change and start performing a gap assessment.

The Mandatory Lane Changing Model

Drivers consider a mandatory lane change in order to:

- connect to the downstream link of their path,
- bypass a lane blockage downstream,
- avoid entering a restricted use lane, or,
- respond to lane use or variable message signs.

At each time step of the simulation, a probabilistic model is used to decide when a driver is in MLC state. The probability is a function of the remaining distance to the point at which lane change must be completed by ($L_n^{rem}(t)$), the number of lanes to cross to be in the target lane ($m_n(t)$), and the traffic density. The probability is given by:

$$\mathrm{P}_n(MLC(t)) = \begin{cases} \exp\left[\frac{(L_n^{rem}(t)-97.5)^2}{\sigma_{MLC}^2(t)}\right] & \text{if } L_n^{rem}(t) > L_0 \\ 1 & \text{otherwise.} \end{cases} \tag{7.1}$$

where, $\sigma_{MLC}(t)$ is defined as follows:

$$\sigma_{MLC}(t) = 402.3\ (1 + 0.5\ m_n(t) + 1.0\ k_n(t)/k_j) \tag{7.2}$$

where, $k_n(t)$ and k_j denote the traffic density of the segment and the jam density (130 veh/km/lane) respectively. Once a vehicle is tagged MLC, it keeps the tag until it performs the lane change operation or moves into a downstream link. An MLC tagged driver then searches for an acceptable gap in the target lane.

The Gap Acceptance Model

In the gap assessment phase, drivers compare the lead and lag gaps in the target lane to the critical lead and lag gaps respectively. The specifications for the lead and lag critical gaps under mandatory and discretionary lane changing situations for driver

n at time t are:

$$G_{n,DLC}^{cr,lead}(t) = 0.5 \times \max(0.914,\ 0.914 + 0.05\ V_n(t) - 0.10\ \Delta V_n^{lead}(t)) \quad (7.3)$$

$$G_{n,DLC}^{cr,lag}(t) = 0.5 \times \max(1.524,\ 1.524 + 0.10\ V_n(t) + 0.30\ \Delta V_n^{lag}(t)) \quad (7.4)$$

where,

$$\begin{aligned} G_{n,DLC}^{cr,lead}(t) &= \text{lead critical gap for DLC (m)}, \\ G_{n,DLC}^{cr,lag}(t) &= \text{lag critical gap for DLC in (m)}, \\ V_n(t) &= \text{subject vehicle's speed (m/s)}, \\ \Delta V_n^{lead}(t) &= \text{lead veh. speed less subject speed (m/s)}, \\ \Delta V_n^{lag}(t) &= \text{lag veh. speed less subject speed (m/s)}. \end{aligned}$$

At 10 m/s speed, the DLC lead critical gap increases from 0.46 to 0.96 meters as the lead relative speed decreases from 10 m/s to -5 m/s. Similarly, the DLC lag critical gap increases from 0.76 to 2.76 meters as the lag relative speed increases from -5 m/s to 10 m/s. These values are rather small from a behavioral standpoint.

We expect drivers to be more aggressive under MLC situations compared to DLC situations. To capture this, the lead/lag critical gaps under MLC situations are assumed to decrease with decreasing remaining distance to the point at which lane change must be completed by. The specifications for the MLC lead and lag critical gaps are given by:

$$\begin{aligned} G_{n,MLC}^{cr,lead}(t) = \max(&0.914, \\ &0.914 + [0.05\ V_n(t) - 0.10\ \Delta V_n^{lead}(t)][1 - e^{-2.5E-5\ L_n^{rem}(t)}]) \end{aligned} \quad (7.5)$$

$$\begin{aligned} G_{n,MLC}^{cr,lag}(t) = \max(&1.524, \\ &1.524 + [0.10\ V_n(t) + 0.30\ \Delta V_n^{lag}(t)][1 - e^{-2.5E-5\ L_n^{rem}(t)}]) \end{aligned} \quad (7.6)$$

where,

$$\begin{aligned} G^{cr,lead}_{n,MLC}(t) &= \text{lead critical gap for MLC (m)}, \\ G^{cr,lag}_{n,MLC}(t) &= \text{lag critical gap for MLC in (m)}. \end{aligned}$$

7.2 Validation Methodology

7.2.1 Number of Replications

MITSIM is a stochastic simulation model. As a result, the output from one simulation run may be different from another. Each output represents a sample and a number of simulations are required to get statistics with a prespecified accuracy. Hence, an important aspect of the validation methodology is the determination of the number of replications required to obtain reliable estimates of the measures of interest.

Let, y^s_r be an output from the r–th run of the simulator corresponding to a field observation y. Therefore, y^s_r is a realization of the random variable y^s corresponding to the actual observation y. An unbiased estimator of y^s is the mean of the R observations of y^s_r from R different simulation runs. Mathematically,

$$\hat{y}^s = \frac{1}{R} \sum_{r=1}^{R} y^s_r \tag{7.7}$$

where,

$$\begin{aligned} \hat{y}^s &= \text{an estimator of } y^s, \\ R &= \text{number of replications}. \end{aligned}$$

Assume that, the R different realizations of the random variable y^s are distributed *iid* normal with an unknown variance[2]. Then, the number of replications required to

[2]Although, the independence assumption may be violated due to the stochastic nature of the simulator, we still make these assumptions in order to get a closed form solution to estimate the required number of replications.

obtain a certain accuracy (e) at a certain level of significance (α) is given by:

$$R^{reqd} = \left(\frac{s \; t_{\alpha/2}}{\hat{y}^s \; e} \right)^2 \tag{7.8}$$

where,

$$\begin{aligned} s &= \text{an estimate of the standard deviation of } y^s, \\ e &= \text{allowable error,} \\ \alpha &= \text{desired level of significance,} \\ t_{\alpha/2} &= \text{critical value of the } t\text{–distribution at a level of significance } \alpha. \end{aligned}$$

Generally, output from the simulation includes speeds, flows and other quantities that have spatial as well as temporal dimensions. For each of these types of output for each time–space point, the required number of replications needs to be calculated. Then, the desired number of replications would be the most conservative value — in other words, the maximum number of replications required by all the output elements.

7.2.2 Measures of Goodness–of–fit

In this section, different measures of goodness–of–fit to compare the simulated data with their field counterparts are presented (see, for example, Pindyck and Rubinfeld, 1981).

Let, y_i^s be a simulation estimate corresponding to a field observed quantity y_i, where, subscript i denotes a time–space point. For each time–space point i, the percent error, d_i is given by:

$$d_i = \frac{y_i^s - y_i}{y_i} \times 100 \tag{7.9}$$

A positive percent error represents an overprediction whereas a negative percent error represents an underprediction. To evaluate systemwide performance, a useful measure is the bias or mean percent error over all the time–space points. The mean percent

error, b, is:

$$b = \frac{1}{I} \sum_{i=1}^{I} d_i \tag{7.10}$$

where, I is the total number of time–space points. To identify whether an overprediction or an underprediction dominates the bias, a useful measure is the mean positive and negative percent error. The mean positive percent error, b_p, is given by:

$$b_p = \frac{1}{J} \sum_{j=1}^{J} d_j \tag{7.11}$$

where,

j = index representing the time–space point at which the percent error was positive,

J = total number of positive percent error observations.

Similarly, the mean negative percent error is defined for all the observations showing underpredictions.

To penalize larger errors at a higher rate, the root mean square error is used. The root mean square error (RMS) is given by:

$$RMS = \sqrt{\frac{1}{I} \sum_{i=1}^{I} (y_i^s - y_i)^2} \tag{7.12}$$

The RMS percent error is another measure that takes the scale of y_i into account and is given by:

$$RMS\ percent\ error = \sqrt{\frac{1}{I} \sum_{i=1}^{I} \left(\frac{y_i^s - y_i}{y_i} \times 100 \right)^2} \tag{7.13}$$

Another useful measure of fit is the Theil's inequality coefficient (Pindyck and

Rubinfeld 1981), defined as

$$U = \frac{\sqrt{\frac{1}{I}\ \sum_{i=1}^{I}\left(y_i^s - y_i\right)^2}}{\sqrt{\frac{1}{I}\ \sum_{i=1}^{I}\left(y_i^s\right)^2} + \sqrt{\frac{1}{I}\ \sum_{i=1}^{I}\left(y_i\right)^2}} \tag{7.14}$$

The value of U will always fall between 0 and 1. A value of U equal to 0 implies a perfect fit. Related to the Theil's inequality coefficient are three proportions: the bias (U^M), the variance (U^S), and the covariance (U^C) proportions. The proportions are given by

$$U^M = \frac{\left(\overline{y}^s - \overline{y}\right)^2}{\frac{1}{I}\ \sum_{i=1}^{I}\left(y_i^s - y_i\right)^2} \tag{7.15}$$

$$U^S = \frac{\left(\sigma_s - \sigma\right)^2}{\frac{1}{I}\ \sum_{i=1}^{I}\left(y_i^s - y_i\right)^2} \tag{7.16}$$

$$U^C = \frac{2\ (1-\rho)\ \sigma_s\ \sigma}{\frac{1}{I}\ \sum_{i=1}^{I}\left(y_i^s - y_i\right)^2} \tag{7.17}$$

where, $\overline{y}^s, \overline{y}, \sigma_s$, and σ are the means and standard deviations of the simulated and the original series respectively, and ρ denotes the correlation between the two series. Basically, these proportions allow us to determine the contribution of the bias and the variance in the simulation error. Note that,

$$U^M + U^S + U^C = 1 \tag{7.18}$$

The bias proportion (U^M) reflects the systematic error. The variance proportion (U^S) indicates how well the fluctuation in the original data is replicated by the simulation. Therefore, lower values (close to zero) of U^M and U^S are desired. Finally, the covariance proportion (U^C) measures the unsystematic error. This is the remaining error after the deviations from the average values have been accounted for and it is of less worrisome as we desire smaller U^M and U^S.

In addition to these statistical measures, a plot of the real and simulated quantities over time and space may be useful in identifying any systematic under or overpredictions at any particular time and/or space.

7.3 Case Study

7.3.1 The Network

A small network in the Boston area, for which actual flow observations exist, was used in the case study (see Figure 7-1). The network is a 2.7 km (1.68 miles) long segment of the Storrow Drive in Boston. The network is a two lane freeway with two

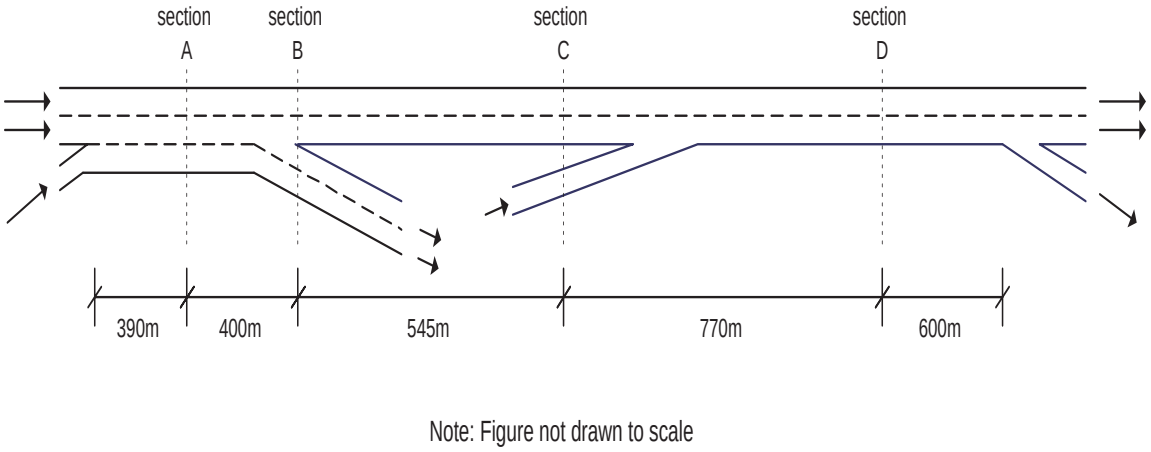

Figure 7-1: The network used in the validation exercise.

on–ramps and two off–ramps. Video of traffic during the morning peak (7:30am to 9:15am) on February 10, 1998 was recorded at four locations marked sections A to D in Figure 7-1.

The part of the network between sections A and D, that are 1.7 km apart, was simulated. Three 30 meters long dummy links were added to the upstream of section A to load vehicles in appropriate lanes based on the O–Ds estimated from the counts. The simulated freeway was extended arbitrarily by 100 meters beyond section D. Traffic sensors were placed at all four sections in the simulated network to collect aggregate counts and average speeds. The speed limit for the freeway was 17.9 m/s (40 mph).

The above network was selected for the following reasons:

1. Traffic was light at the beginning and at the end of the data collection time and was congested in between. Therefore, initial conditions for congestion oc-

currence could be simulated accurately,

2. The bottleneck formation originated due to conditions within the network (traffic merging from the on–ramp near section C) and was not affected by conditions downstream, and

3. The input flows for the network was not affected by spillbacks from the bottleneck, and therefore, the input flows represent the demand exactly.

A limitation of the network though, is that due to the geometric configuration of the on–ramp and the freeway merge area, the mandatory lane changing and forced merging models could not be validated. Although few mandatory lane changes take place between sections A and B, the number of mandatory lane changes is too small to validate the model. Figure 7-2 shows the schematic diagram of the merging area

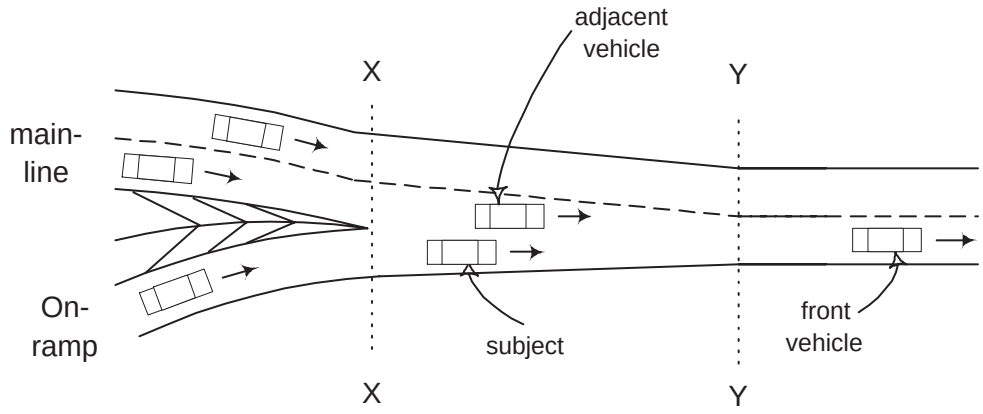

Figure 7-2: Schematic diagram of the on–ramp and Storrow Drive merging area.

between the on–ramp and Storrow Drive (downstream from section C in Figure 7-1) where two lanes merge into one lane and no lane change takes place.

In geometric configurations like this, the mainline vehicles have priority over the on–ramp vehicles. Two vehicles can overlap laterally at this location since the lane width is more than that of a single lane (see location of the subject and the adjacent vehicle in Figure 7-2) but less than that of two lanes. In this case, vehicles from the two upstream lanes merge without any lane changing taking place. In addition, the subject vehicle is not necessarily following its leader as is assumed in developing the

car–following model, since the headway is negative. Therefore, the acceleration and lane changing models developed in this thesis or those implemented in the original version of MITSIM do not apply here.

In MITSIM, lanes are discrete and such geometry cannot be represented. An *ad hoc* merging model (Yang and Koutsopoulos 1996) is implemented to capture the merging phenomenon in such areas. The on–ramp vehicle checks whether there is any vehicle from the adjacent mainline and executes the merge only if the gap is acceptable.

7.3.2 Traffic Data

Minute by minute traffic counts were collected from video tapes for 1 hour 40 minutes beginning at 7:33am. At section A, counts were collected for the left two lanes combined and the rightmost lane (that directly feeds into the rightmost lane of the off–ramp 400 meters away). At section B, the mainline (the two leftmost lanes) counts and the off–ramp (the two rightmost lanes) counts were collected. At section C, before the merge, the mainline counts and the on–ramp counts were collected. Finally, at section D the mainline counts were collected.

Figure 7-3 shows the minute by minute flow through the left two lanes and the rightmost lane at section A and through the on–ramp near section C. The mean flow values at these locations were 1650, 700, and 900 veh/hr/lane respectively with a standard deviation of 350, 300, and 250 veh/hr/lane respectively. Although, the on–ramp volume was not high, a bottleneck formed near the on–ramp and freeway merging area due to merging. A spillback from the bottleneck reached section B briefly, but never reached section A nor the upstream end of the on–ramp at section C. Therefore, the input flows for the network were not affected by spillbacks from the bottleneck and they represent the demand accurately.

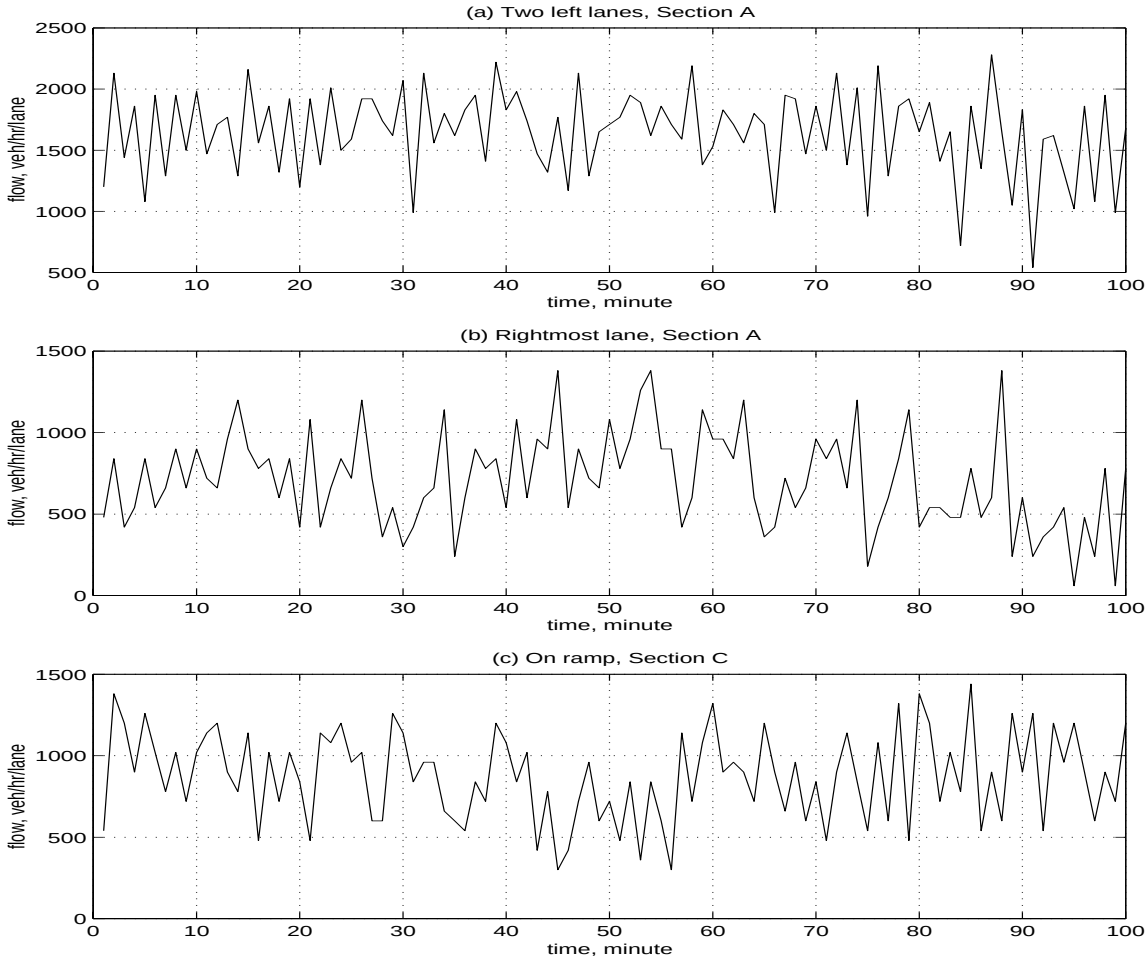

Figure 7-3: Flow of traffic entering the network.

7.3.3 O–D Estimation from Traffic Counts

A required input to the simulator is a time–dependent O–D matrix. The minute by minute O–D matrix was estimated from the minute by minute traffic counts at section A, the exit counts at section B, and the on–ramp counts at section C by using an *ad hoc* method. Note that, the method is developed considering the geometry and counts of this particular network, and is not applicable to a general network. It was assumed that, a certain percentage (p) of the traffic from the rightmost lane at section A (the exit only lane) takes the exit ramp near section B. Since p is unknown, different sets of O–D matrices were created by varying p from 70% to 100% to investigate the effect of the assumption of p on the validation results.

The O–D matrix for a particular minute (say, the t^{th} minute) is estimated from the

counts of the corresponding minute by using the following equations (see Figure 7-4 (c)):

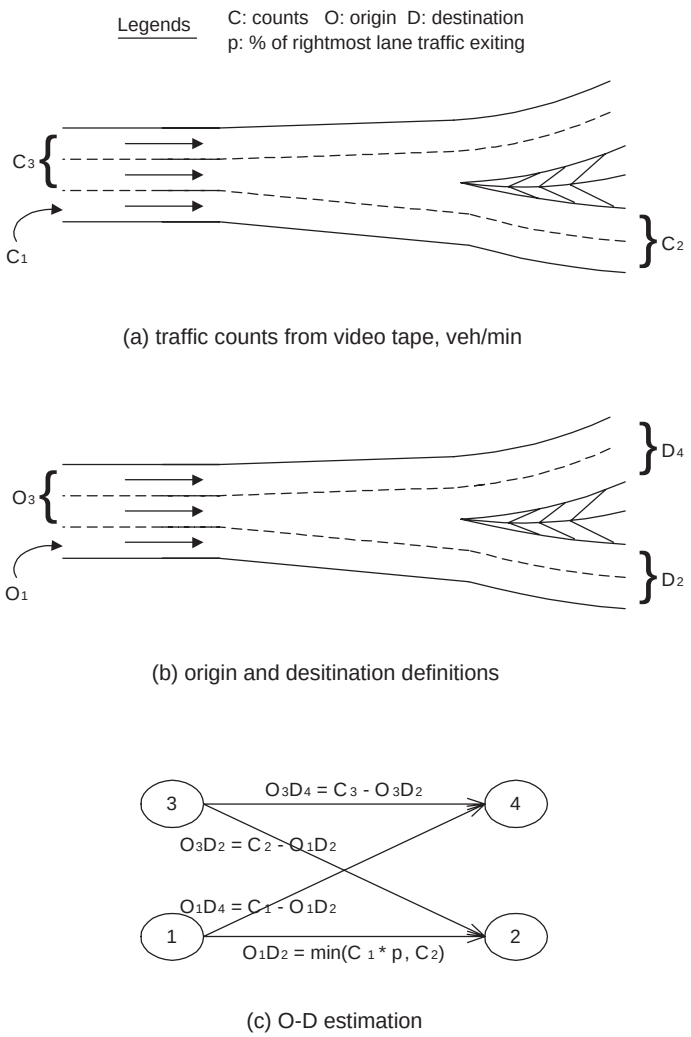

Figure 7-4: O–D estimation from traffic counts for the case study.

$$O_1D_2(t) = \min(C_1(t)\ p, C_2(t+tt)) \quad (7.19)$$

$$O_1D_4(t) = C_1(t) - O_1D_2(t) \quad (7.20)$$

$$O_3D_2(t) = C_2(t+tt) - O_1D_2(t) \quad (7.21)$$

$$O_3D_4(t) = C_3(t) - O_3D_2(t) \quad (7.22)$$

where (see Figures 7-4 (a) and (b)),

t = time period between minutes t and $(t+1)$,

tt = average travel time between sections A and B,

$C_1(t)$ = counts at the rightmost lane at section A,

$C_2(t)$ = counts at the exit ramp at section B,

$C_3(t)$ = counts at the left two lanes at section A,

$O_1D_2(t)$ = number of vehicles from the rightmost lane at section A exiting at section B,

$O_1D_4(t)$ = number of vehicles from the rightmost lane at section A that continue on the freeway,

$O_3D_2(t)$ = number of vehicles from the left two lanes at section A exiting at section B,

$O_3D_4(t)$ = number of vehicles from the left two lanes at section A that continue on the freeway.

The count C_2 was advanced by tt to take into account that a vehicle counted at section A at time t_o would reach section B at time $(t_o + tt)$. It was assumed that tt is the travel time between sections A and B for everyone. We conducted a sensitivity analysis on tt to investigate its impact on the O–D estimations. The average travel time to reach section B from section A ranged from 19 to 28 seconds (observations from simulation). Within this range of tt, $C_2(t+tt)$ differed by less than 2 vehicles/minute for 92% of the cases. Therefore, the assumption on tt does not affect the O–D estimation significantly. The variable tt was set to 22.4 seconds which assumes that vehicles traveled at the speed limit.

From the rightmost lane at section A, the minimum of a certain percent p of C_1 and the exit ramp count at section B (C_2) is assigned to take the exit ramp at section B (O_1D_2). The remaining C_1 is assigned to continue on the freeway (O_1D_4). This will guarantee that at least $(1-p)$ percent of the rightmost lane drivers would perform a

mandatory lane change to continue on the freeway.

The number of vehicles from the left two lanes exiting section B (O_3D_2) is estimated by deducting O_1D_2 from the off–ramp counts at section B (C_2). The remaining traffic counted at the left two lanes at section A (i.e., $C_3 - O_3D_2$) continues in the freeway (O_3D_4). Finally, all vehicles entering the network through the on–ramp at section C have only one destination, i.e., they travel through section D.

7.3.4 MITSIM Modifications

As mentioned above, two additional versions of MITSIM were created by incorporating the models developed in this thesis. In MITSIM ONE, only the acceleration model was replaced with the one estimated in this thesis. In MITSIM TWO, both the acceleration and lane changing models were replaced with those estimated in this thesis. A version of MITSIM with only the lane changing model replaced with the one estimated in this thesis was not created due to the following reason.

Early testing using the original version of MITSIM indicated that, it was not capable of handling the demand used in this case study due to over prediction of congestion and the resulting spillback. Vehicles were queued outside of the network and were loaded only when spaces to load them became available. As a result, vehicles could not be loaded on time according to their O–D and departure times. By replacing the default lane changing model with the one developed in this thesis, the problem still persisted. Therefore, the results from such simulation runs would not be reliable, and MITSIM with only the lane changing model replaced was not tested.

In addition to replacing the acceleration and lane changing models with those estimated in this thesis, the following changes to MITSIM parameters were introduced (see Appendix B for a general approach to calibrate the simulation model parameters):

- The lower (headway) threshold of the acceleration model was set to 0.4 seconds and the upper threshold was adopted from Equation 6.5. The lower threshold was set after some trial and error to avoid vehicle to vehicle collisions. Compared to the 1.36 seconds upper threshold used in the original version of MITSIM, the

upper threshold estimated in this thesis was much higher. For example, the 5 percentile and the median upper headway thresholds were 1.75 and 3.17 seconds respectively.

- Since the data collection site used to estimate the models in this thesis and the network used for the validation case study have different geometric configurations, the constant of the car–following acceleration model was adjusted to make the model predictions more realistic for the validation network. The constant of the car–following acceleration model (α^{acc} in Equation 6.2) was increased from 0.023 to 0.040.

7.3.5 Experimental Design

The three versions of MITSIM were used under different scenarios with respect to the O–D flows (values of p were set equal to 100%, 85%, and 70%). In order to determine the number of replications required, we need estimates of the mean and standard deviation of the measures of interest (discussed in Section 7.2.1). To get estimates of mean and standard deviation, all three versions of the simulator were run 10 times using the three different sets of O–D matrices. Then the required number of replications for all the cases were estimated using Equation 7.8. The most conservative estimate was 4 and in subsequent computations output from all 10 runs were used.

Traffic counts and speeds for each scenario were aggregated over 5 minute periods. The counts were compared to the corresponding real traffic counts. Speeds predicted by different versions of the simulators were also compared. The statistics reported in Section 7.2.2 were used to measure the goodness of fit of the various simulation runs.

7.3.6 Validation Results

Table 7.3 summarizes the comparison of the original MITSIM with the two revised MITSIM versions using three different set of O–D matrices (assuming that 100, 85, and 70% of the drivers from the rightmost lane at section A took the exit at section B). Observations corresponding to the first five minutes were not used in computations

since vehicles were loaded into an empty network and it took approximately 2 minutes to fill the network.

As evident in Table 7.3, by varying the values of p, the percent of the rightmost drivers at section A exiting at section B, the statistics did not show significant variation. This may be due to low flow through the rightmost lane at section A and the exit at section B. Therefore, based on the low sensitivity of the results to the value of p, the conclusion drawn should be valid for the actual O–D flows as well.

For all cases, MITSIM ONE and TWO performed consistently better than the original MITSIM version. Traffic in the original MITSIM got jammed 15 minutes after the beginning of simulation and continued to be jammed throughout the simulation period. The congestion originated near the on–ramp merge. Traffic spilled back all the way up to section A and beyond, and affected vehicle loading into the network. Whereas, in reality, the merging area near section C was congested from 8:04am to 9:05am and the effect of spillback reached section B briefly but never reached section A. MITSIM ONE and TWO performed much better in this respect. This is also reflected by consistently low average speeds at sections B and C for the original MITSIM as shown in Figures 7-5, 7-6, and 7-7.

Due to lack of speed observations from the field, simulated speeds could not be compared to the field observations. At section B, the average speeds were around 12 to 14 m/s for MITSIM ONE and TWO compared to 5 m/s for the original MITSIM. The speed limit of the freeway is 17.9 m/s (40 mph). Average speeds from the original MITSIM were significantly lower than expected.

The RMS Percent Error in counts for the original MITSIM was 9.08% which reduced to 8.09% and 7.53% for MITSIM ONE and TWO respectively. The root mean square error was 28, 24, and 22 vehicles per 5 minutes for the original MITSIM and MITSIM ONE and TWO respectively. The Theil's inequality coefficient was 0.050, 0.042, and 0.039 for the original MITSIM and MITSIM ONE and TWO respectively. Note that, a smaller coefficient implies a better fit.

The mean percent error contributed significantly toward the RMS Percent Error for the original MITSIM and is equal to -5.81% compared to -1.95% and -1.56% for

Table 7.3: Summary statistics of the comparison of the field observed counts with those obtained from different versions of MITSIM using three different O–D sets.

Percent vehicles from the rightmost lane taking exit = 100%			
Statistical Measure	Original MITSIM	Revised MITSIM, Acc only	Revised MITSIM, Acc & LC
RMS percent error (%)	9.08	8.09	7.53
RMS error (veh. per 5 min)	27.82	24.23	22.22
mean percent error (%)	-5.81	-1.95	-1.56
Theil's inequality coefficient	0.050	0.042	0.039
U^M (bias proportion)	0.419	0.073	0.059
U^S (variance proportion)	0.063	0.005	0.011
avg. positive error(%)	4.53	6.78	5.99
no. of positive errors	12	18	20
max. positive error(%)	9.13	20.85	20.49
avg. negative error (%)	-8.56	-5.98	-5.64
no. of negative errors	45	39	37
max. negative error(%)	-19.97	-18.99	-16.17
Percent vehicles from the rightmost lane taking exit = 85%			
Statistical Measure	Original MITSIM	Revised MITSIM, Acc only	Revised MITSIM, Acc & LC
RMS percent error (%)	9.08	7.83	7.44
RMS error (veh. per 5 min)	27.76	23.44	22.02
mean percent error (%)	-5.77	-2.13	-1.96
Theil's inequality coefficient	0.049	0.041	0.038
U^M (bias proportion)	0.415	0.090	0.088
U^S (variance proportion)	0.059	0.008	0.012
avg. positive error(%)	3.90	5.86	5.72
no. of positive errors	14	19	19
max. positive error(%)	10.24	19.46	18.74
avg. negative error (%)	-8.92	-6.12	-5.81
no. of negative errors	43	38	38
max. negative error(%)	-20.10	-17.28	-16.10
Percent vehicles from the rightmost lane taking exit = 70%			
Statistical Measure	Original MITSIM	Revised MITSIM, Acc only	Revised MITSIM, Acc & LC
RMS percent error (%)	9.17	8.13	7.71
RMS error (veh. per 5 min)	28.06	24.21	23.00
mean percent error (%)	-5.83	-2.25	-2.20
Theil's inequality coefficient	0.050	0.042	0.040
U^M (bias proportion)	0.416	0.091	0.099
U^S (variance proportion)	0.060	0.003	0.011
avg. positive error(%)	4.41	6.85	6.65
no. of positive errors	12	17	16
max. positive error(%)	8.97	20.72	19.69
avg. negative error (%)	-8.56	-6.11	-5.79
no. of negative errors	45	40	40
max. negative error(%)	-20.51	-17.65	-16.41

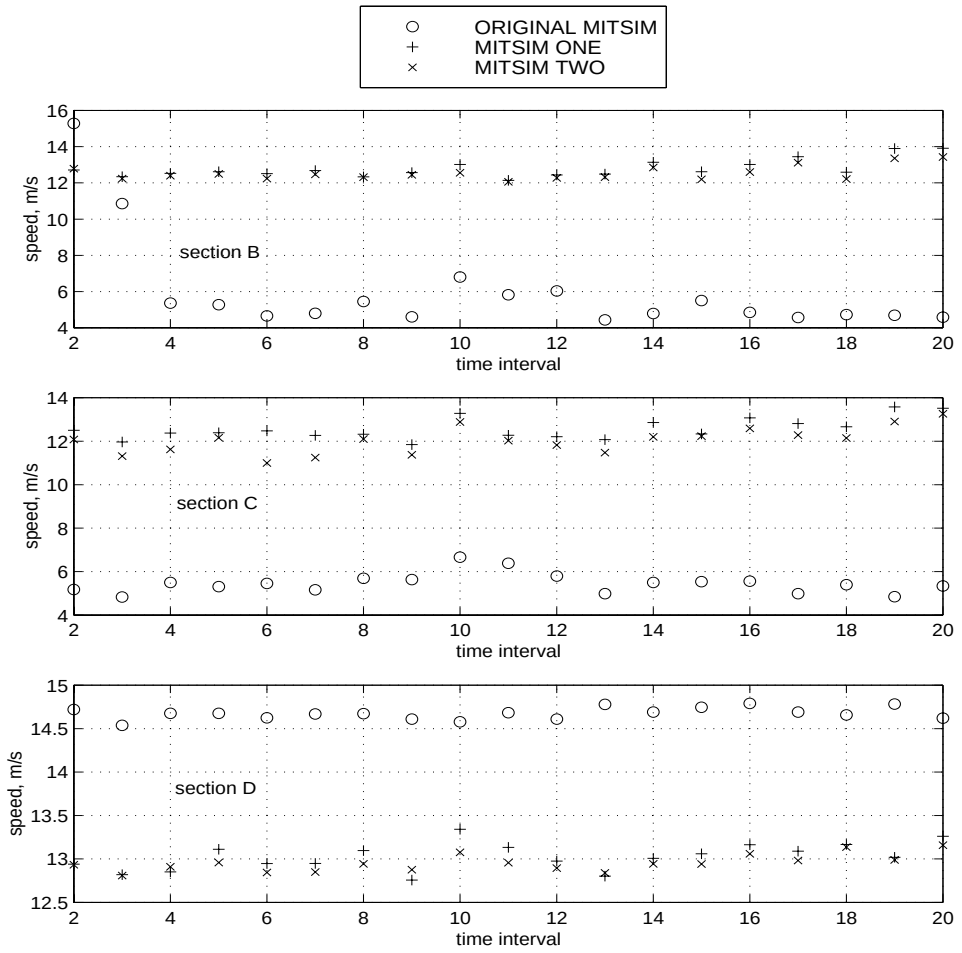

Figure 7-5: Comparison of average speeds obtained from different versions of MITSIM for $p = 100\%$.

MITSIM ONE and TWO respectively. The bias proportion (U^M) for the original MITSIM is 0.419 which is very high. The bias proportions for MITSIM ONE and TWO were 0.073 and 0.059 respectively. The variance proportions were 0.063, 0.005, and 0.011 for the original MITSIM and MITSIM ONE and TWO respectively.

As a result of the systematic underrepresentation of flow, the number of positive errors for the original MITSIM was small and the corresponding average and maximum positive errors were low compared to those for the two other MITSIMs. The mean positive percent errors were 4.53%, 6.78%, and 5.99% for the original MITSIM and MITSIM ONE and TWO respectively. The negative mean percent error for the original MITSIM was -8.56% compared to -5.98% and -5.64% for MITSIM ONE and

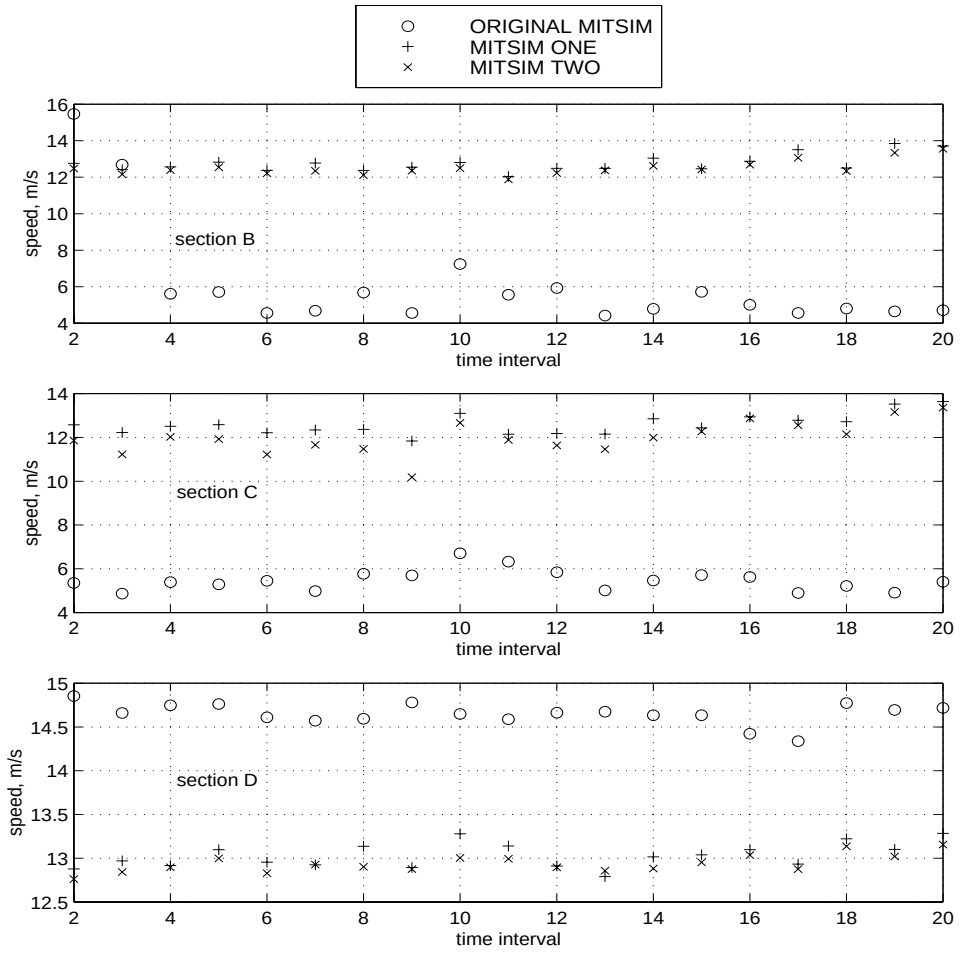

Figure 7-6: Comparison of average speeds obtained from different versions of MITSIM for $p = 85\%$.

TWO respectively.

Compared to MITSIM ONE and TWO, the performance of the original MITSIM was poor at all three sections (see Figures 7-8, 7-9, and 7-10). Performances of MITSIM ONE and TWO at section D were not as good as they were at sections B and C. This may be due to the fact that, section D is near the simulated network boundary where all traffic exits the network. As a result, vehicles leave the network at speeds higher than the real speed. Therefore, the fluctuation in the flow for section D could not be reproduced well.

Performance of the original MITSIM improved significantly after the acceleration model was replaced with the one estimated in this thesis (MITSIM ONE). Due to

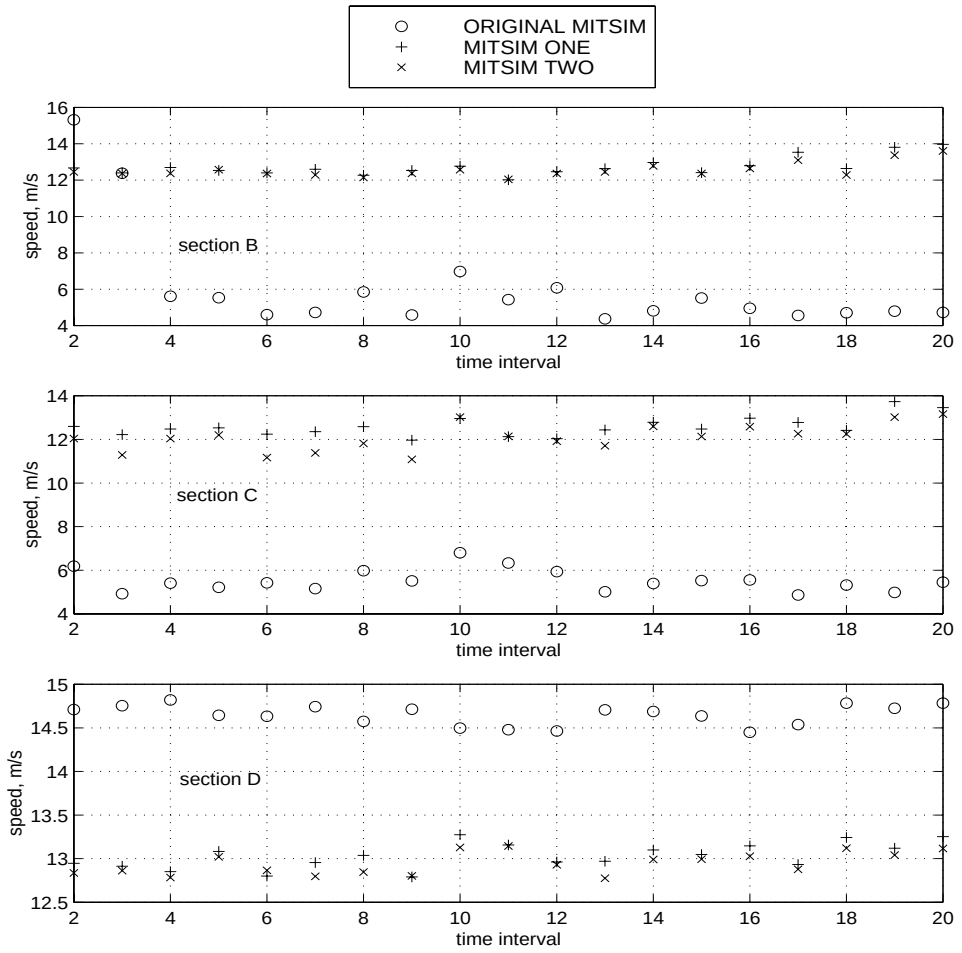

Figure 7-7: Comparison of average speeds obtained from different versions of MITSIM for $p = 70\%$.

the high congestion level, drivers traveled with low headways most of the time. As shown in Figure 6-3, the deceleration calculated by the deceleration model used in the original MITSIM (adopted from (Subramanian 1996)) is too high at low headways. This may have contributed to vehicles moving slowly in the original MITSIM, and thereby reducing the volume of traffic the network could handle, especially, near the merging area.

Finally, MITSIM TWO performed better than MITSIM ONE with respect to all the statistics except the variance proportion (U^S) and the bias proportion (U^M) for the $p = 70\%$ case. However, the RMS and the mean percent errors for MITSIM TWO were smaller than its MITSIM ONE counterparts. This may be due to the fact that

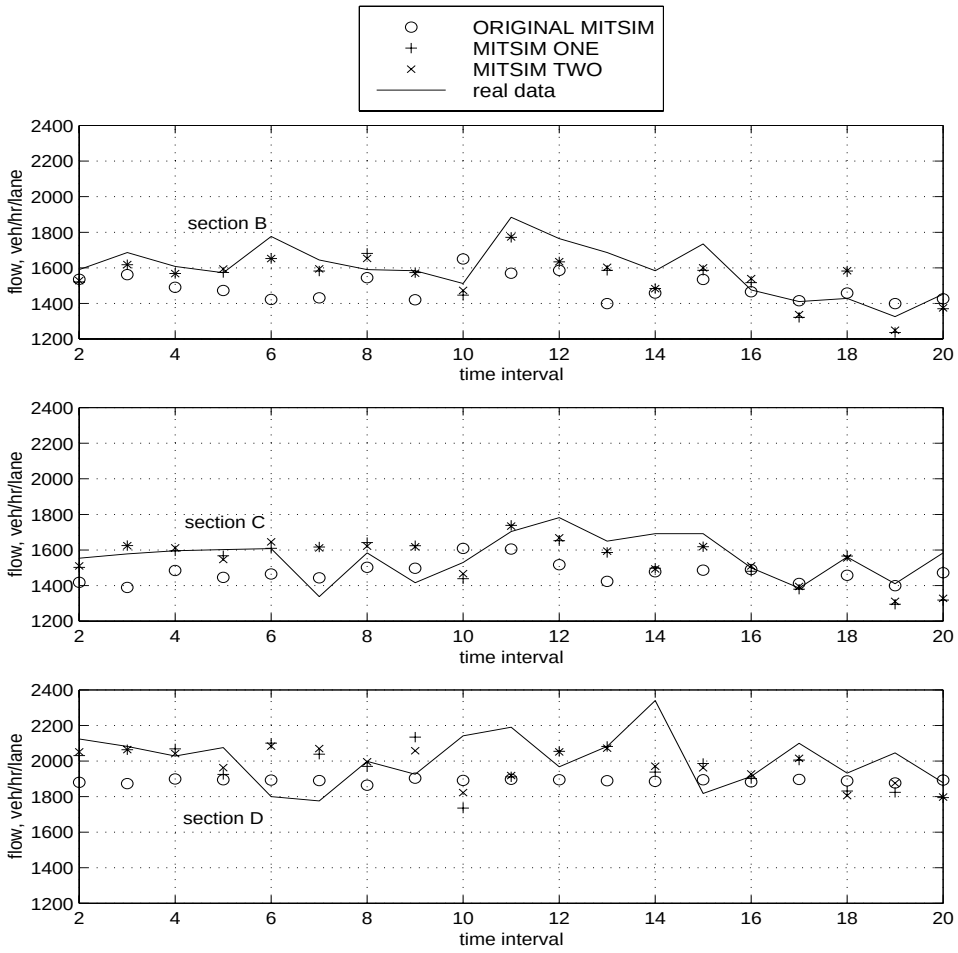

Figure 7-8: Comparison of the real traffic counts with those obtained from different versions of MITSIM for $p = 100\%$.

the variance and the bias proportions do not take into account the scale of the errors (the differences between the simulated and the original traffic counts) with respect to the original counts. Therefore, MITSIM TWO demonstrates the effectiveness of the discretionary lane changing model.

7.4 Conclusions

The acceleration and discretionary lane changing models were tested using a microscopic traffic simulator, MITSIM. Traffic on a 1.83 km long segment of a freeway with one on– and one off–ramps was simulated using different versions of MITSIM: the original MITSIM, MITSIM with only the acceleration model replaced with the

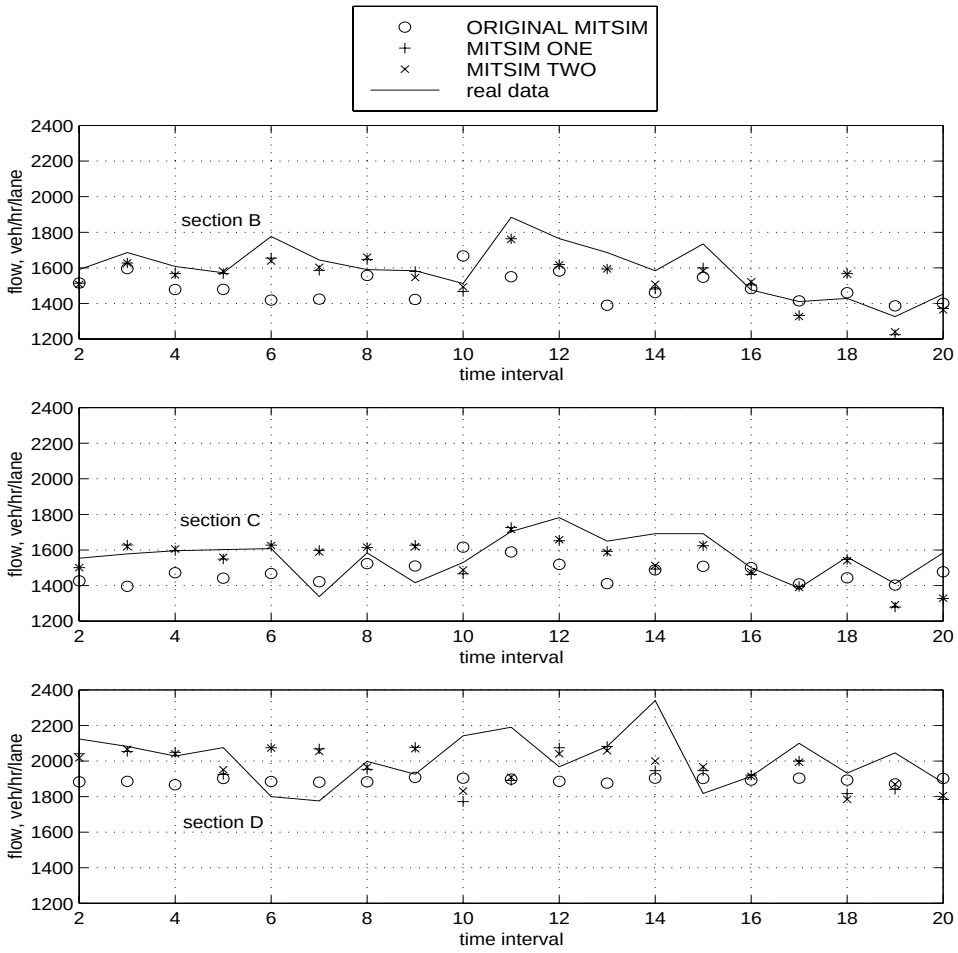

Figure 7-9: Comparison of the real traffic counts with those obtained from different versions of MITSIM for $p = 85\%$.

model estimated in this thesis, and MITSIM with both the acceleration and the lane changing model replaced with the corresponding models estimated in this thesis. Simulated counts aggregated over five minute intervals at different locations were compared to the corresponding field observations.

Performance of the original MITSIM significantly improved after the acceleration model was replaced with the one estimated in this thesis (MITSIM ONE). It improved further when the lane changing model of the original MITSIM was replaced with the one estimated in this thesis in addition to replacing the acceleration model (MITSIM TWO). For a full evaluation, a wider set of experiments covering different weather, geometry, and congestion conditions is needed.

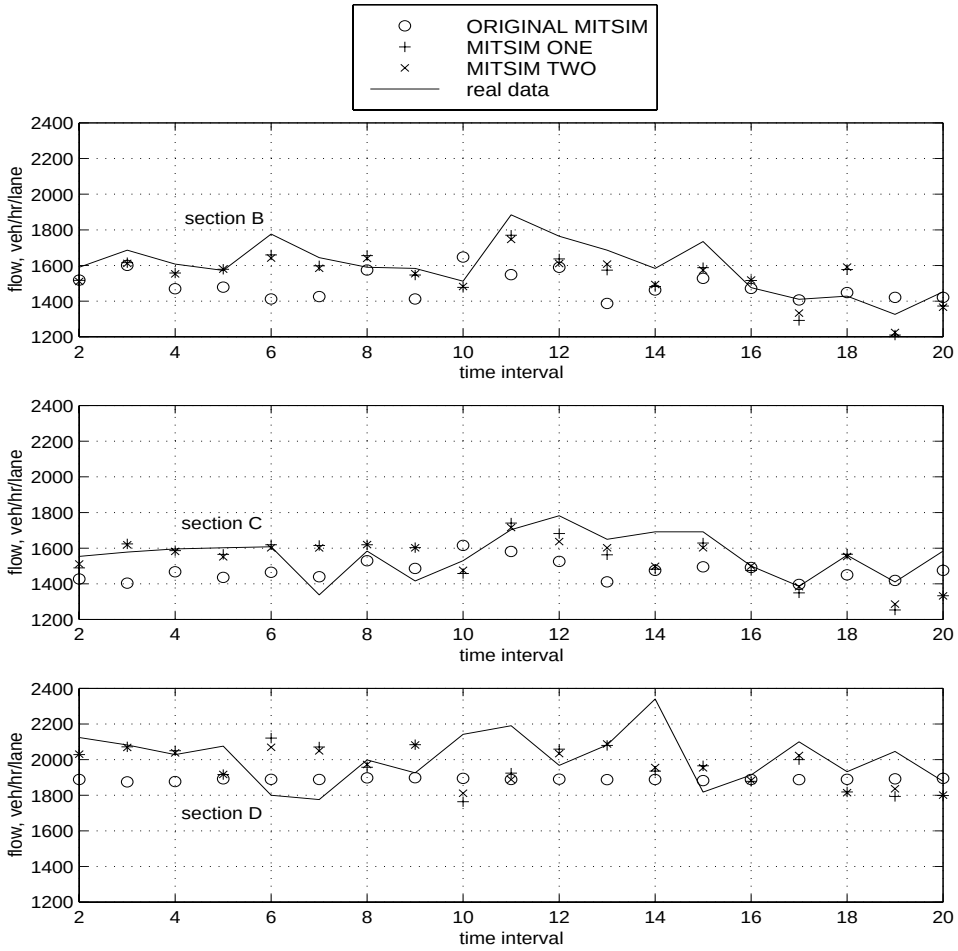

Figure 7-10: Comparison of the real traffic counts with those obtained from different versions of MITSIM for $p = 70\%$.

Chapter 8

Conclusions and Future Research Directions

This chapter summarizes the conceptual framework and estimation results of the proposed acceleration and lane changing models. Major contributions of this thesis are also discussed. Finally, suggestions for future research are presented.

8.1 Summary of Research

8.1.1 The Acceleration Model

A comprehensive framework for estimating a general acceleration model is developed that is applicable to both congested and uncongested traffic. The model defines two regimes based on a time headway threshold: the car–following regime and the free–flow regime. At headways less than the threshold, a driver is assumed to be in the car–following regime trying to match its leader's speed, and at headways larger than the threshold, the driver is assumed to be in the free–flow regime trying to attain its desired speed.

A headway threshold distribution is assumed to capture the variability among drivers. A reaction time distribution is also assumed which captures the effect of response lag to stimulus. The mean of the reaction time distribution depends on the

traffic environment.

Both the car–following and free–flow acceleration models employ the *response equal to the stimulus times the sensitivity* structure. The car–following model uses the *GM Nonlinear Model* as a basis and extends it. The original model was modified to include the effect of density in the sensitivity term and allow the stimulus to be a nonlinear function of the front relative speed (i.e., leader speed less the subject speed). In addition, the estimation allows for capturing the fact that, drivers may update their perception of the traffic environment after they recognize the stimuli for the car–following acceleration (the lead relative speed). In the free–flow acceleration model, the sensitivity term is a constant and the difference between the desired speed and the current speed provides the stimulus.

The parameters of all the component models were estimated jointly using the maximum likelihood estimation method and microscopic data collected from the video of real freeway traffic. The network is a part of Interstate 93, the Central Artery in Boston. The section has a three lane mainline and a weaving lane.

The estimation results show that the impact of speed, space headway, and density of traffic is different under acceleration and deceleration situations. The sensitivity term of the car–following acceleration is a function of the subject speed, the space headway, and the density of traffic, while that of the car–following deceleration is a function of the space headway and the density of traffic. The stimulus is a nonlinear function of the lead relative speed. The free–flow acceleration is a function of the subject speed, its leader speed, an indicator whether the subject vehicle is a heavy vehicle (i.e., vehicle length greater than 9.14 meters or 30 ft), and an indicator whether traffic density is low (level of services A through C).

The mean and standard deviation of the headway threshold distribution were estimated to be 3.17 and 0.87 seconds respectively. The median, mean, and standard deviation of the reaction time distribution were estimated to be 1.31, 1.34, and 0.31 seconds respectively.

8.1.2 The Lane Changing Model

The lane change model is based on a decision that proceeds in the following three steps:

- decision to consider a lane change,
- choice of a target lane, and
- acceptance of a gap in the target lane.

Modeling such a process is extremely complicated due to its latent nature. To simplify, drivers are assumed to make decisions about lane changes at every discrete point in time irrespective of the decisions made during earlier time periods.

The proposed gap acceptance model recognizes that for merging into an adjacent lane, both the lead and lag gaps must be acceptable. Drivers are expected to be more aggressive under mandatory lane changing situations compared to discretionary lane changing situations. The proposed model captures this behavior by allowing different parameters for the gap acceptance model under the two situations. The models were estimated using the same data as in the estimation of the acceleration model.

Drivers' decision to perform a discretionary lane change is modeled as a two steps decision process. First, drivers examine their satisfaction with the driving conditions of the current lane. Important factors affecting such decision include the difference between the current speed and the driver's desired speed, an indicator whether the subject vehicle is a heavy vehicle, and an indicator whether the subject is tailgated. If the driver is not satisfied with the driving conditions of the current lane, he/she compares the driving conditions of the current lane with those of the other lanes. Such decision is influenced by the the speeds of the vehicles ahead in different lanes compared to the subject's desired speed and the lag relative speed.

Factors affecting a driver's decision to respond to the mandatory lane change situation (MLC) are delay (time elapsed since MLC conditions apply) and an indicator for the first gap (when delay is equal to zero). The estimated median lead and

lag critical gap lengths under MLC situations are lower than their DLC situations counterparts, as expected.

A forced merging model is developed to capture drivers' lane changing behavior in heavily congested traffic where gaps larger than their minimum acceptable length are hard to find. In such situations, it is assumed that a driver changes lanes either through courtesy yielding the lag vehicle in the target lane or through the subject forcing the lag vehicle to slow down. Important factors that affect drivers' forced merging behavior include lead relative speed (only when the lead vehicle is slower), remaining distance to the point at which the lane change must be completed by, and total clear gap in excess of the subject vehicle's length.

8.1.3 Validation by Microsimulation

The acceleration and lane changing models were tested using a microscopic traffic simulator, MITSIM. A 1.83 km long segment of a freeway with one on– and one off–ramps was simulated using different versions of MITSIM: the original MITSIM, MITSIM with only the acceleration model replaced with the one estimated in this thesis, and MITSIM with both the acceleration and lane changing models replaced with the corresponding models estimated in this thesis. Simulated counts at different time intervals, aggregated over five minutes, at different locations were compared to the corresponding field observed counts.

Performance of the original MITSIM significantly improved after the acceleration model was replaced with the one estimated in this thesis. It improved further when the lane changing model of the original MITSIM was replaced with the one estimated in this thesis in addition to replacing the acceleration model.

8.2 Contributions

This thesis contributes to the state of the art in modeling drivers' acceleration and lane changing behavior in two major areas: enhancing existing models and proposing new models, and estimating the models using statistically rigorous methods and real

microscopic traffic data. Contributions in each of these two areas are listed below.

- Contribution to the modeling framework:
  - The car–following model is extended by assuming that the stimulus is a nonlinear function of the lead relative speed and that the sensitivity term is also a function of the traffic conditions ahead of the driver.
  - The existing models restricts the stimulus (the lead relative speed) and other factors (such as subject speed, gap in front of the subject) that affect the acceleration decision to be observed at the same time. This corresponds to an assumption that drivers base their decisions on the traffic environment at the time they were stimulated into action. The proposed model relaxes this assumption by allowing drivers to update their perception of the traffic environment during the decision making process.
  - A headway threshold distribution is introduced that allows any driver behavior to be captured (aggressive or conservative).
  - An individual driver specific reaction time is introduced which is allowed to be sensitive to the traffic situation under consideration.
  - A probabilistic lane changing model is developed that captures drivers' lane changing behavior under both the mandatory and discretionary lane changing situations. This is a significant improvement over the existing deterministic rule–based lane changing models.
  - The proposed lane changing model allows for different gap acceptance model parameters for mandatory and discretionary lane changing situations. It also captures the variability within driver and amongst drivers in the lane changing decision process.
  - A forced merging model is proposed that captures merging in a heavily congested traffic by gap creation either through force or through courtesy yielding.

- Contribution to model estimation:
  - A methodology to estimate instantaneous speed and acceleration (that is required for model estimation) from discrete trajectory data (that can be obtained from real traffic) is developed.
  - All the components of the acceleration model are estimated jointly using real microscopic traffic data. The component models are the car–following acceleration and deceleration models, the free–flow acceleration model, and the headway threshold and reaction time distributions. Estimation results demonstrate the robustness of the modeling framework.
  - Separate car–following model parameters under acceleration and deceleration situations are allowed in the estimation. This captures the fact that, the sensitivity of different factors on drivers' acceleration behavior may not be same under these two situations.
  - Separate gap acceptance models for the mandatory and discretionary lane changing situations are estimated. This captures the fact that, driver are expected to be more aggressive under mandatory lane changing situations compared to discretionary lane changing situations.
  - The proposed models were estimated using the maximum likelihood estimation method and real microscopic traffic data.

8.3 Future Research Directions

8.3.1 Modeling

- The proposed acceleration model should be extended to capture the impact of lane changing decisions on the acceleration decision. For example, drivers may need to accelerate or decelerate to fit into a gap in the target lane. In such cases, the headway and speed of the lead and lag vehicles in the target lane will influence drivers' acceleration decisions.

- The proposed lane changing model does not capture the impact of past lane changing decisions on the current lane changing decision and various modeling approximations should be considered.

- The forced merging model and the mandatory lane changing model should be combined into a single framework. In reality, drivers consider forced merging only when they perceive the probability of finding an acceptable gap to be very low.

- Models capturing driver behavior in a merging area where two lanes gradually become one (see Figure 7-2 for an example) have to be developed.

8.3.2 Estimation and Validation

To enhance the ability of the models proposed in this thesis to predict drivers' acceleration and lane changing behavior, the models should be estimated with richer data that has more variability than the one used in this thesis. For example, the car–following model proposed in this thesis predicts acceleration that is smaller than expected which should be reestimated using richer data. In addition, from an estimation point of view, a major research activity is the estimation of the models using richer data that provide the required variability to assess the impact of various factors, such as geometric characteristics etc. More specifically,

- The impact of geometric characteristics of a roadway, for example, lane width, curvature, grade, pavement surface quality, on driver behavior was not captured due to lack of data. The models should be estimated using data from different sites with different geometric characteristics.

- The discretionary lane changing behavior, when mandatory lane changing situations apply, cannot be estimated due to lack of appropriate data. This requires data collected over a long stretch of a roadway (1500 $\sim$ 3000 meters long).

- The discretionary lane changing model was estimated using a data set in which the choice set was the current lane and one adjacent lane. Ideally, data set with

two adjacent lanes in the choice set would be preferable.

- The identification problem that arose while estimating the discretionary lane changing model in which serial correlation was captured should be further investigated.

Further validation, using more extensive networks, is also required.

8.4 Conclusion

A comprehensive framework for modeling drivers' acceleration and lane changing behavior was developed in this thesis. Both the acceleration and lane changing models were estimated using real microscopic traffic data, and validated from a behavioral standpoint as well as using microsimulation. Overall, the empirical results are encouraging and demonstrate the effectiveness of the modeling framework.

Appendix A

Specification of the Random Utility Model Appropriate for Panel Data

Panel data contains one or more observations for each individual driver. Different observations from a given driver are likely to be correlated which may introduce bias in the parameter estimates. To capture this correlation, the random disturbance of the utility function used to model the decisions at various levels is assumed to have two components: an individual specific random term (that does not vary for a given individual), and a generic random term (Heckman 1981). Hence, the utility formulation associated with a decision d within the hierarchy is given by:

$$U_n^d(t) = X_n^d(t)\beta^d + \alpha^d\nu_n + \epsilon_n^d(t) \tag{A.1}$$

where,

$$\begin{aligned} n &= \text{individual driver,} \\ t &= \text{time instance,} \\ U_n^d(t) &= \text{unobserved utility of responding to decision } d \text{ at time } t, \\ X_n^d(t) &= \text{vector of explanatory variables,} \\ \beta^d &= \text{vector of parameters,} \end{aligned}$$

ν_n = individual specific random term assumed to be distributed standard normal,

α^d = parameter of ν_n for decision d,

$\epsilon_n^d(t)$ = generic random term that varies across all three dimensions, i.e., $d, t,$ and n.

These assumptions on the random terms imply:

$$\text{cov}(\epsilon_n^d(t), \epsilon_{n'}^{d'}(t')) = \begin{cases} \sigma^2_{\epsilon^d} & \text{if } t = t',\ n = n' \text{ and } d = d' \\ 0 & \text{otherwise} \end{cases} \tag{A.2}$$

$$\text{cov}(\nu_n^d, \epsilon_{n'}^{d'}(t)) = 0, \forall t,\ n,\ d,\ n',\ d' \tag{A.3}$$

$$\text{cov}(U_n^d(t), U_{n'}^{d'}(t')) = \begin{cases} (\alpha^d)^2 + \sigma^2_{\epsilon^d} & \text{if } d = d',\ n = n' \text{ and } t = t' \\ (\alpha^d)^2 & \text{if } d = d',\ n = n' \text{ and } \forall t \neq t' \\ \alpha^d \alpha^{d'} & \text{if } d \neq d',\ n = n' \text{ and } \forall t \\ 0 & \text{otherwise} \end{cases} \tag{A.4}$$

where, $\sigma^2_{\epsilon^d}$ denotes the variance of $\epsilon_n^d(t)$. Conditional on ν_n, different discrete choice models can be obtained by making different assumptions on the distribution of $\epsilon_n^d(t)$, such as a logit or a probit model.

Appendix B

Calibration of the Simulation Model Parameters

Figure B-1 illustrates a systematic approach to calibrate simulation model param-

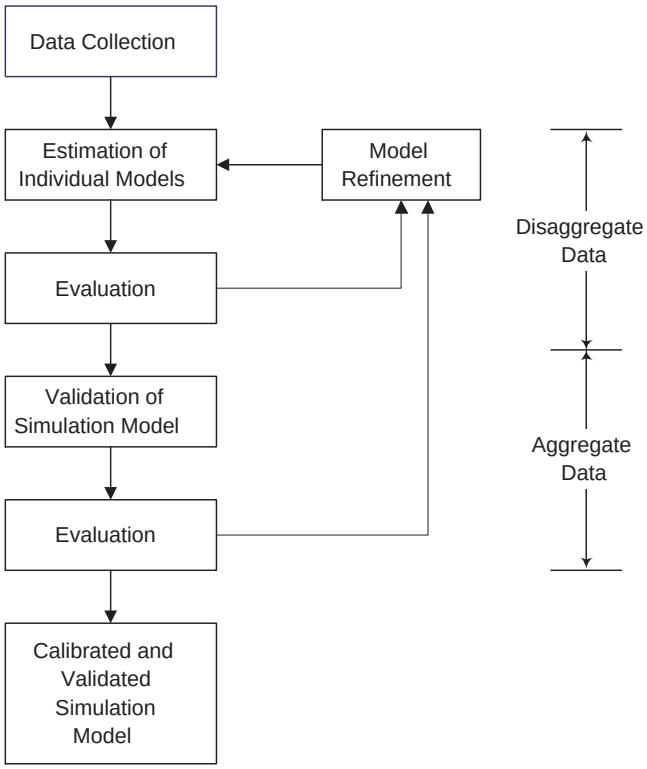

Figure B-1: Model parameter calibration approach.

eters. Data collection involves collecting both disaggregate (microscopic) and ag-

gregate (macroscopic) data. Chapter 5 provided a detailed description of the data required to estimate driver acceleration and lane changing behavior and the actual disaggregate data collected from real traffic. The disaggregate data are used to estimate individual models (as is done in this thesis presented in Chapter 6). Then the parameter estimates are evaluated both from statistical and behavioral standpoints. This may suggest refinement of the model structure which is followed by reestimation of the models.

In the next phase, aggregate data is used to validate the overall performance of the simulation model. Examples of aggregate data include speeds, counts, occupancies at different locations of a roadway aggregated over a period of time. At that point further refinement and calibration may take place. For example, the constant of the models estimated using disaggregate data, collected at other locations, may be recalibrated using aggregate data from the location where the application takes place.

Bibliography

AASHTO (1990). *A Policy on Geometric Design of Highways and Streets*. Washington D. C.: AASHTO.

Ahmed, K. I., M. E. Ben-Akiva, H. N. Koutsopoulos, and R. G. Mishalani (1996). Models of freeway lane changing and gap acceptance behavior. In J. Lesort (Ed.), *Transportation and Traffic Theory*, pp. 501–515. Pergamon.

Aycin, M. F. and R. Benekohal (1998). A linear acceleration car–following model development and validation. *Transportation Research Board, 77th Annual Meeting*.

Ben-Akiva, M. E. and S. R. Lerman (1985). *Discrete Choice Analysis*. Cambridge, MA: MIT Press.

Benekohal, R. and J. Treiterer (1988). Carsim: Car-following model for simulation of traffic in normal and stop-and-go conditions. *Transportation Research Record 1194*, 99–111.

Bexelius, S. (1968). An extended model for car-following. *Transportation Research 2*(1), 13–21.

Cassidy, M. J., S. M. Madanat, M. Wang, and F. Yang (1995). Unsignalized intersection capacity and level of service : Revisiting critical gap. *Transportation Research Board, 74th Annual Meeting*.

Chandler, R., R. Herman, and E. Montroll (1958). Traffic dynamics; studies in car following. *Operations Research 6*, 165+.

Chen, S. (1996). Estimation of car-following safety: Application to the design of intelligent cruise control. Phd dissertation, MIT, Department of Mechanical Engineering, Cambridge, Massachusetts.

Cleveland, W. S. and S. J. Devlin (1988). Locally weighted regression: an approach to regression by local fitting. *Journal of the American Statistical Association 83*(403), 596–610.

Cleveland, W. S., S. J. Devlin, and E. Grosse (1988). Regression by local fitting, methods, properties, and computational algorithms. *Journal of Econometrics 37*, 87–114.

Daganzo, C. F. (1981). Estimation of gap acceptance parameters within and across the population from direct roadside observation. *Transportation Research Part B 15B*, 1–15.

Drew, D. R., L. R. LaMotte, J. H. Buhr, and J. A. Wattleworth (1967). Gap acceptance in the freeway merging process. *Texas Transportation Institute 430-2*.

Edie, L. (1961). Car-following and steady-state theory for noncongested traffic. *Operations Research 9*, 66+.

FHWA (1980). *Development and Testing of INTRAS: a Microscopic Traffic Simulation Model — vol. 1–3*. Report FHWA/RD–80/106–108, Federal Highway Administration, US–DOT, McLean, Virginia.

FHWA (1994). *FREESIM User Guide* (4.5 ed.). Technical Report, Federal Highway Administration, US–DOT, McLean, Virginia.

FHWA (March, 1998). *CORSIM User Manual* (1.04 ed.). US DOT, Office of Safety and Traffic Operations R&D, Intelligent Systems and Technology Division (HSR-10), McLean, Virginia.

Gazis, D., R. Herman, and B. Potts (1959). Car-following theory of steady–state traffic flow. *Operations Research 9*, 449+.

Gazis, D., R. Herman, and R. Rothery (1961). Nonlinear follow–the–leader models of traffic flow. *Operations Research 9*, 545+.

Gerlough, D. and M. Huber (1975). *Traffic Flow Theory, TRB Special Report 165*, pp. 78–79. Washington D. C.: TRB, National Research Council.

Gipps, P. G. (1981). A behavioural car-following model for computer simulation. *Transportation Research–B 15B*, 105–111.

Gipps, P. G. (1986). A model for the structure of lane changing decisions. *Transportation Research 20B*(5), 403–414.

Greenberg, H. (1959). An analysis of traffic flow. *Operations Research 7*, 79–85.

Greenshields, H. (1934). A study in highway capacity. *Highway Research Board Proc. 14*, 468+.

HCM (1985). *Highway Capacity Manual: TRB Special Report 209*. Washington D. C.: Office of Research, FHWA.

Heckman, J. J. (1981). Statistical models for discrete panel data. In C. F. Manski and D. McFadden (Eds.), *Structural Analysis of Discrete Data with Econometric Applications*, pp. 114–178. Cambridge, MA: MIT Press.

Herman, R. and R. Potts (1961). Single–lane traffic theory and experiment. In R. Herman (Ed.), *Theory of Traffic Flow*, pp. 131. Elsevier Publishing Company.

Herman, R. and G. H. Weiss (1961). Comments on the highway crossing problem. *Operations Research 9*, 828–840.

Homburger, W. S. and J. H. Kell (1988). *Fundamentals of Traffic Engineering*, pp. 3–3. Univ. of California, Berkeley, CA: Institute of Transportation Studies.

ITE (1982). *Transportation and Traffic Engineering Handbook* (4 ed.). Englewood Cliffs, NJ: Prentice–Hall Inc.

Johansson, G. and K. Rumer (February, 1971). Drivers' brake reaction time. *Human Factors 13*(1), 23+.

KBB (1998). *Used Car Guide: Consumer Edition, 1983–1997 Models*, Volume 6. Irving, CA: Kelly Blue Book Co.

Kita, H. (1993). Effect of merging lane length on the merging behavior at expressway on–ramps. In C. F. Daganzo (Ed.), *Transportation and Traffic Theory*, pp. 37–51. Elsevier Science Publishers.

Lerner, N., R. Huey, H. McGee, and A. Sullivan (1995). *Older Driver Perception–Reaction Time for Intersection Sight Distance and Object Detection*, Volume 1, pp. 33–40. Report FHWA–RD–93–168, Federal Highway Administration, US–DOT, McLean, Virginia.

Leutzbach, W. (1968). *Introduction to the Theory of Traffic Flow*, pp. 143–146.

Mahmassani, H. and Y. Sheffi (1981). Using gap sequences to estimate gap acceptance functions. *Transportation research, Part B 15B*, 143–148.

May, A. and H. Keller (1967). Non–integer car–following models. *Highway Research Record 199*, 32–32.

Miller, A. J. (1972). Nine estimators of gap acceptance parameters. In G. F. Newell (Ed.), *Proceedings, 5th International Symposium on the Theory of Traffic Flow and Transportation*, New York, pp. 215–235. Elsevier.

Newell, G. (1961). Nonlinear effects in the dynamics of car–following. *Operations Research 9*, 209+.

NSC (1992). *Accident Facts*. Itasca, IL.

Ozaki, H. (1993). Reaction and anticipation in the car–following behavior. In C. F. Daganzo (Ed.), *Proceedings of the 12th International Symposium on the Theory of Traffic Flow and Transportation*, New York, pp. 349–366. Elsevier.

Pindyck, R. S. and D. L. Rubinfeld (1981). *Econometric Models and Economic Forecasts*. New York: McGraw–Hill.

Pline, J. L. (1992). *Traffic Engineering Handbook*. Englhwood Cliffs, New Jersey: Prentice Hall.

Smith, S. A. (1985). *Freeway Data Collection for Studying Vehicle Interaction*, Volume 1. Technical Report FHWA/RD–85/108, Federal Highway Administration, Office of Research, Washington D. C.

Subramanian, H. (1996). Estimation of car-following models. Master's thesis, MIT, Department of Civil and Environmental Engineering, Cambridge, Massachusetts.

Winsum, W. and A. Heino (1996). Choice of time–headway in car–following and the role of time to collision information in braking. *Ergonomics 39*, 579–592.

Yang, Q. (1993). A microscopic traffic simulation for IVHS applications. Master's thesis, MIT, Department of Civil and Environmental Engineering, Cambridge, Massachusetts.

Yang, Q. (1997). A simulation laboratory for evaluation of dynamic traffic management systems. Phd dissertation, MIT, Department of Civil and Environmental Engineering, Cambridge, Massachusetts.

Yang, Q. and H. N. Koutsopoulos (1996). A microscopic traffic simulator for evaluation of dynamic traffic management systems. *Transportation Research C 4(3)*, 113–129.